

PELA

47-05

ILC 1a
Lehigh
Lawrence Co

**APPLICATION FOR NEW SITE APPROVAL OF A
TYPE III RESTRICTED WASTE DISPOSAL FACILITY**

Attachment I

**KARST INVESTIGATION OF THE
PLANNED CEMENT KILN DUST MONOFILL SITE AT THE
LEHIGH PORTLAND CEMENT COMPANY IN MITCHELL, INDIANA**

**VOLUME 1 OF 2
Text, Tables, and Figures**

RECEIVED

MAY 8 1998

DEPARTMENT OF
ENVIRONMENTAL MANAGEMENT
SOLID HAZARDOUS WASTE MANAGEMENT

Prepared for

**Lehigh Portland Cement Company
121 North First Street
Mitchell, Indiana 47446
(812) 849-2191**

Prepared by

**P.E. LaMoreaux & Associates, Inc. (PELA)
106 Administration Road
Oak Ridge, Tennessee 37830
(423) 483-7483**

PELA Project No. 595200

March 18, 1998

P.E. LaMoreaux & Associates

KARST INVESTIGATION OF THE
PLANNED CEMENT KILN DUST MONOFILL SITE AT THE
LEHIGH PORTLAND CEMENT COMPANY IN MITCHELL, INDIANA

VOLUME 1 OF 2
Text, Tables, and Figures

Prepared for

Lehigh Portland Cement Company
121 North First Street
Mitchell, Indiana 47446
(812) 849-2191

Prepared by

P.E. LaMoreaux & Associates, Inc. (PELA)
106 Administration Road
Oak Ridge, Tennessee 37830
(423) 483-7483

PELA Project No. 595200

Barry F Beck
Dr. Barry F. Beck, Indiana C.P.G. #1858

March 18, 1998

—P.E. LaMoreaux & Associates—

TABLE OF CONTENTS

LIST OF TABLES.....	iii
LIST OF FIGURES	iv
LIST OF ACRONYMS AND ABBREVIATIONS	v
EXECUTIVE SUMMARY	viii
I. INTRODUCTION	I-1
II. HYDROGEOLOGIC SETTING	II-1
A. REGIONAL HYDROGEOLOGY	II-1
1. Stratigraphy	II-1
2. Structural Geology	II-4
3. Geomorphology	II-6
B. SITE HYDROGEOLOGY	II-9
1. Location and Physical Description	II-9
2. Site Geology	II-10
III. SINKHOLES	III-1
A. SINKHOLE FORMATION	III-1
B. SINKHOLES ON THE MITCHELL PLAIN	III-4
C. SINKHOLES IN THE SITE AREA	III-6
D. FRAMEWORK FOR EVALUATING SINKHOLE COLLAPSE RISK	III-6
IV. EXPLORATORY DRILLING	IV-1
V. GEOPHYSICAL INVESTIGATIONS	V-1
A. NATURAL POTENTIAL (NP) SURVEY	V-1
1. Introduction to the Natural Potential (NP) Technique	V-1
2. Natural Potential (NP) Data Acquisition	V-3
3. Natural Potential (NP) Data Analysis and Results	V-7
a) Temporal Drift Correction	V-7
b) Topographic Correction	V-8

TABLE OF CONTENTS (Continued)

4.	Interpretation and Discussion	V-13
a)	Sources of Interference	V-13
b)	Topographic Effect—Streaming Potential from Lateral Groundwater Flow	V-14
c)	Residual NP—Streaming Potential from Vertical Groundwater Recharge	V-15
B.	ELECTRICAL RESISTIVITY TOMOGRAPHY	V-17
1.	Introduction to Electrical Resistivity Tomography	V-17
2.	Resistivity Data Acquisition	V-20
3.	Data Analysis and Results	V-23
4.	Interpretation and Discussion	V-26
VI.	GROUNDWATER TRACING	VI-1
A.	DESIGN OF GROUNDWATER TRACING INVESTIGATION	VI-1
1.	Previous Groundwater Tracing	VI-1
2.	Inventory of Karst Features	VI-4
3.	Groundwater Tracing Methodology	VI-7
a)	Background Monitoring	VI-8
b)	Groundwater Tracing Events	VI-9
B.	RESULTS OF GROUNDWATER TRACING INVESTIGATION	VI-13
VII.	DISCUSSION	VII-1
VIII.	CONCLUSIONS	VIII-1
	REFERENCES CITED	References-1
	EXTENDED BIBLIOGRAPHY	Bibliography-1
	APPENDICES	
	APPENDIX A Results of Fluorometric Analyses of Water Samples	A-1
	APPENDIX B Dye Breakthrough Curves	B-1
	APPENDIX C Natural Potential Data	C-1
	APPENDIX D Natural Potential Graphs	D-1
	APPENDIX E Results of Electrical Resistivity Tomography	E-1
	APPENDIX F Interpretation of Electrical Resistivity Tomography Results	F-1
	APPENDIX G Geologic Drilling Logs	G-1

LIST OF TABLES

<u>TABLE</u>	<u>TITLE</u>	<u>PAGE</u>
V-1	Natural Potential Survey Lines	V-5
V-2	Locations of Soil Borings on the Natural Potential Grid	V-6
V-3	Natural Potential Topographic Effect	V-10
V-4	Electrical Resistivity Tomography Transects	V-22
V-5	Comparison of Bedrock Elevations Interpreted from True Resistivity and Borings	V-29
V-6	Verification of the Bedrock Surface Elevation by Drilling	V-33
VI-1	Tracer Monitoring Locations (with Abbreviations)	VI-6
VI-2	Summary of Groundwater Tracing Results	VI-15
VI-3	Results of Analyses for Fluorescein in Dye Bugs	VI-22
VI-4	Results of Analyses for Rhodamine WT in Dye Bugs	VI-23
VI-5	Results of Analyses for Fluorescein in Water Samples	VI-24
VI-6	Results of Analyses for Rhodamine WT in Water Samples	VI-25

LIST OF FIGURES

<u>FIGURE</u>	<u>TITLE</u>	<u>PAGE</u>
I-1	Site Map.....	I-2
II-1	Stratigraphy of the Mitchell Area	II-2
II-2	Idealized Karst Geomorphology of the Mitchell Plain Area.....	II-5
II-3	Orientation of Joints in an Outcrop—S.R.37 at U.S.50, Bedford.....	II-6
II-4	Orientation of Joints in Lehigh Quarry Spring Cave	II-7
II-5	Physiographic Provinces of Southern Indiana	II-8
II-6	Locations of Exploratory Borings and Cross Sections	II-12
II-7	East-West Cross Section Near the Site Based on 1960-61 Exploratory Borings.....	II-13
II-8	North-South Cross Section Through the Site Based on 1960-61 Exploratory Borings...	II-14
III-1	Types of Sinkholes	III-3
IV-1	WSW-ENE Cross Section Through the Site Based on 1997 Exploratory Borings	IV-2
V-1	Natural Potential Response to Groundwater Pumping	V-2
V-2	Natural Potential Data Collection Grid	V-4
V-3	Drift-Corrected Natural Potential Profile for Line 9.....	V-8
V-4	Drift-Corrected Natural Potential Profile for Line 41	V-8
V-5	Drift-Corrected Natural Potential vs. Elevation.....	V-9
V-6	Topography-Corrected Natural Potential Profile for Line 9	V-11
V-7	Topography-Corrected Natural Potential Profile for Line 41	V-11
V-8	Natural Potential with Drift and Topography Corrections.....	V-12
V-9	Natural Potential Noise Levels at the Site	V-14
V-10	Cumulative Error Distribution for Natural Potential	V-15
V-11	Resistivity Anomaly Caused by a Shale-Filled Sinkhole.....	V-18
V-12	Generalized Layout of Multiple-Electrode Electrical Resistivity Tomography Surveys..	V-19
V-13	Electrical Resistivity Tomography Transects	V-21
V-14	Measured Apparent Resistivity Pseudosection	V-23
V-15	Calculated Apparent Resistivity Pseudosection and Inverse Model Resistivity Section	V-24
V-16	RMS Error Distribution Obtained from RES2DINV.....	V-25
V-17	Variation of Standard Deviation of Measured Apparent Resistivity with Depth	V-26
V-18	Interpreted Limestone/Clay Contact Along Line 41A	V-27
V-19	Limestone Elevation Differences Between Data from Borings and Resistivity	V-31
V-20	Generalized Elevation of the Bedrock Surface as Interpreted from Electrical Resistivity Tomography	V-32
VI-1	Results of Previous Groundwater Tracing near Mitchell.....	VI-2
VI-2	Tracer Monitoring Locations	VI-5
VI-3	Dye Insertions at Sinkholes B and F	VI-10
VI-4	Dye Monitoring at Quarry Road Spring (QRS)	VI-11
VI-5	Dye Breakthrough Curve for RLB-2	VI-13
VI-6	Groundwater Tracing Results.....	VI-14
VI-7	Typical Dye Breakthrough Curve	VI-17
VI-8	Rhodamine WT Discharging from Grissom Spring	VI-18
VI-9	Dye Breakthrough Curve for RLB-4	VI-19
VI-10	Dye Breakthrough Curves for RLB-1 and QNS.....	VI-20
VI-11	Joints in Bedrock Streambed of Rock Lick Branch.....	VI-21

P.E. LaMoreaux & Associates

LIST OF ACRONYMS AND ABBREVIATIONS

-	minus
%	percent
±	plus or minus
~	approximately
+	plus
=	is equal to
a	electrode spacing (in electrical resistivity survey)
A	Sinkhole A; also designation for a base station (in NP survey); also designation for soil borings drilled in 1994
AMSL	above mean sea level
B	Sinkhole B; also designation for a base station (in NP survey)
BDL	below detection limit
BH	borehole
BLS	below land surface
Br.	Branch
BsC	Blue Spring Cave
BsS	Blacksmith Spring
BTOC	below top of (well) casing
C	Sinkhole C; also designation for a base station (in NP survey)
C ₁ , C ₂	current electrodes (in electrical resistivity survey)
CaCO ₃	calcium carbonate
CBS	Crusher Building Spring
CCC	CCC Spring
CKD	cement kiln dust
CM	centimeter
D	Sinkhole D
D.H.	drill hole
DA	designation for soil borings drilled in 1994
DnC-1	Donaldson Cave-main stream
DnC-2	Donaldson Cave-small stream
DnC-3	Donaldson Cave-PVC pipe
DRS	Downhill from Rockpile Seep
E	east
E	Sinkhole E
e.g.	<i>exempli gratia</i> (for example)
ENE	east-northeast
ESC	Erwin Spring (Rock Lick) Cave
F	Sinkhole F; also designation for "F-Series" boreholes drilled in 1960-61
Fm	Formation
G	Sinkhole G
gpm	gallons per minute
GrS	Grissom Spring
h _{0j}	elevation of the first measurement on line j (in NP survey)
h _j	elevation of the station where V _j is measured (in NP survey)

P.E. LaMoreaux & Associates

LIST OF ACRONYMS AND ABBREVIATIONS (Continued)

HmC	Hamer Cave
horiz.	horizontal
i	base station (in NP survey)
i.e.	<i>id est</i> (that is)
IDEM	Indiana Department of Environmental Management
Inc.	Incorporated
IP	induced polarization
j	line (in NP survey)
Jan.	January
K _j	topographic correction factor for line j (in NP survey)
km	kilometer(s)
L	left
Lehigh	Lehigh Portland Cement Company
LhC	Lehigh Cave
LQD	Lehigh Quarry Discharge
LQS	Lehigh Quarry Spring Cave
LQS-2	Lehigh Quarry Spring #2
Ls	Limestone
LSp	Lehigh Quarry Seep
m, M	meter(s)
Mar.	March
μg/L	micrograms per liter
MgCO ₃	magnesium carbonate
mV	millivolt(s)
n	data layer (in electrical resistivity survey)
N	Munsell Color classification for soils and rocks
N/A	not applicable
NFS	North Face Seepage
NGVD	national geodetic vertical datum
No.	number
NP	natural potential
ohm.m	ohm-meters (in electrical resistivity survey)
OQS	Old Quarry Seep
OvR	Orangeville Rise
p'	true resistivity for limestone
p''	true resistivity for shale
P ₁ , P ₂	potential electrodes (in electrical resistivity survey)
PELA	P.E. LaMoreaux & Associates, Inc.
pH	acidity or alkalinity (on the standard scale from 0 to 14)
Ps.Z.	pseudo depth (in electrical resistivity survey)
PVC	polyvinyl chloride (well casing)
QBS	Quarry Road Block Spring
QNS	Quarry Road New Spring

LIST OF ACRONYMS AND ABBREVIATIONS (Continued)

QPS	Quarry Road Pipe Spring
QRS	Quarry Road Spring
QSp	Quarry Road Seep
QUS	Quarry Road Upstream Spring
r	radius
R	right; also Munsell Color classification for soils and rocks
RES2DINV	computer software used to process electrical resistivity tomography data
RLB	Rock Lick Branch (may be followed by a station number, 1 through 5)
RMS	Root-Mean-Square error (in electrical resistivity tomography)
RQR	Rabbitville Quarry Rise
RSD	Rock Lick Branch Spring-downstream
RSM	Rock Lick Branch Spring-middle
RSU	Rock Lick Branch Spring-upstream
S.R.	State Route
Sh	Shale
ShS	Springhouse Seep
SP	self potential, spontaneous potential, and streaming potential
Spr.	Spring
SPS	Sewage Plant Spring
St	Saint (male)
Ste	Saint (female)
T_j	time of measurement in line j (in NP survey)
T_{ni}	time of subsequent (next) reading at base station i (in NP survey)
T_{pi}	time of previous reading at base station i (in NP survey)
TM	trademark
U.S.	United States
V_0	reference NP value which is the first reading at Base Station A
V_{cj}	drift-corrected NP value for the measured V_j at time T_j in line j
V_{cj}'	topography-corrected NP, also called the residual NP
vert.	vertical
V_j	measured NP value
V_{ni}	subsequent (next) reading at base station i at time T_{ni} (in NP survey)
V_{pi}	previous reading at base station i at time T_{pi} (in NP survey)
W	west
W.Q.	water quality
WhC-1	Whistling Cave-main stream
WhC-B	Whistling Cave-downstream
WL	water level
WnC	Wind Cave
WSW	west-southwest
WT	water tracing, a part of the name for one form of dye—i.e., rhodamine WT
x	times (multiplication)
YR	a Munsell Color classification for soils and rocks

EXECUTIVE SUMMARY

Lehigh Portland Cement Company is applying to the Indiana Department of Environmental Management (IDEM) for a permit to establish a Type III waste disposal facility for Cement Kiln Dust (CKD) on its property in Mitchell, Indiana. The site is in a karst terrane¹ characterized by limestone bedrock, caves, sinkholes, and springs. According to Indiana regulations, siting such a facility in a karst area requires "provisions to collect and contain all of the leachate generated; and...a demonstration that the integrity of the landfill will not be damaged by subsidence" (329 IAC 10-33-1(a)(4)). This document was prepared by P.E. LaMoreaux & Associates, Inc. (PELA) to supplement the *Application for New Site Approval of a Type III Restricted Waste Disposal Facility* prepared for Lehigh by Keramida Environmental, Inc. It is intended to answer three questions.

- 1) Is there a significant risk of sinkhole collapse or subsidence at the site?
- 2) If so, what can be done to minimize the potential hazards?
- 3) Can groundwater at the site be monitored effectively?

Lehigh's waste disposal site is located on 10.3 acres of undeveloped land. The site lies on the eastern slope of the small valley of Rock Lick Branch. It is underlain by approximately 10 to 40 feet of clayey sediment; the permeability of the clay ranges from 10^{-7} to 10^{-9} centimeters per second. The site area is underlain by the St. Louis and Salem Limestones. Bedrock exposures are rare throughout the area because the clayey sediment is up to 80 feet thick. Four borings were made at the site to investigate the limestone. The depth to limestone ranged from 15 to 39 feet; several small cavities were encountered in the limestone, both open and sediment-filled, as is typical of karst terrane.

Several sinkholes exist in the area around the site. The boundaries of the site were selected to avoid berm construction or the placement of CKD over any sinkholes. A number of small springs discharge groundwater to Rock Lick Branch downslope from the site. The discharge of all the springs on the east side of Rock Lick Branch in the vicinity of the site is small.

The site is located on the Mitchell Plain of southern Indiana—a karst area covering 1,125 square miles. Sinkholes and dendritic cave systems have developed in response to the entrenchment of the streams. The most highly developed portions of the Mitchell Plain have more than 1,000 sinkholes per square mile.

¹ The spelling *terrane*, rather than *terrain*, is used to denote that karst includes both land surface features and features below ground, such as caves and groundwater conduits.

The characteristic features of a karst terrane are caused by the dissolution of the bedrock by natural water. *Solution sinkholes* are broad, bowl-shaped basins produced primarily by the concentrated dissolution of limestone around localized groundwater recharge points. They form gradually. *Cave-collapse sinkholes* occur when the rock roof of a cave collapses suddenly. *Cover-collapse sinkholes* develop where unconsolidated sediment covering the limestone is eroded downward through solutionally-widened shafts in the limestone, undermining the land surface. As subterranean erosion continues, the ground surface may collapse suddenly or settle gradually. The vast majority of sinkholes which develop today and which impact human activity are cover-collapse sinkholes.

The larger and deeper sinkholes on the Mitchell Plain have formed by cave-roof collapse over large, hydrologically active cave passages. Noted sinkhole authorities agree that the incidence of cave-roof collapse is extremely rare within the human time frame. On that basis alone, the risk of cave-roof collapse beneath a 10.3-acre site is negligible. The sinkholes surrounding the site do not show any evidence of being formed by cave-roof collapse, and the available data indicate that any caves beneath the site are small.

The majority of the sinkholes on the southern Mitchell Plain are forming by a combination of limestone solution and cover-sediment erosion. On the southern Mitchell Plain, cover-collapse sinkholes develop over plugged drainage conduits of existing sinkhole basins. No sinkhole basins are apparent on the site. In view of the absence of any surface expression of a sinkhole basin, the risk of a cover-collapse sinkhole developing is negligible. However, two geophysical investigations were undertaken to investigate the possible existence of drainage shafts in the limestone beneath the site.

The natural potential technique (NP) was used to detect subsurface areas of localized groundwater recharge. The NP method involves the measurement of naturally occurring electrical currents. NP anomalies have been detected in and around sinkholes and correlate with areas of localized groundwater movement. The magnitude of the NP anomaly is related to the rate of water flow. Approximately 1,200 voltage measurements were made at 25-foot intervals over the site and adjacent areas. Readings were made at the base station every hour to record the temporal drift. The drift-corrected NP data were further corrected by the corresponding topographic correction factor, K, defined as the NP change per unit elevation increase.

Each drift-corrected NP value consists of three components: the topographic effect, residual NP, and noise. The residual NP response caused by localized hydrogeologic conditions was plotted on a site map. Two negative anomalies were observed off site to the north, corresponding with two known sinkholes. There is only one negative anomaly within the site boundary—a broad, low-magnitude anomaly which may be caused by background noise. Its magnitude is lower and it is much less concentrated than the anomalies associated with the off-site sinkholes. Therefore, any groundwater

recharge associated with this anomaly must be smaller and more diffuse. By itself, this anomaly is certainly not an indication of a sinkhole-collapse risk.

Electrical resistivity tomography was used to identify depressions in the limestone surface which can indicate the existence of enlarged groundwater recharge channels in the bedrock. Tomographic resistivity surveys employ a linear array of electrodes on the ground surface. Computerized instrumentation permits selection of three or four electrodes from the array for each measurement. An inversion program converts the measurements of apparent resistivity into a two-dimensional model of the geology (a tomograph). The interpreted limestone/clay boundary is generalized, but the accuracy of the interpretation can be improved by averaging data from several transects crossing the same point. The elevation of the interpreted limestone surface was plotted in map form. Borings that were not used to calibrate the interpretation were used to evaluate the accuracy of the map. The average difference between the interpreted and measured depth to limestone is only 3.5 feet.

The areas of potential concern for sinkhole development are those which appear as anomalies in *both* the resistivity *and* NP data: those marked by groundwater recharge and a depression in the limestone surface indicating the presence of an open recharge conduit. The only anomalies detected by both methods coincided with an off-site, mature, solution sinkhole and a small valley on-site. Because of the low magnitude and dispersed nature of the on-site NP anomaly, it does not appear to result from a significant zone of concentrated groundwater recharge of the type necessary to cause a sinkhole collapse.

A groundwater tracing investigation was also conducted to determine whether groundwater at the site can be monitored effectively and to provide data to design an effective monitoring strategy. Published information allowed coverage of approximately 150 square miles by monitoring numerous features near the site and only three regional discharge points: Spring Mill State Park, Blue Spring Cave, and Orangeville Rise. Field reconnaissance located 71 karst features in the vicinity of the site, including sinkholes, sinking streams, caves, springs, and seeps.

Five sinkholes adjacent to the site were used to introduce dye into the karst aquifer. At each insertion, the dye was introduced with a 2,000-gallon slug of potable water, followed by one or two additional slugs. Water samples were collected at nearby springs. Drainage from the sinkholes flowed to springs adjacent to the site or to fractures in the streambed of Rock Lick Branch. The data do not indicate the existence of any karst groundwater connections between sinkholes at the site and monitoring locations at Spring Mill State Park, Blue Spring Cave, or Orangeville Rise.

The following conclusions are based on these investigations.

1. The karstic nature of the site does not preclude its acceptability for use as a Type III waste disposal facility.
2. The risk of a cave-collapse sinkhole developing on the 10.3-acre site is infinitesimally small, because there is no evidence of any large caverns beneath the site.
3. Based on the cover-collapse processes in the Mitchell area and site data, the risk of a cover-collapse sinkhole developing beneath the 10.3-acre site is also negligible. In general, the occurrence of a cover-collapse sinkhole is a rare event, even in a mature karst area. Moreover, most cover-collapse sinkholes on the Mitchell Plain occur within existing sinkhole basins, and the site does not contain any sinkhole basins.
4. Dye tracing has demonstrated that groundwater beneath the site discharges through several small springs immediately adjacent to the site. Groundwater associated with any facility at the site can be monitored effectively by analyzing samples collected at these nearby springs.
5. There is no indication of the existence of any karst groundwater connections between the site and regional discharge areas, including Spring Mill State Park, Blue Spring Cave, and Orangeville Rise.

P.E. LaMoreaux & Associates

I. INTRODUCTION

Lehigh Portland Cement Company (Lehigh) is applying to the Indiana Department of Environmental Management (IDEM) for a permit to establish a Type III waste disposal facility (the location of which will be referred to herein as "the site") on its property in Mitchell, Indiana (Figure I-1). This facility will be a monofill for the on-site disposal of Cement Kiln Dust (CKD). Proper siting and design of such a facility requires thorough geologic evaluation of the site (Bleuer, 1970).

The site lies on the Mitchell Plain of southern Indiana, a karst terrane¹ characterized by limestone bedrock, caves, sinkholes, and springs. According to Indiana regulations, siting such a facility in a karst area requires "provisions to collect and contain all of the leachate generated; and...a demonstration that the integrity of the landfill will not be damaged by subsidence" (329 IAC 10-33-1(a)(4)).

P.E. LaMoreaux & Associates, Inc. (PELA) has performed an investigation to address the karstic nature of the site selected by Lehigh for development. This document was prepared to supplement the permit application prepared for Lehigh by Keramida Environmental, Inc. and is intended to answer three questions.

- 1) Is there a significant risk of sinkhole collapse or subsidence at the site?
- 2) If so, what can be done to minimize the potential hazards?
- 3) Can groundwater at the site be monitored effectively?

This report documents the results of a series of extensive investigations conducted by PELA to answer these questions. Published maps and literature regarding the geology of the Mitchell area were collected and reviewed, especially those related to karst and sinkholes. An extensive examination of sinkholes in the Mitchell area was conducted, and Indiana sinkhole authorities were interviewed. A groundwater tracing investigation was conducted to determine the nature and pattern of groundwater flow at the site. Two independent geophysical investigations were conducted to characterize subsurface conditions at the site, and exploratory borings were made to obtain *in-situ* data on the geologic materials beneath the site. The results of these investigations are presented in this Volume I of this document, and the data is presented in a series of appendices in Volume II.

¹ The spelling *terrane*, rather than *terrain*, is used to denote that karst includes both land surface features and features below ground, such as caves and groundwater conduits.

FIGURE 1-1
SITE MAP

LEGEND

- E SINKHOLE
- LANDFILL BOUNDARY
- SPRING MONITORING STATION
- STREAM MONITORING STATION
- > CAVE
- == PAVED ROAD
- UNPAVED ROAD
- STREAM
- SPRING DISCHARGE CHANNEL

N TRUE

CONTOUR INTERVAL = 2 FEET



DRAWING NO. BASE98	 P.E. LaMoreaux & Associates, Inc. Hydrologists, Geologists, Environmental Scientists, & Engineers © P. E. LaMoreaux & Associates, Inc., 1998		
DRAWN POL			
APPROVED			
DATE 03/05/98	FIGURE NO. 1-1	LEHIGH PROJECT NO. 595200	REV. NO. 5

II. HYDROGEOLOGIC SETTING

This chapter provides information regarding the hydrogeologic setting of the site with respect to the stratigraphy, structural geology, and geomorphology of the Mitchell Plain. Information about the regional setting was derived from a review of available maps and publications, all of which are included in the *References Cited* section near the end of this document.

A description of the site and its geology is also presented. This information was derived from published information, as well as data collected during this investigation and previous studies by Lehigh.

Additional publications listed in the *Extended Bibliography* section are included for future reference. They are not cited within the text of this document because they are not directly relevant to this investigation or because they are not readily available. In addition to this material, Hasenmueller and Tankersley (1987) present an annotated bibliography of publications related to the geology of Indiana for the period 1956 through 1975. Miller and Waldron (1988) present a bibliography of descriptive and scientific papers regarding the karst areas of Indiana.

A. REGIONAL HYDROGEOLOGY

In the following sections, the hydrogeologic setting of the site is described with respect to the stratigraphy, structural geology, and geomorphology of the Mitchell Plain. This information was derived from a review of available maps and publications, all of which are listed in the *References Cited* section near the end of this document.


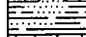



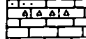

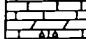
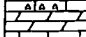
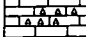

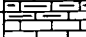
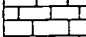
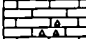
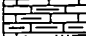
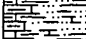
1. STRATIGRAPHY

A generalized stratigraphic section is shown in Figure II-1. According to Gray and others (1970, 1985, and 1987), the area around the site is underlain by the St. Louis Limestone, a unit ranging from 10 to 300 feet in thickness which comprises the lower half of the Blue River Group. The Salem Limestone lies immediately below the St. Louis and comprises the upper half (50 to 100 feet) of the Sanders Group. These rock units were deposited during the Chesterian and Valmeyeran Epochs of the Mississippian Period. In the site area, these Paleozoic-age limestones are generally overlain by less than 50 feet of overburden (Ault, 1993; Gray, 1983).

Gray and others (1970) present a regional topographic and stratigraphic cross section which passes within 0.5 miles of the site. It shows the position of the site area (marked as Mitchell on the section) relative to the underlying rock units. Rexroad and Gray (1979) mapped the elevation of the contact between the St. Louis Limestone and the underlying Salem Limestone ranging from 590 to 610 feet within Spring Mill State Park, approximately 2 miles southeast of the site. Based on published observations that the

P.E. LaMoreaux & Associates

FIGURE II-1 Stratigraphy of the Mitchell Area

TIME UNIT			THICKNESS (FEET)	LITHOLOGY	ROCK UNIT			
PERIOD	EPOCH	SIGNIF. MEMBER			FORMATION	GROUP		
MISSISSIPPIAN	CHESTERIAN	100 to 130			Elwren Fm.	West Baden		
					Reelsville Ls.			
					Sample Fm.			
					Beaver Bend Ls.			
					Bethel Fm.			
		250 to 490			Paoli Ls.	Blue River		
				Lovias	Ste. Genevieve Ls.			
				Rosiclair				
				Fredonia				
					St. Louis Ls.			
		130 to 230			Salem Ls.	Sanders		
					Harrodsburg Ls.			
					Muldraugh Fm.			
				150 to 780			Edwardsville Fm.	Borden
							Spickert Knob Fm.	
					New Providence Sh.			

SOURCE: Adapted from Gray and others (1970 and 1985).

regional dip is toward the west or southwest (see Section A2), the contact should lie at approximately the same elevation beneath the site. Data collected in the immediate vicinity of the site is consistent with this dip direction (see Section B2).

More detailed stratigraphic descriptions are provided by Shaver and others (1970), as revised by Shaver and others (1986). The St. Louis Limestone, which is conformably underlain by the Salem Limestone and conformably overlain by the Ste. Genevieve Limestone, is described as follows (Shaver and others 1986, p. 126).

The lower St. Louis on outcrop consists mainly of pellet-micritic limestone, calcareous shale, and silty dolomite. In the subsurface in a large belt across southern Illinois, southwestern Indiana, and north-central Kentucky, these are interbedded with anhydrite and gypsum to a total thickness exceeding 160 feet (49 m) (McGregor, 1954, pl. 2; Jorgensen and Carr, 1973, p. 46). Evaporite deposition was cyclical and produced as many as 18 distinct repetitions of lithologies.

Droste and Carpenter (1990) present additional lithostratigraphic data on the formations of the Blue River Group, including the St. Louis Limestone. They use well samples or electric logs from 2,000 wells in Indiana to characterize the formations of the Blue River Group and to correlate them with outcrop rocks.

The underlying Salem limestone, which is known in the building-stone industry as Indiana Limestone, is described as follows (Shaver and others, 1986, p. 133).

Crossbedded calcarenite that is medium to coarse grained, tan, gray tan, and light gray, porous, and fairly well sorted and that occurs in exceptionally thick beds is the most widely known rock type of the Salem Limestone and is the internationally known building-stone facies. Individual grains are mostly microfossils (including especially the foraminiferid *Globoendothyra baileyi*), macrofossil fragments, and whole diminutive forms of macrofossils. Coated grains are also common. Other lithologies, besides the shale of the Somerset, include much finer and coarser calcarenites, biocalcirudites, very fine grained argillaceous dolomite commonly containing wavy black carbonaceous laminae, very fine to dense limestone in places including oolites, and dense argillaceous dark-gray to dark-brown limestone (Pinsak, 1957). ...vertical transition or even lateral gradation between lithologies representative of the Salem and the overlying St. Louis Limestone is the general situation in the subsurface of the Illinois Basin (Lineback, 1972), but in part of the Indiana outcrop belt the evidence of continuity of deposition between the Salem and the St. Louis is not strong.

In a discussion written for cave explorers, Moore (1973) presents the following descriptions of the St. Louis and Salem Limestones (p. 7):

The lower part of the [St. Louis Limestone] formation is a gray, tan and brown microcrystalline, thin-bedded, dolomitic limestone that contains silt to sand size quartz grains and clay. Black, gray, and greenish shales are commonly intercalated. In the subsurface there are extensive deposits of gypsum and anhydrite.... Many caves in the Lost River region occur in the lower St. Louis.

The Salem has often been termed oolitic, but true oolites are rare and most of the small, rounded particles are fossil foraminifers, *Endothyra baileyi*, pellets, or mechanically rounded fossil debris. Nevertheless, the massive, even-grained texture of the building

stone facies is typical of the Salem. It contains few horizontal bedding planes, and solutionally widened vertical joints play a major role in karst development in terrains underlain by this formation. Near the top of the Salem in Washington County are several thin, fissile black shales which exert a hydrologic control far in excess of their relative proportion of the rock column. The longest caves in Indiana are formed in the Salem, notably Blue Spring, Binkley, Pless, Fredericksburg, and Dog Hill-Donnehue.

According to Palmer and Palmer (1975), the St. Louis Limestone is the uppermost rock layer beneath most of the sinkhole plain. Bedrock exposures are rare because the limestone is generally covered by as much as 80 feet of unconsolidated material consisting of a clay-rich, cherty residuum from the weathering of the underlying limestone, as well as colluvium, alluvium, and lacustrine material. Although this unconsolidated material is called residuum by Palmer and Palmer (1975), Powell (1961), and Thomas (1985), substantial evidence is presented to suggest that it has a transported sedimentary origin (Hall, 1973, 1976a, and 1976b; Olson and others, 1980).

Palmer and Palmer (1975) state that most known cave passages in the sinkhole plain exist within less than 25 percent of the total limestone exposure, particularly within the massive, prominently jointed beds of the Salem Limestone. However, more than 90 percent of the associated sinkholes are located in the thinner overlying layers of the St. Louis. These observations are confirmed by Rexroad and Gray (1979) for caves and sinkholes within Spring Mill State Park.

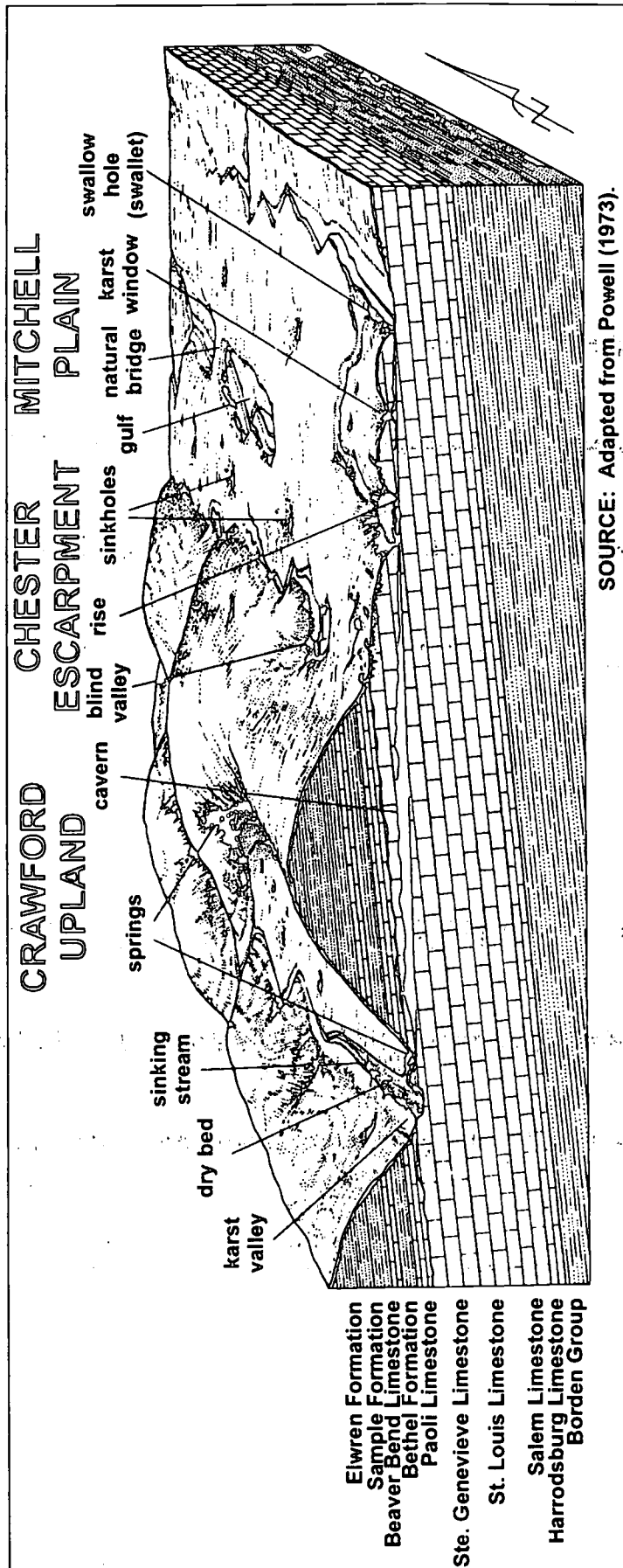
2. STRUCTURAL GEOLOGY

The Mitchell Plain lies on the western flank of the Cincinnati Arch where the rock layers dip toward the center of the Illinois Basin (Palmer and Moore, 1976; Powell, 1973). This regional dip is evident in a generalized structural cross section through the region (Gray and others, 1970) which passes within 0.5 miles of the site (see also Figure II-2). Regionally, the dip of the limestone formations ranges from 20 to 30 feet per mile toward the west or southwest (Bassett, 1976; Duwelius and others, 1995; Malott, 1922; Palmer, 1967 and 1970; Powell, 1961 and 1973). Ruhe (1977) states that the regional dip is about 40 feet per mile toward the southwest and that this dip controls the slope of the Mitchell Plain surface, which is 20 to 30 feet per mile toward the southwest.

The distribution of passages in caves of the Mitchell Plain is controlled primarily by the northwesterly topographic slope, the westerly dip of the bedrock, and the prominent north-south and east-west joint sets within the Salem Limestone (Palmer, 1967; Ash and Ehrenzeller, 1983; Johnson, 1992; Johnson and Gomez, 1994). Groundwater tends to flow downdip, following natural irregularities along bedding-plane partings between adjacent rock layers (Palmer, 1968). Relatively minor differences in lithology, such as an underlying layer of shaley or silty rock, may result in more groundwater movement along a particular bedding-plane parting. Where there is no downdip outlet for groundwater to discharge to a surface stream, it tends to flow along the strike (Powell, 1970; Palmer and Palmer, 1975). Palmer (1969) reports a strong relationship

P.E. LaMoreaux & Associates

FIGURE II-2 Idealized Karst Geomorphology of the Mitchell Plain Area



between joint trends and cave passage orientation in several caves of the Mitchell Plain. Within the Salem Limestone, the influence of joints on groundwater movement is at least as significant as that of bedding planes (Palmer, 1970). However, joint control is less in the St. Louis Limestone, where bedding-plane control predominates (Palmer and Palmer, 1975).

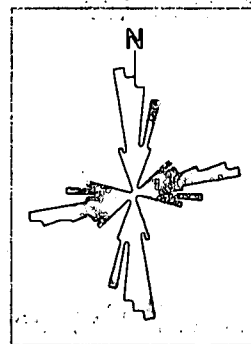
Powell (1977) suggests a stronger relationship between jointing and groundwater flow beneath the Mitchell Plain.

Essentially all integrated solution channels and cavern passages in Indiana have developed along joints, including those passages that exhibit a sinuous pattern (p. 255).

...nearly all significant transmission of subterranean water prerequisite to solution channel and cavern development in central southern Indiana has been along joints within particular stratigraphic units rather than along bedding-plane separations between such units (p. 256-57).

Ault (1989) presents a rose diagram (Figure II-3) depicting joint orientations measured in the road cut at the intersection of State Route 37 and U.S. 50, approximately 6.5 miles north-northwest of the site. At that location, the joints strike predominantly north-northwest and east-northeast. Powell (1976) shows similar diagrams for several locations in Lawrence County which indicate that the strike of jointing is predominantly east-northeast and north-northwest. Joint orientations measured by Powell (1976) in Lehigh Quarry Spring Cave indicate that the primary strike direction is east-northeast with a secondary trend oriented north-south (Figure II-4). A very strong relationship between the orientations of joints and cave passages is demonstrated in Lehigh Quarry Spring Cave; the main cave passages are oriented east-northeast with a minor offset along a short passage trending north-northwest.

FIGURE II-3 Orientation of Joints in an Outcrop—S.R.37 at U.S.50, Bedford

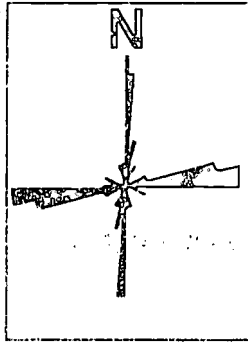


SOURCE: Adapted from Ault (1989).

3. GEOMORPHOLOGY

The Mitchell Plain of southern Indiana (Figure II-5) is a 1,125-square-mile limestone plateau characterized by abundant underground drainage and few streams on the land surface (Powell, 1961; Lehmann, 1975; McConnell and Horn, 1972). It ranges in elevation from 550 to 750 feet above mean sea level (AMSL) and is eroded to elevations below 500 feet along the East Fork White River and its tributaries (Duwelius and others, 1995).

FIGURE II-4 Orientation of Joints in Lehigh Quarry Spring Cave



SOURCE: Adapted from Powell (1976).

Physiographically, the Mitchell Plain of southern Indiana is a subunit of the Highland Rim Section of the Interior Low Plateaus Province (Malott, 1919; Fenneman, 1938). To the south in Kentucky, it is known as the Pennyroyal Plateau; to the north, it is covered with a thick blanket of Pleistocene till (McConnell and Horn, 1972; Palmer and Palmer, 1975). A sinkhole plain occupies the westernmost 30 percent of the Mitchell Plain (Palmer and Palmer, 1975). The Mitchell Plain is bordered on its western side by the Crawford

Upland, a hilly, dissected sandstone highland; and these two areas are separated by the eastward-facing Chester Escarpment (Powell, 1961; McConnell and Horn, 1972). On its eastern side, the Mitchell Plain is bordered by the Norman Upland, which consists of the same resistant shales and siltstones which underlie the Mitchell Plain (Palmer, 1973; Powell, 1964).

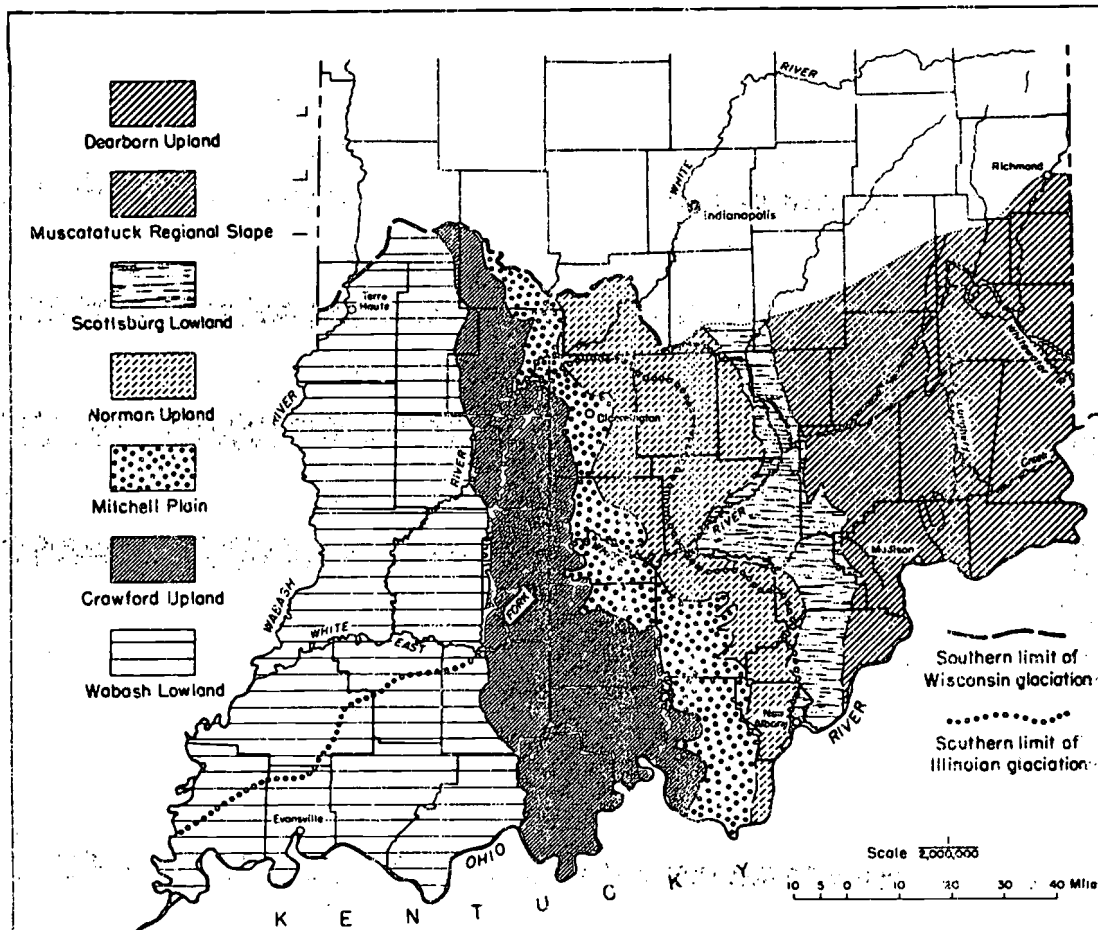
The current configuration of the Mitchell Plain land surface began to evolve during the early Pleistocene, when the present course of the Ohio River was established. At least twice during the early to middle Pleistocene, the Ohio River and its tributaries have been entrenched well below their current levels—i.e., cut downward into the landscape by erosion. During those times, streams on the Mitchell Plain began to sink into the ground in a headward (progressively upstream) manner and return to the land surface via springs in the entrenched river valleys (Gray and Powell, 1965).

During each entrenchment (or episode of erosional downcutting), the land surface and subterranean drainage network of fractures and caves adjusted to drain at the elevation of nearby rivers, such as East Fork White River. Palmer (1976) identifies three surfaces on the Mitchell Plain, suggesting that they are remnants of former land surfaces created in response to three separate base levels that have existed during its history. These base-level-controlled surfaces are referred to as the "upper Mitchell Plain surface," the "lower Mitchell Plain surface," and the "Blue River strath." This interpretation of three previous base levels is supported by the observation that Blue Spring Cave contains three distinct passage levels, each apparently resulting from cessations in the downcutting of the East Fork White River (Palmer, 1967).

Sinkholes and dendritic cave systems developed in response to the dissection of the Mitchell Plain by the entrenching (downcutting) streams (Palmer and Palmer, 1975). Powell (1961) provides brief descriptions of selected caves and summarizes several of the prevailing theories regarding the origin of caves beneath the Mitchell Plain. Ash (1980) also presents a generalized description of cave development beneath the

P.E. LaMoreaux & Associates

FIGURE II-5 Physiographic Provinces of Southern Indiana



SOURCE: Adapted from Powell (1973).

Mitchell Plain. Most known caves lie within the massive, prominently jointed Salem Limestone, while the majority of sinkholes occur in the thinner beds of the overlying St. Louis Limestone (Palmer and Palmer, 1975).

Despite the relatively uniform stratigraphy throughout the Mitchell Plain, the distribution of karst features is very uneven (Palmer and Palmer, 1975). The sinkhole density ranges from less than 10 percent to greater than 60 percent per square mile (Ruhe, 1977). In the most highly developed portions of the Mitchell Plain, more than 100 sinkholes are indicated per square mile on 1:24,000-scale topographic maps with 10-foot contour intervals (Palmer and Palmer, 1975). However, field studies have shown that the actual density is about ten times greater. Malott (1945) found 1,022

P.E. LaMoreaux & Associates

sinkholes in a single square mile near Orleans and estimated that there may be as many as 300,000 sinkholes on the Mitchell Plain. Palmer and Palmer (1975) state that sinkhole development increases with proximity to entrenched streams, such as East Fork White River.

In addition to caves and sinkholes, the Mitchell Plain is characterized by joints which have been enlarged by solution to form fissures known as "grikes". Also known as "cutters," these features are separated by upward-protruding limestone features known as "lapies" or "pinnacles". These vertical channels in the limestone surface are generally filled with soil, forming a subsoil network that provides for drainage of water into the underlying fractures or caves (Malott, 1945; Powell, 1961 and 1966). This subsoil drainage network weathered into the upper 10 to 30 feet of limestone is generally referred to as the epikarstic zone. Gruver and Krothe (1991) demonstrate that the epikarstic zone is capable of storing large volumes of water, which may be flushed into the underlying karst aquifers during storm events.

B. SITE HYDROGEOLOGY

A description of the site and its geology is presented in the following sections. This information was derived from published information, as well as data collected during this investigation and previous studies by Lehigh.

1. LOCATION AND PHYSICAL DESCRIPTION

The site is located on 10.3± acres of undeveloped land north of 840 South Road and east of Rock Lick Branch (Figure I-1). As shown by the Mitchell quadrangle topographic map (U.S. Geological Survey, 1960), the site lies at an elevation of approximately 670 to 695 feet AMSL in the NE¼ NE¼ NW¼ Section 31, T4N, R1E. Its latitude and longitude are approximately 38° 44' 42" north and 86° 27' 13.5" west, respectively. Surrounding areas are included on the Bedford East, Bedford West, and Georgia quadrangles (U.S. Geological Survey, 1978, 1979, and 1965, respectively).

The property, which is owned by Lehigh Portland Cement Company, is located south of the active limestone quarry and north of the cement manufacturing facility. Unpaved roads are located immediately east and west of the site. The road west of the site, which is adjacent to Rock Lick Branch, goes to the quarry and is referred to herein as Quarry Road. The road east of the site, which goes from the plant to the current CKD disposal area, is referred to as the CKD Haul Road. The site is also immediately south of Lehigh's active CKD disposal area.

The site lies on the eastern slope of the small valley of Rock Lick Branch. Rock Lick Creek and Rock Lick Branch are surface streams which are incised approximately 100 feet below the surrounding sinkhole plain in this area. Rock Lick Branch flows north to join Rock Lick Creek which flows into East Fork White River, approximately 3 miles north of the site. The immediate site area slopes from an elevation of 670 to

P.E. LaMoreaux & Associates

690 feet AMSL along the CKD Haul Road on the east to an elevation of 625 feet AMSL at its western extremity: a slope of approximately 6 percent. In this vicinity Rock Lick Branch is at an elevation of 590 to 600 feet AMSL. The lowest portion of the site is well above the valley floor.

The site is approximately half wooded and half cleared field. The margins of the wooded areas are shown in Figure I-1. The majority of the area has never been developed. However, several small houses once existed at the western end of the site near Rock Lick Branch. Old building foundations, cisterns, roofing metal, barbed wire fences, and other debris can be found in this part of the site. The central portion of the site has been excavated by Lehigh for clay to use elsewhere on the property. This includes most of the area which is cleared of trees.

2. SITE GEOLOGY

The site is underlain by 5 feet of a yellowish-brown sandy clay soil. These soils are mapped as two units of the Frederick silt loam which are differentiated primarily by the slope of the land surface. According to Thomas (1985), soils of the Frederick Series are deep and moderately permeable. They are well drained during most of the year but tend to dry out slowly after precipitation. Frederick soils occur on the tops and side slopes of ridges and are formed in limestone residuum.

A red plastic clay underlies the soil; it contains chert fragments at various levels, is occasionally mottled with brownish yellow slightly plastic clay, and is rarely interbedded with thin strata of sandy clay containing up to 20% sand (see Geologic Drilling Logs in Appendix G). Laboratory analyses determined that the permeability of the clay ranges from 10^{-7} to 10^{-9} centimeters per second (see Section III-A, Soil Testing Information, of the Application for New Site Approval of a Type III Restricted Waste Disposal Facility prepared by Keramida Environmental, Inc.) The clayey overburden, including the soil, is referred to collectively as "red clay." It varies in thickness from approximately 10 to 40 feet, depending on the ground topography and the surface of the underlying limestone.

The clayey overburden is underlain by the St. Louis and Salem Limestones (and dolomites) of Mississippian age. The geologist for Lehigh Portland Cement Company, Tom Kessler, has cored numerous exploratory borings to evaluate limestone reserves in the vicinity of the active quarry and two inactive ones. Several of their "F Series" borings, which were drilled in 1960-61, are near the site (Figure II-6). Lehigh's file data on these cores provide calcium carbonate (CaCO_3) and magnesium carbonate (MgCO_3) concentrations, but no detailed lithologic description. Based on this data, dolomite, calcite, and insoluble mineral proportions can be calculated. This is adequate to establish the approximate stratigraphy of the site. Kessler assigns the uppermost, dolomitic, in some areas impure, limestones to the St. Louis Limestone and the underlying *pure limestone—dolomitic limestone—pure limestone* sequence to the Salem Limestone (Kessler, 1997).

P.E. LaMoreaux & Associates

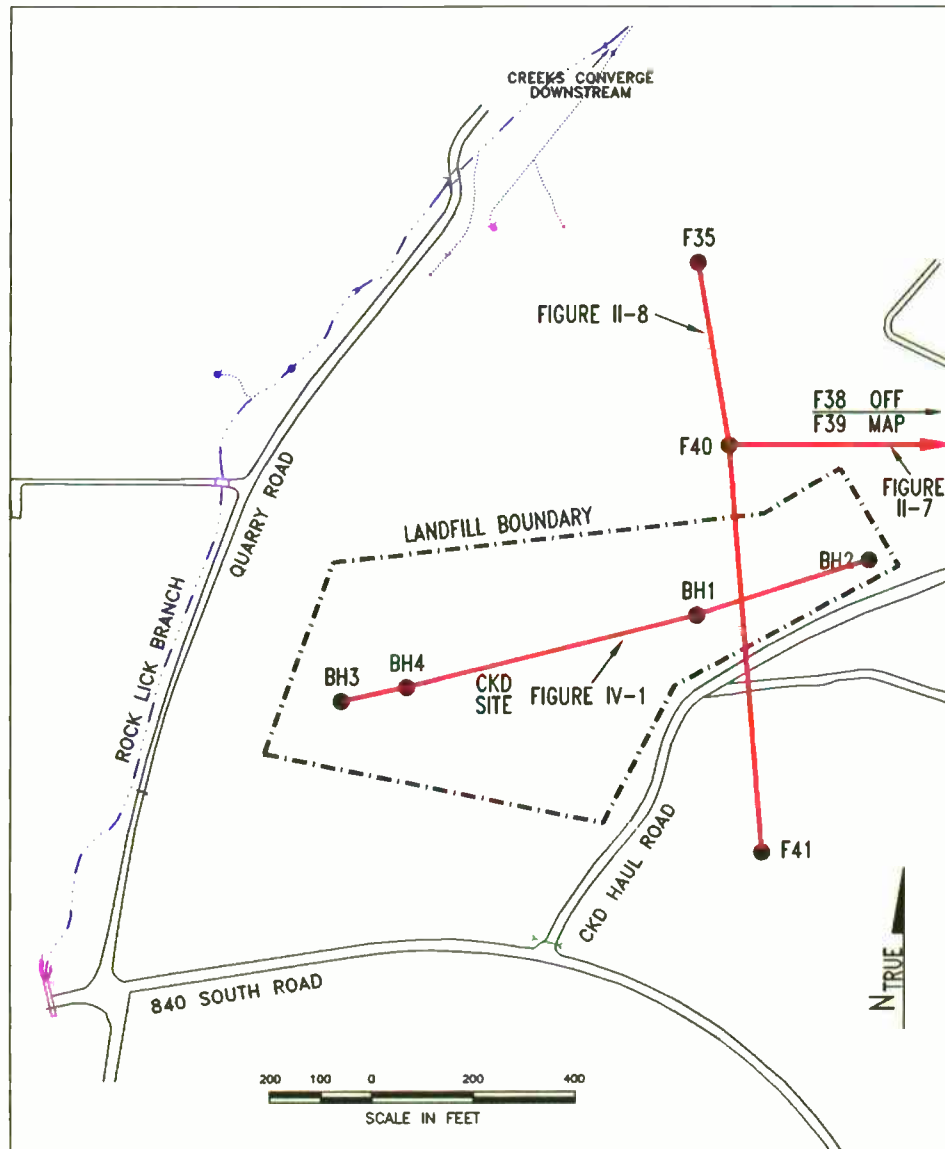
Based on the file records of Lehigh's exploratory drilling, North—South and East—West cross-sections have been constructed through, or within a few hundred feet of, the site (Figures II-7 and II-8). The higher portions of the site are underlain by approximately 80 feet of St. Louis Limestone above the Salem Limestone, whereas the St. Louis is only 50 feet thick beneath the lower portion of the site. On the East-West cross-section (Figure II-7), which is generally parallel to the regional dip, the basal contact of the St. Louis Limestone indicates that the strata beneath the site are approximately horizontal.

The site is located on the eastern slope of the small valley of Rock Lick Branch (Section B1 of Chapter II). The flat upland into which this valley is incised is the Mitchell [Sinkhole] Plain (see Section A of this chapter and Section B of Chapter III) which extends approximately to the CKD Haul Road. In this area large sinkholes, *circa* 500 to 1,000 feet in diameter and up to 40 or 50 feet deep, are common. Sinkholes also occur on the valley slope, but they are much smaller than those on the upland. Several sinkholes (labeled A through G) exist in the area around the site (Figure I-1). They are described in Section C of Chapter III. Sinkhole F is located on the upland, whereas Sinkholes A through E are on the valley slope. The contrast in size is obvious on the site map (Figure I-1). The boundaries of the site were selected to avoid berm construction or the placement of CKD over any sinkholes.

A number of small springs discharge groundwater to Rock Lick Branch along the base of the valley slope, where it meets the valley floor of Rock Lick Branch, below the lowest site elevation (Figure I-1). These springs are located upstream and downstream of the site with respect to Rock Lick Branch. Several of these springs, such as Quarry Road New Spring (QNS) are located at the head of short, steep valleys. Others, such as Quarry Road Spring (QRS), emerge from small openings in the valley floor or from fractures in the bed of Rock Lick Branch, such as Grissom Spring.

The discharge of all the springs on the east side of Rock Lick Branch in the vicinity of the site is small, even after rainfall, and several of the springs cease flowing during the driest time of the year. They respond quickly to recharge, as was shown during the introduction of dye and "chase water" into the sinkholes. The broad, shallow, highly vegetated, and meandering nature of the spring discharge channels indicates that the maximum flow is relatively low.

FIGURE II-6 Locations of Exploratory Borings and Cross Sections

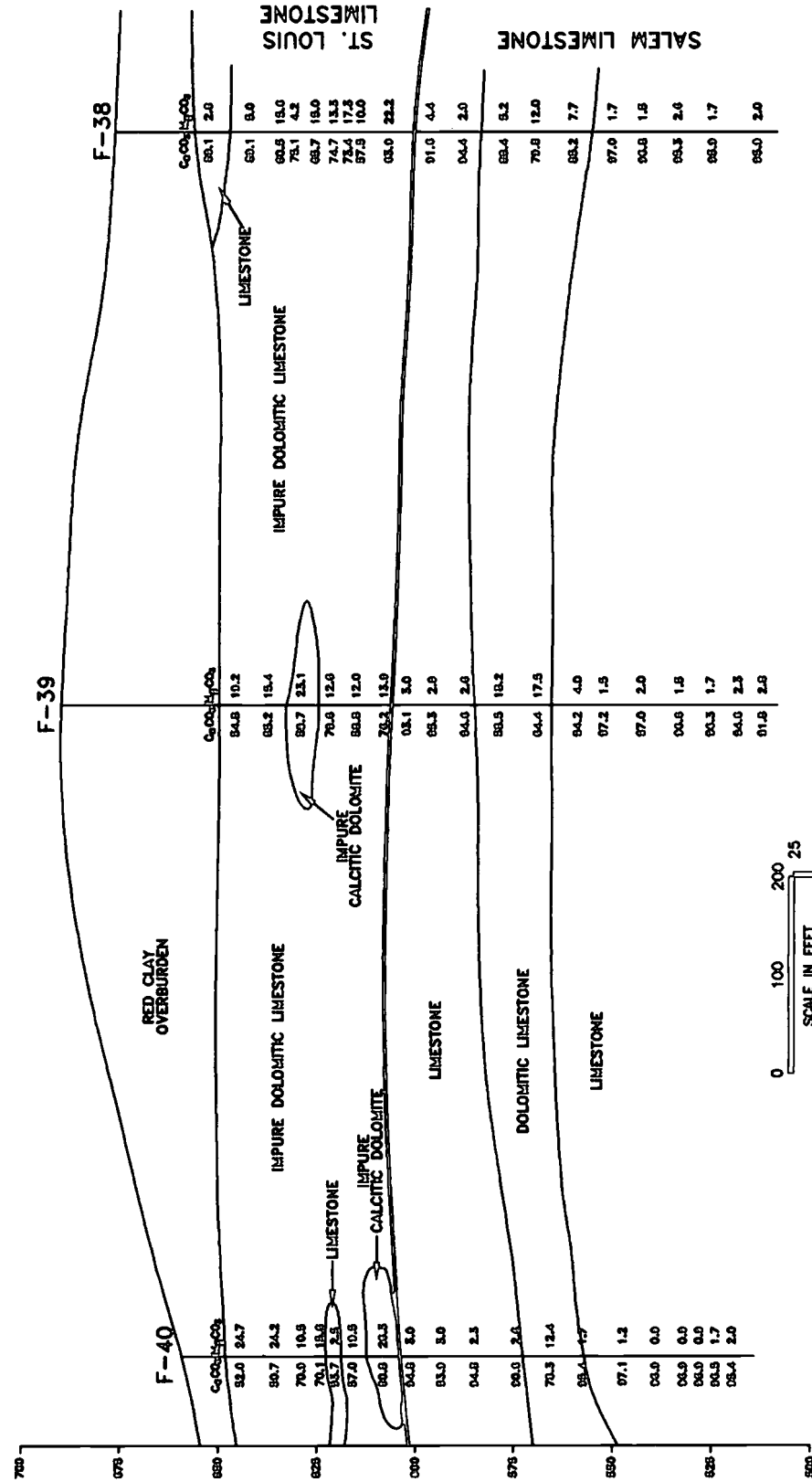


F35, F38, F39, F40, F41: 1960-61 EXPLORATORY BORINGS
BH1, BH2, BH3, BH4: 1997 EXPLORATORY BORINGS

FIGURE II-7 East-West Cross Section Near the Site Based on 1960-61 Exploratory Borings

WEST

EAST

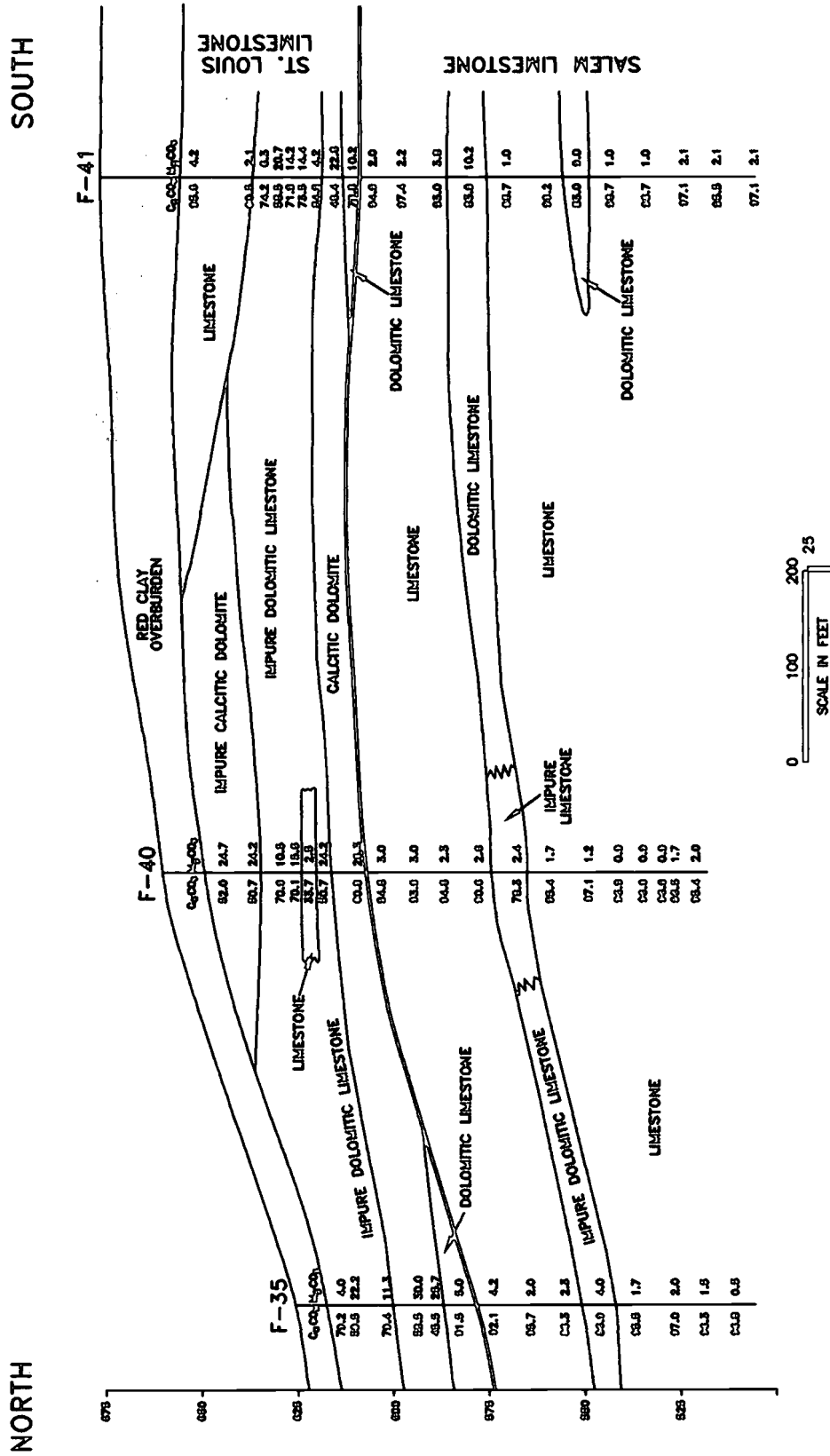


NOTE: LOCATION OF CROSS-SECTION IS SHOWN IN FIGURE II-6.

DRILLING NO. USED-1A
DRAWN BY PDL

P.E. LaMoreaux & Associates

FIGURE II-8 North-South Cross Section Through the Site Based on 1960-61 Exploratory Borings



NOTE: LOCATION OF CROSS-SECTION IS SHOWN IN FIGURE II-6.

PELA PROJECT NO. 595200

III. SINKHOLES

Sinkholes are common geologic features of the landscape in the Mitchell area of southern Indiana. Most sinkholes are broad depressions in the land surface, hundreds of feet across and tens of feet deep. Smaller sinkholes are occasionally featured in the news media when the ground surface collapses suddenly and damages a road or building. This chapter explains how these different types of sinkholes form in southern Indiana and how they are related to underlying karst processes. In particular, this chapter examines the potential risk of sinkhole collapse or subsidence impacting the site.

A. SINKHOLE FORMATION

Sinkholes are the most obvious and characteristic landforms of karst terrane. According to the *Glossary of Geology*, a sinkhole is "A circular depression in a karst area. Its drainage is subterranean, its size is measured in meters or tens of meters, and it is commonly funnel-shaped" (Bates and Jackson, 1987, p. 616). In fact, sinkholes are not so easily definable. They occur in a variety of shapes and sizes for a variety of reasons. The broad, internally drained depressions which are common on the Mitchell Plain are not the same type of features as the small, steep-sided holes which collapse suddenly and without warning. Because both types of sinkholes occur in southern Indiana, it is important to understand how they differ. The following discussion of sinkholes is modified from Beck (1991).

All of the characteristic features of a karst terrane ultimately owe their origins to the dissolution of the bedrock by natural water. As rainwater percolates downward through the soil and any unconsolidated sediment overlying the limestone, it absorbs carbon dioxide and becomes acidic. When it reaches the limestone the water can no longer seep downward, because of the low permeability of the bedrock compared to soil. At this level the infiltrating water flows laterally over the rock surface until it encounters a crack or fracture down which it can flow deeper into the rock. The most permeable pathways tend to occur where two fractures intersect.

Over time these fracture intersections become the preferred pathways for the downward flow of infiltrating water. As the acidified water flows through the limestone, it dissolves and widens the walls of the fractures through which it flows. The most favored pathways widen most rapidly because more water flows through them. As they grow larger, they transmit even more water, "pirating" or capturing drainage from the surrounding rock mass. This self-accelerating process results in a few greatly enlarged vertical conduits, termed solution pipes, which penetrate downward through the limestone, leaving the rock between them only slightly modified.

The concentration of carbon dioxide in the water is greatest when it first encounters the rock, and therefore the solution process is most aggressive at the limestone surface. It decreases as the water seeps downward into the limestone and the CO₂ is consumed

P.E. LaMoreaux & Associates

by reacting with the rock. Because water flow is converging toward the dissolved shafts, the solution process is most concentrated in the area around the shaft. Thus, the bedrock surface is lowered faster here by dissolution. This eventually results in a broad, bowl-shaped depression: the classic *solution sinkhole*, or *doline* (Figure III-1.A). This solution process is extremely slow. The formation of a solution sinkhole requires tens of thousands to hundreds of thousands of years; its enlargement is imperceptible within the human time frame (as compared with the geologic time frame).

If the limestone contains insoluble minerals, they may be left behind on the bedrock surface as a thin soil residue which tends to accumulate in the bottom of the sinkhole basins. If the residual soil becomes thick enough, over thousands of years of limestone dissolution, the terrane is termed a *subsoil karst*. If the limestone is covered by sediments from an external source (marine sands or glacial debris, for example), the terrane is termed a *mantled karst*. However, the origin of the unconsolidated material overlying the limestone does not affect the sinkhole forming process, and this material is simply referred to as "cover."

Although the limestone is covered, the configuration of its surface and the water/rock interaction remain the same, except that the sinkhole basin and the solution pipe which drains it are filled with loose sediment (Figure III-1.C.1). Precipitation infiltrates through the sediment and seeps along the limestone surface toward the solution pipe which drains the area. The loose sediment directly over the solution pipe may be gradually eroded by infiltrating water and transported down the pipe, leaving a soil cavity above the pipe.

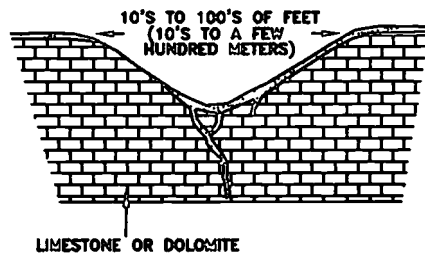
If the sediment is somewhat cohesive, this void may gradually grow upward as the ceiling material continues to be removed (Figure III.C.2). Eventually the upward growth of the void will leave only a thin roof of soil which is not strong enough to support its own weight; at this point collapse occurs. At that moment, a steep-walled hole suddenly appears in the ground surface: a *cover-collapse sinkhole* (Figure III-1.C.3). The limestone and the solution pipe may be visible at the bottom of the hole, or the hole may be choked with sediment. **The vast majority of all the sinkholes which occur today and which impact human activity are cover-collapse sinkholes** (Waltham, 1989; White, 1988; Beck, 1984; Moore, 1980; William's & Vineyard, 1976; Newton and Hyde, 1971).

If the cover sediment is loose rather than cohesive, this process of downward erosion may be gradual and continuous. As one grain settles down the shaft it is followed by another and another, etc. This may happen in loose sand or in clay. The erosion process is very slow, and the settlement of the overlying land surface is imperceptible. Jancin and Clark (1993) have shown how clay in an apparently solid state can "flow" down into caves through solution pipes at a rate of inches per year, thus slowly undermining the land surface. Although the rate of settlement is much slower, this type of subsidence is also a sinkhole: a *cover-subsidence sinkhole* (Figure III-1.D.1-3).

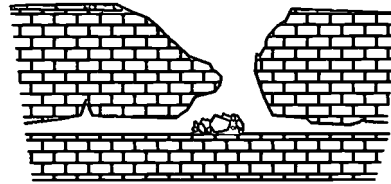
P.E. LaMoreaux & Associates

FIGURE III-1 Types of Sinkholes

A. SOLUTION SINKHOLE

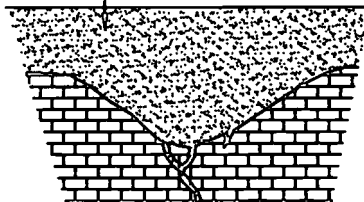


B. CAVE-COLLAPSE SINKHOLE

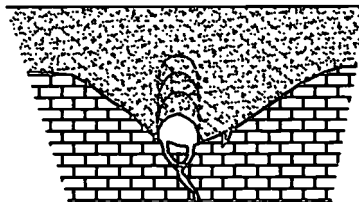


C. FORMATION OF A COVER-COLLAPSE SINKHOLE (L. TO R.)

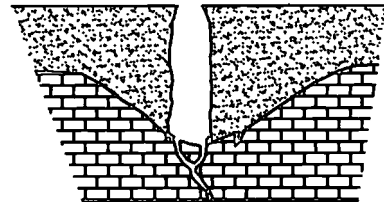
UNCONSOLIDATED SEDIMENT



1. SOLUTION SINKHOLE (A) IS PARTIALLY INFILLED AND PLUGGED, OR COMPLETELY COVERED AS SHOWN. IF IT IS COMPLETELY COVERED, IT IS CALLED A **BURIED SINKHOLE**.

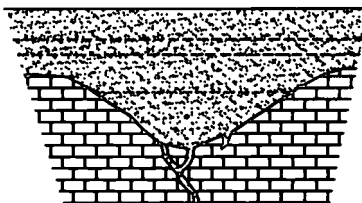


2. WATER INFILTRATING THROUGH THE SOIL AND DOWN THE CENTRAL SHAFT INITIATES EROSION OF SOIL, FORMING A VOID IN THE SOIL ABOVE THE SHAFT. THE ROOF OF THE SOIL VOID GRADUALLY BREAKS DOWN AND THE VOID GROWS UPWARD.

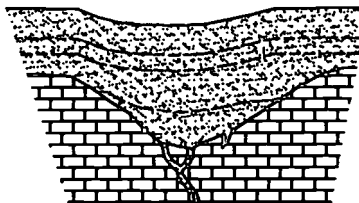


3. UPWARD EROSION EVENTUALLY REACHES THE GROUND SURFACE, WHICH COLLAPSES LEAVING A STEEP-WALLED PIT IN THE SOIL. THE LIMESTONE SHAFT MAY BE VISIBLE OR MAY BE COVERED WITH COLLAPSED SEDIMENT. SURFACE EROSION WILL MODIFY THE SHAFT TO A FUNNEL SHAPE OVER TIME.

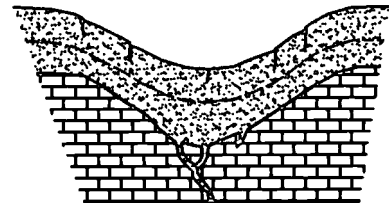
D. FORMATION OF A COVER-SUBSIDENCE SINKHOLE (L. TO R.)



1. SOLUTION SINKHOLE (A) IS PARTIALLY INFILLED OR COMPLETELY COVERED AS SHOWN.

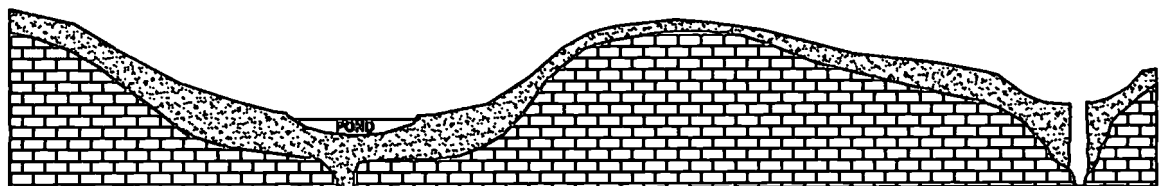


2. SLOW MOVEMENT OF SEDIMENT DOWN THE CENTRAL SHAFT OF THE SINKHOLE GRADUALLY UNDERMINES THE LAND SURFACE.



3. OVERLYING UNCONSOLIDATED SEDIMENTS SLOWLY SETTLE AND DEFORM IN RESPONSE TO THE UNDERMINING. THE RATE OF SETTLEMENT MAY BE INCHES (CM'S) PER YEAR.

E. GENERALIZED CONCEPTUAL CROSS-SECTION OF MATURE TOPOGRAPHY IN A MANTLED KARST



NOTE: FOR THE SAKE OF SIMPLICITY THE LIMESTONE SURFACE IS SHOWN TO BE SMOOTH AND REGULAR. HOWEVER, IN DETAIL IT IS WELL-KNOWN TO BE HIGHLY IRREGULAR, ON A SCALE OF FEET TO A FEW TENS OF FEET (A FEW TENTHS TO SEVERAL METERS).

PREPARED BY: PEL

P.E. LaMoreaux & Associates

All of the aforementioned processes have involved erosion at the limestone surface, through dissolution of the limestone and transportation of loose overburden sediment down through solution-widened channels. The solution process also continues deeper within the limestone, eventually forming a network of caves through which the groundwater flows to springs. The details of cave formation are complex and are not relevant to the present discussion¹. However, as caves within the limestone enlarge over time by dissolution, erosion, and collapse, they may reach a condition where only a thin roof of limestone remains between the cavernous passageway and the land surface. When this roof becomes too thin to support its own weight, and the weight of any load added to the land surface above, the roof may collapse into a gaping hole in the bedrock. The "pit" created by this process is also a sinkhole: a *cave-collapse sinkhole* (also, called a bedrock-collapse sinkhole; see Figure III-1.B). Although evidence of cavern collapse can be found, such events are extremely rare within the human time (Beck, 1991; Waltham, 1989; White, 1988; Williams and Vineyard, 1976; Newton 1976; Davies, 1951). Tharp and others (1985) presents an equation for the rate at which a cave void rises toward the surface by successive roof falls. For large cave passages spanning 100 feet, it takes around 2.8 million years for the void to rise 330 feet through rock layers that are 3 feet thick. In rock layers that are only 8 inches thick, the time required is around 100,000 years.

B. SINKHOLES ON THE MITCHELL PLAIN

The Mitchell Plain in Southern Indiana is the long-term product of karstic erosion (Palmer & Palmer, 1975). The northern portion of the Mitchell Plain was covered and modified by glacial debris, but the southern portion, in which the site is located, has developed primarily through karst processes. As noted in Section A.1 of Chapter II, the older literature on the Mitchell Plain generally assumes that the characteristic *terra rossa* soil is a residual product from the dissolution of the limestone, and that the topography developed as a subsoil karst. However, Hall (1976a) and Olson and others (1980) conducted detailed analyses and investigations of the sediment blanketing the plain and determined that it does not match the insoluble residue from the limestone and, moreover, that there is a greater thickness of sediment than could reasonably result from limestone dissolution. Olson and others (1980) suggest that these sediments were originally transported from the adjacent clastic uplands.

Sinkholes are ubiquitous on the Mitchell Plain. There are on the order of 100 per square mile shown on the standard U.S. Geological Survey topographic quadrangle maps, and the actual number in the field may be up to ten times greater. The largest and deepest of them are generally formed over major, active cave passages due to roof collapse (Palmer and Palmer, 1975). One of the rare examples of the formation of a cave-collapse sinkhole within historic time occurred at the Colglazier entrance to Blue Spring Cave, southwest of Bedford, Indiana. What had formerly been a shallow

¹ Generalized accounts may be found in Ford and Williams (1989), White (1988), Ford and Cullingford (1976), or Waltham (1974). A recent summary by Palmer (1991) is considerably more technical.

marshy depression grew into a cave-collapse sinkhole nearly 100,000 ft³ in volume, during a heavy rainstorm in 1941 (Rexroad, 1976). Although other cave-collapse sinkholes exist on the Mitchell Plain over large cave passages, the incidence of collapse within the human time frame is extremely rare, as documented in the previous section.

The vast majority of the sinkholes on the Mitchell Plain are solution sinkholes which are continuing to develop at the surface by erosion of the cover sediment. Surface drainage converges into sinkholes, and all soil eroded from the land surface is transported into sinkholes, except near the few entrenched streams. This sediment is transported down the central drainage shaft into deeper cavernous conduits where it may be removed by the turbulent flow of groundwater. The erosion process within the surficial sinkhole is a balance between sediment delivery from the entire catchment area of the sinkhole and removal of this sediment by subterranean cavernous flow. If delivery of sediment exceeds the rate of removal, then the sinkhole will fill in for a period of time, and a lake or pond may form. If the rate of removal exceeds the rate of delivery, the sinkhole depth increases until the limestone shaft is exposed at its base (Hansel, 1983).

The process of sediment erosion down the central solution pipe, or shaft, of the sinkhole is often sporadic. The bottom may be plugged and covered for a number of years, only to suddenly open in a rapid episode of collapse. Such cover-collapse sinkholes are normally smaller than the broad surficial depressions which are shown on topographic maps, and are, in fact, one episode in the long-term evolution of these larger basins. In other karst areas, external geomorphic processes may have covered the sinkhole topography with more sediment than karstic erosion can remove quickly. Such is the case in Florida where marine sediments mantle the limestone (Beck, 1988b) and in the northern portion of the Mitchell Plain where glacial debris covers the karst (Hansel, 1983). As the karst terrane is slowly exhumed from this covered condition by internal erosion, sinkholes may suddenly collapse beneath flat ground. In such cases cover-collapse sinkholes can occur unexpected and be extremely hazardous. However, the present topography of the southern Mitchell Plain has developed in response to karstic erosion, and **almost all recent cover-collapse sinkholes have developed at the drainage point of an existing surface depression** (Powell, 1997; Frushour, 1997).

An exception to this generalization occurs where the landscape has been artificially filled and leveled. In such areas karstic erosion continues beneath the ground surface, and the end result may be a cover-collapse sinkhole, as shown in Figure III-1.C. Fortunately, in the southern Mitchell Plain most of these instances occur on agricultural land, although a few may occur beneath roadways or other engineered structures.

In summary, sinkholes form in two ways on the southern Mitchell Plain. The larger and deeper sinkholes, which are located over major, actively enlarging cave passages, result from catastrophic cave-roof collapse. Such events are extremely rare within the human time frame. The second way results from limestone dissolution and erosion of

the cover sediment downward into cavernous conduits. The majority of the sinkholes on the Mitchell Plain form in this manner. If the sinkhole drainage shaft is open, this erosion process may occur continuously. Or, erosion may occur as sporadic surface collapses within the larger sinkhole basin if the shaft is temporarily plugged and the sinkhole is filled. However, on the southern Mitchell Plain these smaller cover-collapse sinkholes almost always occur over the drainage point of mature sinkhole basins, except where the land has been artificially leveled and covered.

C. SINKHOLES IN THE SITE AREA

Sinkholes are numerous on the plain surrounding the small valley of Rock Lick Branch. Sinkholes also occur on the valley slope, but they are much smaller than those on the upland. On the site map (Figure I-1), several sinkholes (designated A-G) can be seen in the surrounding area. The site boundary was selected to avoid the sinkholes.

Sinkholes A, B, C, D, and E are located on the valley slope, generally northwest of the site. None of these sinkholes show any evidence of being formed by cave-roof collapse. Sinkholes A, B, C, and E all capture surface drainage and transmit it underground to a series of small springs along Rock Lick Branch (see Chapter IV.). All have small openings into which the water flows. When first examined the bottom of Sinkhole D was choked with debris and sediment, and there was no outlet visible. For the purpose of dye introduction, a trench was excavated with a backhoe. The trench intercepted a natural soil cavity which readily accepted all the water which was introduced (see Chapter IV).

Sinkhole F is larger than the aforementioned depressions and is located immediately east of the site on the upland. A small drainage channel crosses the broad bottom of this sinkhole and sinks into an open hole near the southern slope. There is no evidence of cave collapse. Sinkhole G is south of the site. The closed depression on the site map is one third of what was formerly a larger sinkhole, as can be seen on the U.S. Geological Survey topographic map of the Mitchell Quadrangle. However, the construction of 840 South Road bisected this sinkhole, and it is probable that the filling for the road base covered the original drain. At present water ponds in sinkhole G and slowly drains by seeping into the soil. There is a potential for long-term karstic erosion to undermine the road and cause eventual damage, but this is not relevant to the site.

D. FRAMEWORK FOR EVALUATING SINKHOLE COLLAPSE RISK

In order to evaluate the potential risk of sinkhole collapse at a site, it is first necessary to understand the mechanisms of sinkhole development which are applicable to that site. The mechanisms of sinkhole collapse which are applicable to the southern Mitchell Plain are explained in Sections A and B of this chapter. The larger and deeper sinkholes on the Mitchell Plain form by cave-roof collapse over major, active caves with passages large enough to create a significant span of unsupported limestone and with

P.E. LaMoreaux & Associates

sufficient flow of water to prevent plugging by sediment and breakdown (ceiling collapse blocks).

As previously documented, noted sinkhole authorities agree that the incidence of cave-roof collapse is extremely rare within the human time frame (Beck, 1991; Waltham, 1989; White, 1988; Williams and Vineyard, 1976; Newton 1976; Davies, 1951). On that basis alone, the risk of cave-roof collapse beneath this small site is negligible. To further minimize this risk, essentially to zero, it is necessary to determine whether "major, active cave passages" exist beneath the site. In order to determine if such passages may occur, the karstic characteristics and the hydrogeology of the site were studied by field investigations, groundwater tracing, and geophysical surveys. After the investigations and results of each of these techniques are documented and explained, the implications for sinkhole collapse will be discussed.

The majority of the sinkholes on the southern Mitchell Plain are forming by a combination of limestone solution and cover sediment erosion. The cover-collapse process is part of this sinkhole evolution, and cover-collapse sinkholes develop over the drainage conduits of existing sinkhole basins. Where pre-existing sinkhole basins have been filled and leveled, cover-collapse sinkholes may develop unexpectedly over the buried sinkhole. However, on the southern Mitchell Plain, instances of naturally buried sinkholes are rare. Filling and leveling of sinkholes occurs primarily through agricultural practices and during construction activities, such as road building.

Therefore, there is only a significant risk of a cover collapse in the bottom of an existing sinkhole basin which is plugged, or in the unlikely instance where a pre-existing sinkhole drainage shaft is covered and has no present surface expression. No sinkholes are apparent within the boundaries of the site. The site was graded circa 1995 to remove clay for use elsewhere on the property, and this could have obscured the topographic indications of any sinkhole that may have been present. However, Tom Kessler, a Lehigh Geologist, conducted investigations on the site prior to the excavation of the clay. He states, "There were no closed depressions, no sinkholes, no breaks in the soil cover that would indicate the presence of a drainage conduit" (Kessler, 1997). An aerial photograph of the site taken on January 9, 1994, prior to the excavation, shows no evidence of sinkholes (Kessler, 1997). In view of the absence of any surface expression of a sinkhole basin, the risk of a cover-collapse developing is negligible. However, in order to investigate the possible existence of drainage basins and shafts in the limestone beneath the unconsolidated cover, two complimentary geophysical investigations of the site have been undertaken. The results and implications of those investigations are discussed in Chapter V.

Furthermore, there is an additional prerequisite for a cover-collapse sinkhole to form. To make room for continued collapse, flowing groundwater must remove the unconsolidated sediment which was previously eroded underground as the surface depression developed, along with any rock debris due to cave breakdown. That is,

cavernous passages draining the area must be characterized by a turbulent flow of groundwater of a volume significant enough to transport the previously collapsed sediment and rock debris (Paimmer and Palmer, 1975). It is obvious from the characteristics of the local spring flow that the groundwater conduits draining this area could only remove such debris extremely slowly. This is an additional reason why the probability of sinkhole collapse beneath this site is negligible.

P.E. LaMoreaux & Associates

IV. EXPLORATORY DRILLING

Because the bedrock at the site is mantled by up to 30 feet of clay, exploratory borings were drilled to permit direct examination of the limestone. The borings were necessary to assess the nature of the weathered zone at the top of the limestone (the epikarstic zone) and to evaluate how extensively the rock is fractured. Moreover, data on the configuration of the bedrock surface is necessary to interpret the results of geophysical investigations of the site (see Chapter 5). The information obtained from exploratory drilling is directly relevant to evaluating the risk of sinkhole collapse or subsidence at the site and to determine what can be done to minimize any potential hazards. The data collected from exploratory drilling will also be useful for designing a groundwater monitoring system. Moreover, Indiana regulations for a Type III Waste Disposal Facility specifically require at least one boring twenty feet into bedrock (329 IAC 10-32).

During 1997 four exploratory boreholes were drilled to obtain detailed information on the geology underlying the site. The locations are shown on Figure II-6. Drilling was performed by Earth Exploration, Inc., of Indianapolis. These holes were sampled continuously by split spoon in advance of 8.25-inch hollow-stem-auger drilling through the overburden and by NX wireline core in the solid rock. A PELA geologist was on site describing the samples and cores as they were obtained. Water levels were measured 24 hours after drilling was completed, with the exception of the last well drilled, BH-3, in which the water level was measured immediately after drilling. The samples and cores are stored at Lehigh's facility in Mitchell.

The generalized lithologic logs of the wells are shown in a cross-section of the site in Figure IV-1. The detailed logs and descriptions of each well are included in Appendix G. It was not possible to correlate the 1997 cores with the 1960-61 exploratory drilling information compiled by Lehigh's geologist, Tom Kessler (see Section B of Chapter II and Figure II-8). The lithology and texture of the 1997 cores were described in detail; but field information on the dolomite content of the rock was obtained by acid testing, which only differentiates nearly pure dolomites from other varieties of calcium-magnesium carbonate. The 1960-61 Lehigh data included precise $MgCO_3$ and $CaCO_3$ content, but no lithologic descriptions. Thus, there was no common criterion by which the data could be combined.

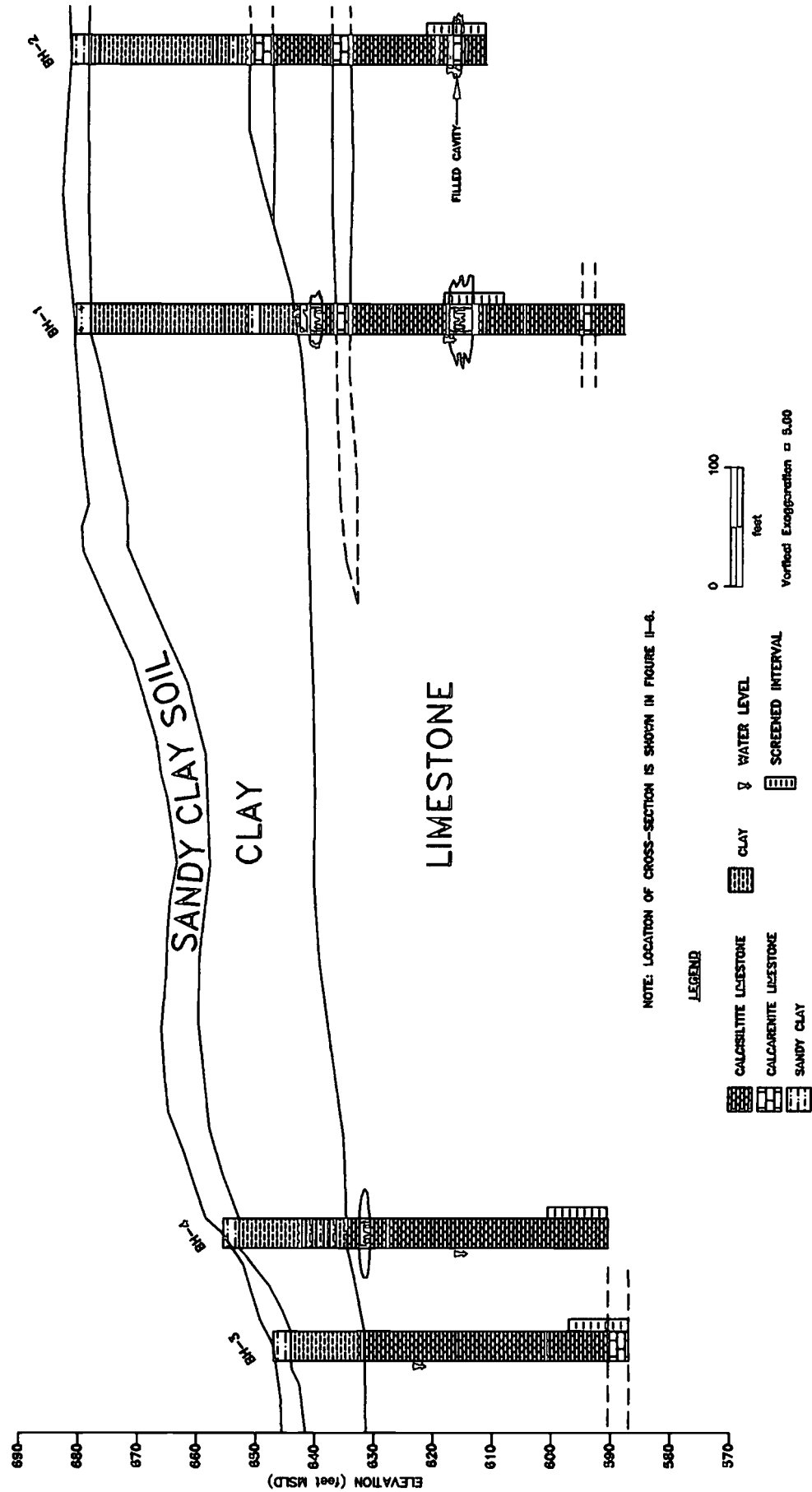
The depth to limestone ranged from 15 to 39 feet in the four exploratory boreholes drilled in 1997. Several small cavities were encountered in the limestone, both open and sediment-filled, as is typical of karst terrane. Well BH-1 penetrated a small cave 4 feet tall, approximately 63 feet below the ground surface; the groundwater level was near the top of this cavity.

P.E. LaMoreaux & Associates

FIGURE IV-1 WSW-ENE Cross Section Through the Site Based on 1997 Exploratory Borings

WSW

ENE



FILE NO. XSEC-881
DRAWN BY FOL

V. GEOPHYSICAL INVESTIGATIONS

Two geophysical investigations have been conducted to evaluate the risk of sinkhole collapse or subsidence at the site. Both geophysical surveys were conducted on a grid established by Lehigh during a soil-boring program conducted in 1994. The natural (electrical) potential (NP) method was used to detect subsurface areas of localized groundwater recharge, which can result in subterranean soil erosion. Electrical resistivity tomography was used to identify depressions in the limestone surface, which can indicate the existence of enlarged channels in the bedrock. The coincidence of localized groundwater recharge and bedrock channels capable of transmitting water and soil into the underlying karst aquifer could indicate a potential location for the development of a cover-collapse sinkhole.

A. NATURAL POTENTIAL (NP) SURVEY

The NP technique was used to detect subsurface areas of localized groundwater recharge, which can result in subterranean soil erosion. Localized groundwater recharge and associated soil erosion have the potential to contribute to the development of cover-collapse sinkholes.

1. INTRODUCTION TO THE NATURAL POTENTIAL (NP) TECHNIQUE

The NP method—also known as self potential, spontaneous potential, streaming potential, and SP—involves the measurement at the ground surface of the naturally occurring voltage resulting from ambient electrical currents which occur everywhere within the earth. These currents are caused by a variety of discrete physical phenomena acting underground, including (a) redox reactions around metallic conductors intersecting the saturated zone; (b) fluid diffusion across soil and lithologic contacts; (c) subterranean chemical and temperature gradients; and (d) the streaming potential gradient resulting from water flowing through pores, fractures and caverns in the ground; i.e., the electrokinetic effect (Kilty and Lange, 1991).

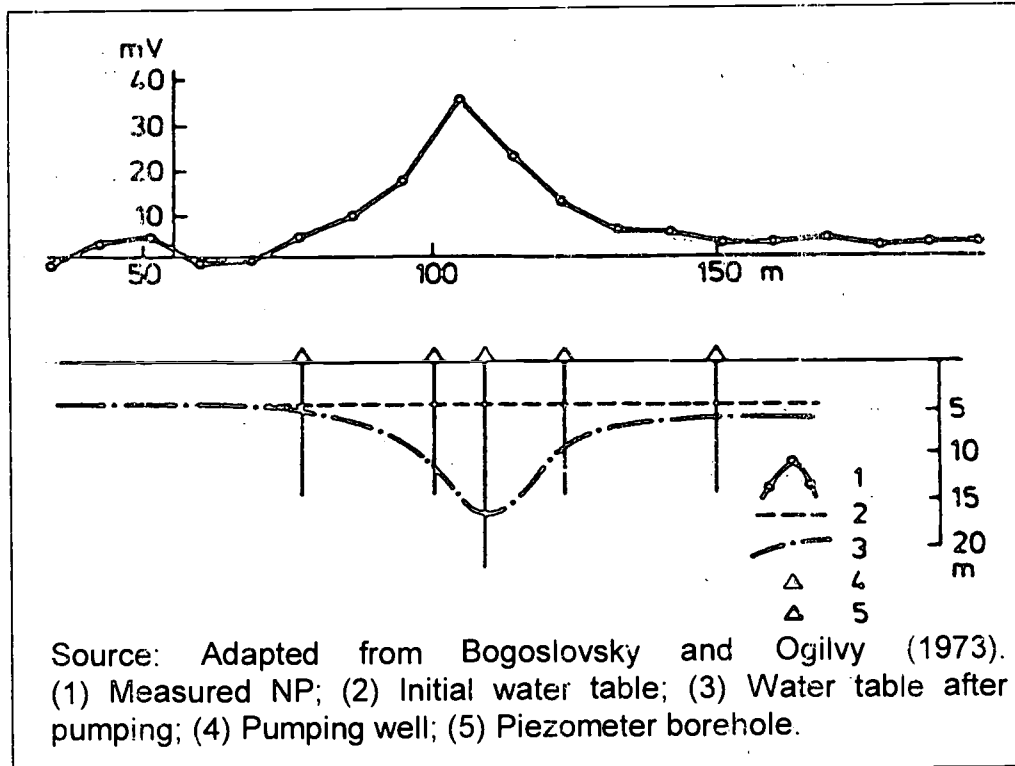
Unlike mining geophysics and oil-well logging where the mineralization potentials and diffusion/membrane potentials are measured, the streaming potential is of primary interest when making engineering and hydrogeologic applications (Ernstson and Scherer, 1986). Cooper and others (1982) report that NP values measured within the same geologic setting result mainly from the streaming potential. Corwin and Hoover (1979) have demonstrated that NP anomalies generated by the streaming potential are larger in amplitude than those generated by other mechanisms.

Theoretically, when water moves through a saturated capillary system by laminar flow, the NP gradient is the product of the water pressure gradient and a coupling constant, known as Helmholtz relation (Aubert and Atangana, 1996). The potential gradient is the result of the electrofiltration process, wherein the natural potential increases positively in the direction of flow. This theory has been proven by laboratory experiments in

—P.E. LaMoreaux & Associates—

which the NP acquired through flow of water in porous material is linearly proportional to Darcian velocity over a broad range of pressure gradients and fluid compositions (Bogoslovsky and Ogilvy, 1972). Field measurement has also revealed a positive NP anomaly that mirrored the groundwater depression cone surrounding a pumping well, as shown in Figure V-1 (Bogoslovsky and Ogilvy, 1973).

FIGURE V-1 Natural Potential Response to Groundwater Pumping



A proportional relationship between NP and the pressure gradient has also been affirmed for fracture flow conditions by studies conducted with channel flow models (Ahmad, 1964). NP values were found to decrease with the width of fissures, but introduction of sand into the fractures could considerably increase the NP values. In a field investigation, Ogilvy and others (1969) observed a NP gradient corresponding to the groundwater flow through fractures. In a study of the application of NP to karst aquifers, Erchul and Slifer (1987) demonstrated that NP anomalies can be detected and monitored in and around sinkholes and appear to indicate areas of groundwater seepage and preferential movement. The magnitudes of NP anomalies and NP change over time are related to the rate of water flow into the sinkhole. Lange and Kilty (1991) and Lange and Barner (1995) provide field evidence that various NP anomalies are associated with groundwater infiltration into cave systems and groundwater flow in karst conduits.

Understanding the basic relationship between NP and groundwater flow through fractures and conduits is critical to distinguish among different types of groundwater

flow regimes in karst systems. For example, there is a fundamental distinction between the lateral flow of groundwater in bedrock fractures and the vertical flow of water infiltrating into and percolating through the overburden. With respect to lateral flow, a potential gradient can develop along the flow path from a recharge area to a discharge area. The upgradient end of the channel can become negatively charged relative to the downgradient end. The typical potential distribution over a discharge point (such as a spring) is a positive anomaly transverse to the flow path. The typical potential distribution over a recharge point (such as a sinkhole or swallet) is a negative expression. Positive potential anomalies are expected over zones of groundwater discharge, whereas negative anomalies may indicate the presence of buried sinkholes or shafts where water is entering the bedrock. Ogilvy (1967) states that the most meaningful NP results could be obtained in karst regions where considerable quantities of water flow into sinkholes (Erchul and Slifer, 1987).

Because localized groundwater recharge and associated soil erosion are important factors in the development of cover-collapse sinkholes (Beck, 1988a), identification of subsurface recharge zones is critical in evaluating the suitability of the site for CKD disposal. The NP technique was used during this investigation to identify any areas of concentrated recharge which may exist at the site.

2. NATURAL POTENTIAL (NP) DATA ACQUISITION

The NP survey was conducted January 7 through January 8, 1997 and March 4 through March 8, 1997. Voltage measurements were made along the ground surface using the voltage averaging mode of a Fluke 87™ multimeter with an input impedance of 10 megohms. The reference and roving probes (3 and 1.25 inches, respectively) were Gisco™ non-polarizing, copper/copper-sulfate, porous-ceramic electrodes. The multimeter was connected to the reference electrode by an 1,800-foot-long, 18-gauge military communication wire, which is also used for induced polarization (IP) surveys.

Voltage measurements were made along forty-seven lines spaced 25 feet apart over an area of approximately 18.8 acres. The NP data-collection grid was established to coincide with the grid established by Lehigh during a soil-boring program conducted in 1994 (Kessler, 1994). Figure V-2 shows the locations of the lines, and Table V-1 lists their parameters. Each NP data point is described by a line number and a station number (distance along that line). Table V-2 shows the locations of the soil borings on the NP grid. Several of the NP lines traversed Sinkholes B and C. The length of the lines varies from 275 to 800 feet. NP measurements were made and recorded every 25 feet along each line. Minor spacing changes were made at locations that were inaccessible because of brush piles. Three base stations were established (Figure V-2) to provide efficient access to the entire site, including extensive areas which are heavily wooded. Base Station A was used for Lines 1 through 20; Base Station B was used for Lines 21 through 32; and Base Station C was used for Lines 33 through 46.

P.E. LaMoreaux & Associates

FIGURE V-2
NATURAL POTENTIAL
DATA COLLECTION GRID

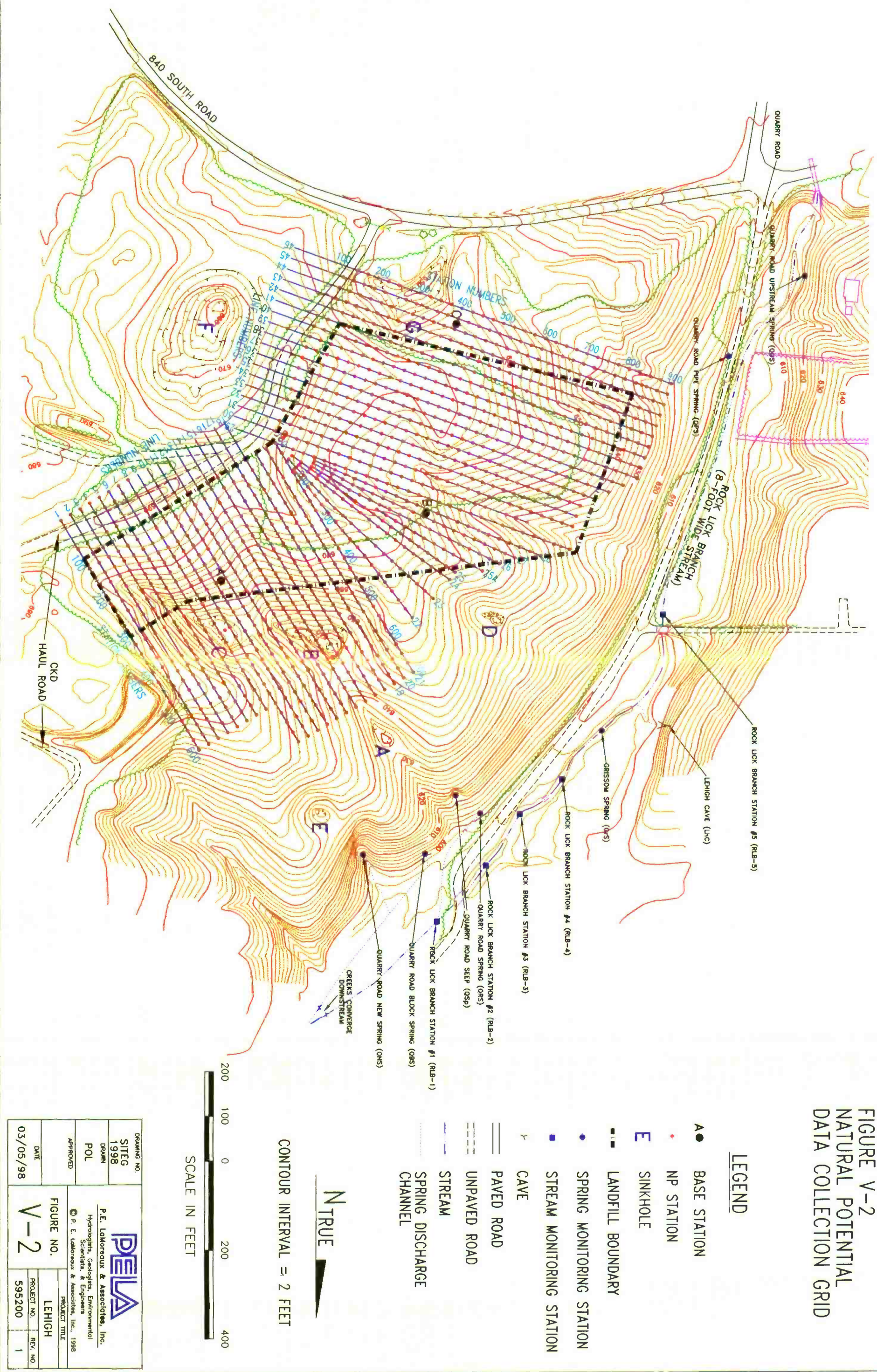


TABLE V-1 Natural Potential Survey Lines

LINE NO.	TOTAL LENGTH (feet)	DATA POINTS	BASE STATION	SURVEY DATE
1	600	23	A	01/07/97
2	600	23	A	01/07/97
3	600	21	A	01/07/97
4	600	22	A	01/07/97
5	600	24	A	01/07/97
6	600	23	A	01/07/97
7	600	22	A	01/08/97
8	600	23	A	01/08/97
9	600	25	A	01/08/97
10	600	25	A	01/08/97
11	600	25	A	01/08/97
12	600	25	A	01/08/97
13	600	25	A	01/08/97
14	600	26	A	03/04/97
15	600	25	A	03/04/97
16	600	25	A	03/04/97
17	600	25	A	03/04/97
18	600	25	A	03/04/97
19	600	25	A	03/04/97
20	600	25	A	03/04/97
21	600	25	B	03/05/97
22	425	18	B	03/05/97
23	450	19	B	03/05/97
24	425	18	B	03/05/97
25	450	19	B	03/05/97
25A	275	12	B	03/05/97
26	475	20	B	03/05/97
27	500	21	B	03/05/97
28	550	23	B	03/05/97
29	675	28	B	03/06/97
30	600	24	B	03/06/97
31	700	29	B	03/06/97
32	700	29	B	03/06/97
33	700	29	B	03/07/97
34	700	29	B	03/07/97
35	700	29	B	03/07/97
36	700	29	B	03/07/97
37	700	29	B	03/07/97
38	700	29	B	03/07/97
39	700	29	B	03/07/97
40	700	29	B	03/07/97
41	700	29	B	03/07/97
42	675	28	C	03/08/97
43	675	28	C	03/08/97
44	675	28	C	03/08/97
45	675	28	C	03/08/97
46	650	27	C	03/08/97

P.E. LaMoreaux & Associates

TABLE V-2 Locations of Soil Borings on the Natural Potential Grid

SOIL BORING	NP GRID		SOIL BORING	NP GRID	
	Line No.	Station No.		Line No.	Station No.
A1	41	100	D4	29	400
A2	41	200	DA3	24	300
A3	41	300	DA4	24	400
A4	41	400	DB2	21	200
A5	41	500	DB3	21	200
A6	41	600	DB4	21	200
A7	39	675	E1	17	100
B1	37	100	E2	17	200
B2	37	200	E3	17	300
B3	37	300	E4	17	400
B4	37	400	F1	13	100
B5	37	500	F2	13	200
B6	37	600	F3	13	300
C1	33	100	F4	13	400
C2	33	200	G1	9	100
C3	33	300	G2	9	200
C4	33	400	G3	9	300
D1	29	100	H1	5	100
D2	29	200	H2	5	200
D3	29	300			

Great care was taken to obtain reproducible and meaningful NP data. At each base station, the reference electrode was buried underground in a shaded location to minimize temperature and polarization effects. At each data-collection station, vegetation was cleared and the electrode was placed approximately 4 inches deep with the aid of a garden-variety bulb planter to ensure good contact with the soil. After the multimeter reading stabilized, the voltage averaging mode was activated, and the measurement was recorded. A duplicate reading was taken at each station to ensure that the measurement was representative of that location. If the difference between the two readings was less than 5 millivolts (mV), the readings were accepted and their average value was used to represent the NP reading at that station (Corwin and Hoover, 1979). If the difference between the two readings was more than 5 mV, additional measurements were made until two successive readings differed by less than 5 mV.

Readings were made at the base station (near the reference electrode) approximately every hour to record the temporal drift. In addition, base station readings were recorded before and after measuring each line. Sixty-two base station readings were recorded (Appendix C).

P.E. LaMoreaux & Associates

NP data were obtained at approximately 1,200 stations along a total survey length of about 6 miles. Data collected at each station includes line and station numbers, two voltage measurements, and time of measurement. These data and the difference and average for each measurement pair are presented in Appendix C.

3. NATURAL POTENTIAL (NP) DATA ANALYSIS AND RESULTS

In most cases where NP is applied to studies of karst groundwater flow in the United States, the data are analyzed on a transect-by-transect basis (e.g., Lange, and Quinlan, 1988; Lange and others, 1990; Lange and Kilty, 1991; Lange and Wiles, 1991; Lange and Barnèr, 1995). However, this investigation utilized a more advanced procedure in which data from the entire site area are contoured after correcting for the influence of topography.

a) Temporal Drift Correction

NP measurements are affected by numerous factors, such as telluric currents, stray currents, conductive mineral deposits, variations in soil moisture and chemistry, temperature changes, and polarization of the electrodes (Corwin and Hoover, 1979). These effects vary during the day and cause temporal drift. To eliminate the drift, additional measurements were made at the base station before, during, and after measuring each transect. Based on the assumption that the factors vary at each measurement station as they do at the base station, the temporal drift was approximated using the linear trend between successive base station readings.

Because three base stations were involved in the data collection, site data were also related to a common reference (Base Station A). All NP values were corrected for temporal drift by the following equation:

$$V_{cj} = V_j - [V_{pi} + (T_j - T_{pi})(V_{ni} - V_{pi})/(T_{ni} - T_{pi}) + V_0]$$

where V_{cj} is the drift-corrected NP value for the measured V_j at time T_j in line j ; V_0 is the reference NP value which is the first reading of Base Station A; V_{pi} and V_{ni} are the previous and subsequent readings at base station i at times T_{pi} and T_{ni} respectively.

The drift-corrected NP profiles for all survey lines are presented in Appendix D. Profiles are shown for Lines 9 and 41 in Figures V-3 and V-4, respectively. Line 9 is on the east side of the site and crosses Sinkhole C. Line 41 is on the south side and crosses a grassy field. For most of the lines, the NP profiles are similar to the one shown in Figure V-4, in which no obvious anomalies are observed. Slight NP anomalies (less than 5 mV) are observed on Line 9, as well as Lines 2, 3, 5, and 10. However, such small anomalies are considered to be attributable to interference (Corwin and Hoover, 1979).

FIGURE V-3 Drift-Corrected Natural Potential Profile for Line 9

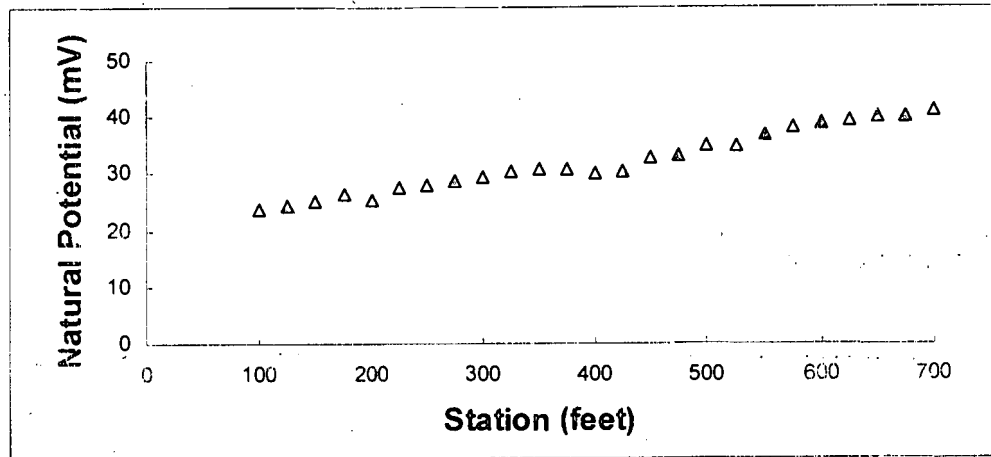
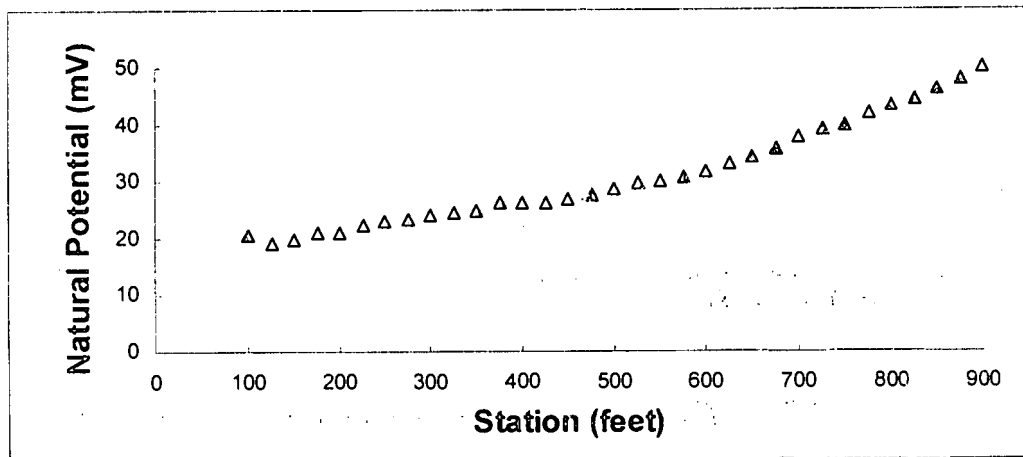


FIGURE V-4 Drift-Corrected Natural Potential Profile for Line 41



b) Topographic Correction

Although no substantial anomalies are evident on the drift-corrected NP profiles, they do reveal an electric field with increasing electrical potential in the downhill direction, as shown in Figures V-3 and V-4, as well as all profiles in Appendix D. This phenomenon is known as the topographic effect (Birch, 1993; Aubert and Atangana, 1996) and has been recognized by geophysics for more than 70 years (Ernstson and Scherer, 1986). The NP profiles also reveal that the topographic effect varies with time, but profiles in which the data were collected on the same day are similar. The time dependence of the topographic effect has been well demonstrated in controlled field experiments (Ernstson and Scherer, 1986). The topography-related potential may

P.E. LaMoreaux & Associates

overshadow anomalies caused by streaming potentials and other NP components of significance to hydrogeological studies (Corwin and Hoover, 1979). Therefore, the topographic effect was mathematically removed from this data.

The survey lines were grouped by date based on the assumption that ground conditions at the site did not change significantly during the course of a single day. For each daily group, two lines with no apparent anomalies were selected to determine the topographic effect. The drift-corrected NP values were plotted against their corresponding elevations, as shown in Figure V-5. The trend line for each group of data indicates that the relationship between NP and elevation is approximately linear. A linear correlation coefficient was calculated for each trend line. NP is inversely proportional to elevation at this site. A correction factor was obtained for each daily group. This topographic correction factor, K , is defined as the NP change per unit elevation increase—i.e., the slope of the linear trend line. The calculated results are summarized in Table V-3. The linear correlation coefficient ranges from 0.83 to 0.99 and averages 0.95. The topographic correction factor, K , varies from -0.38 to -0.75 mV/foot and averages -0.55. These correction factors are within the range reported by other investigators (Aubert and Atangana, 1996; Ernstson and Scherer, 1986).

FIGURE V-5 Drift-Corrected Natural Potential vs. Elevation

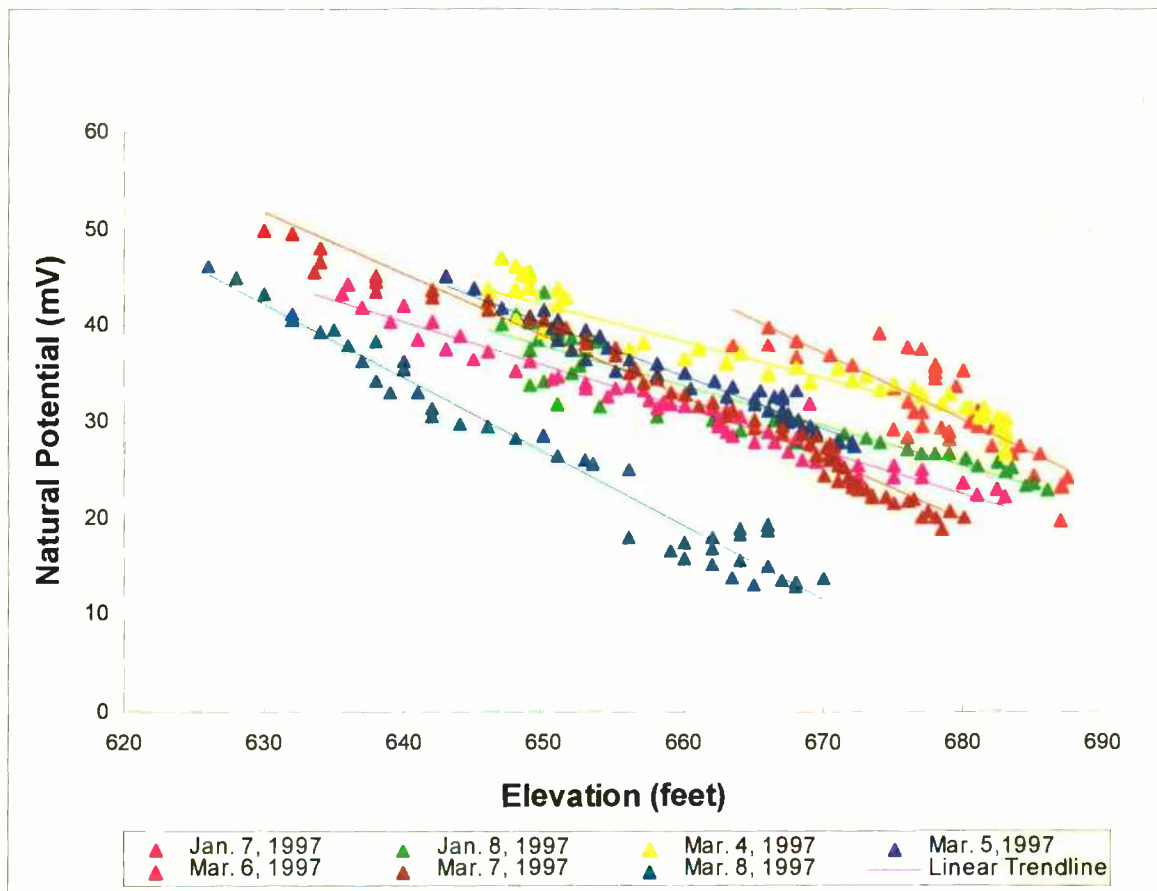


TABLE V-3 Natural Potential Topographic Effect

DATE	SELECTED LINES	CORRELATION COEFFICIENT	CORRECTION FACTOR (mV/foot)
01/07/97	Lines 2 and 3	0.83	-0.69
01/08/97	Lines 12 and 13	0.93	-0.42
03/04/97	Lines 18 and 19	0.95	-0.38
03/05/97	Lines 27 and 28	0.97	-0.55
03/06/97	Lines 31 and 32	0.98	-0.45
03/07/97	Lines 37 and 38	0.99	-0.62
03/08/97	Lines 42 and 43	0.98	-0.75
Average		0.95	-0.55

The drift-corrected NP data were further corrected by their corresponding topographic correction factors using an equation presented by Ernstson and Scherer (1986):

$$V_{cj}' = V_{cj} - K_j(h_j - h_{0j})$$

where V_{cj}' is the topography-corrected NP (also known as the residual NP); K_j is the topographic correction factor for line j ; h_j is the elevation of the station where V_j is measured; h_{0j} is the elevation of the first measurement on line j .

Each drift-corrected NP value consists of three basic components: topographic effect, residual NP, and noise. Using the terminology of Ernstson and Scherer (1986), the residual NP is the component of interest at this site—i.e., the NP response which may vary due to localized hydrogeologic conditions. The data collected on January 7, 1997 (e.g., Lines 2 and 3) exhibit a significantly lower correlation with elevation than the remainder of the data (Table V-3). It is possible that these data are primarily responsive to localized hydrogeologic conditions, although some of the response may be attributable to noise, as discussed in Section 4(a).

The residual NP profiles for all survey lines are presented in Appendix D. Lines 9 and 41 are shown as examples for typical NP profiles (Figures V-6 and V-7). An obvious 10-mV negative anomaly occurs on Line 9 at Station 400 (Figure V-6), which is located at the center of Sinkhole C. The anomaly is much more pronounced than it is in Figure V-3. Similar anomalies with magnitudes ranging from 5 to 20 mV exist at various stations on Lines 4, 5, 6, 7, 8, 10, 11, 12, 13, 14, 15, 16, 17, 18, 19, 42, 43, 44, 45, and 46. Each of these lines crosses or lies close to an off-site sinkhole.

Residual profiles for lines further from the sinkholes are generally similar to the one shown in Figure V-7. Comparison with Figure V-4 reveals that topographic correction removes the trend observed in the drift-corrected NP profiles. Some fluctuations are present, but they are too small to be considered hydrogeologically meaningful.

P.E. LaMoreaux & Associates

FIGURE V-6 Topography-Corrected Natural Potential Profile for Line 9

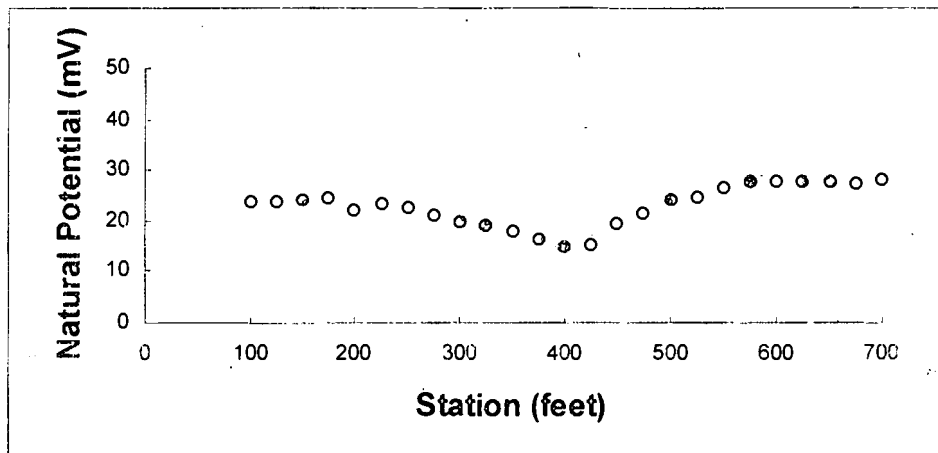


FIGURE V-7 Topography-Corrected Natural Potential Profile for Line 41

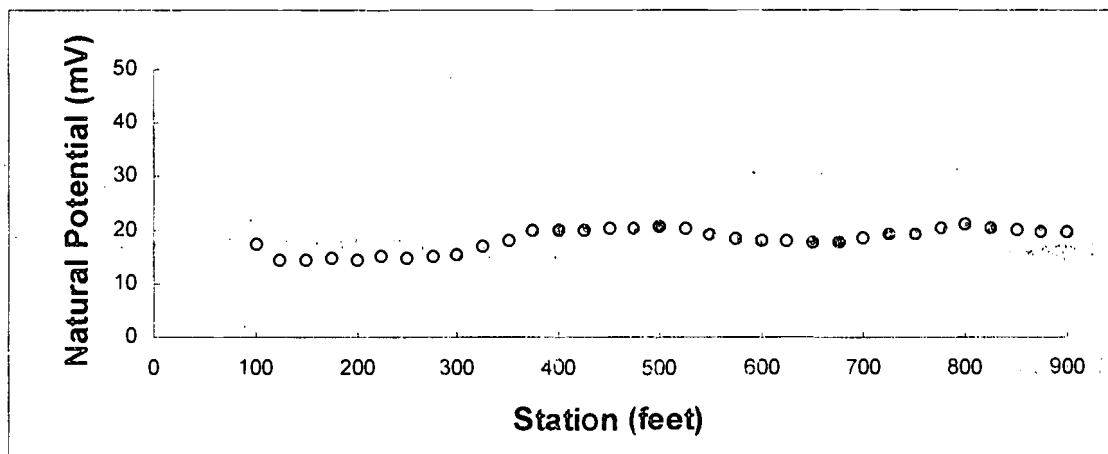
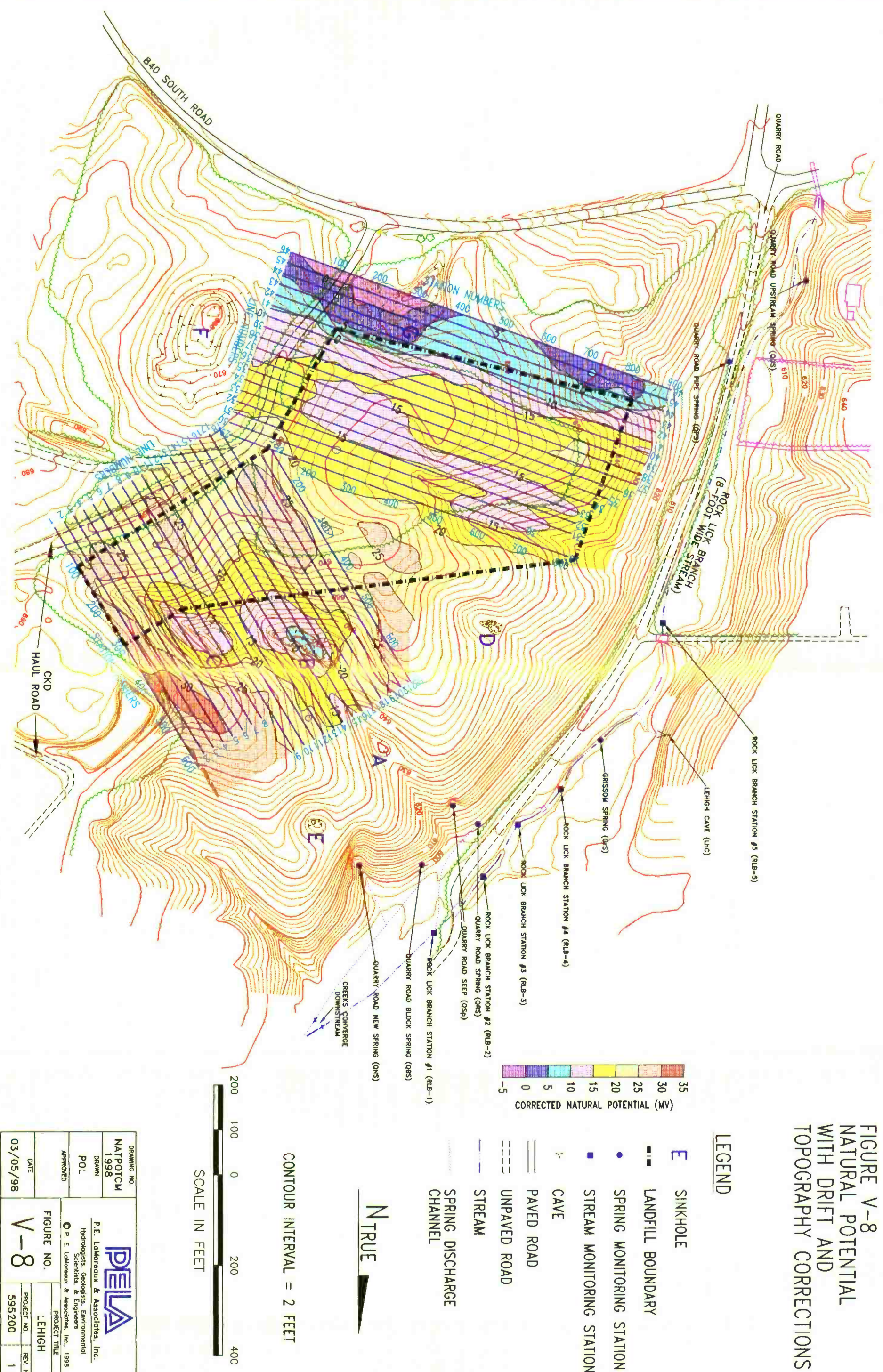


Figure V-8 shows the residual NP, plotted based on the average topographic correction factor and a reference elevation—the elevation of Station 100 on Line 1. Because the typical background geological noise level is approximately ± 5 to ± 10 mV (Corwin and Hoover, 1979), a 5-mV contour interval was selected. Anomalies defined by two contour lines are considered to be significant and possibly related to localized hydrogeologic conditions. Anomalies enclosed by only one contour line are considered to result from background noise (Corwin and Hoover, 1979).

FIGURE V-8
NATURAL POTENTIAL
WITH DRIFT AND
TOPOGRAPHY CORRECTIONS



Moreover, anomalies must be determined in a relative manner; they are not based on absolute NP values. Therefore, anomalies should be identified by comparing NP values only with those in the immediate vicinity (Figure V-8). In general, the topography-corrected NP values are higher and vary over a wider range on the north side of the site (Lines 1 through 21) than those on the south side (Lines 29 through 46). The NP values range from 5 to 35 mV on the north side, while they range from -5 to 20 mV on the south side.

Two negative anomalies are observed on the north side of the site. They are associated with Sinkholes B and C, and their magnitudes are greater than 5 mV. The anomalies are not centered exactly on the respective sinkholes, but they are within 50 feet of the center. On the south side, a negative NP anomaly appears to be associated with Sinkhole G. The contour lines are not enclosed because the anomaly lies near the NP-survey boundary.

Additional small anomalies exist at the site. However, each is less than the 5 mV level attributable to background noise. One is a negative anomaly on the south side of the site, which is enclosed only by the 15-mV contour line. Several positive anomalies are also observed at the site, each of which is enclosed by only one contour line.

4. INTERPRETATION AND DISCUSSION

a) Sources of Interference

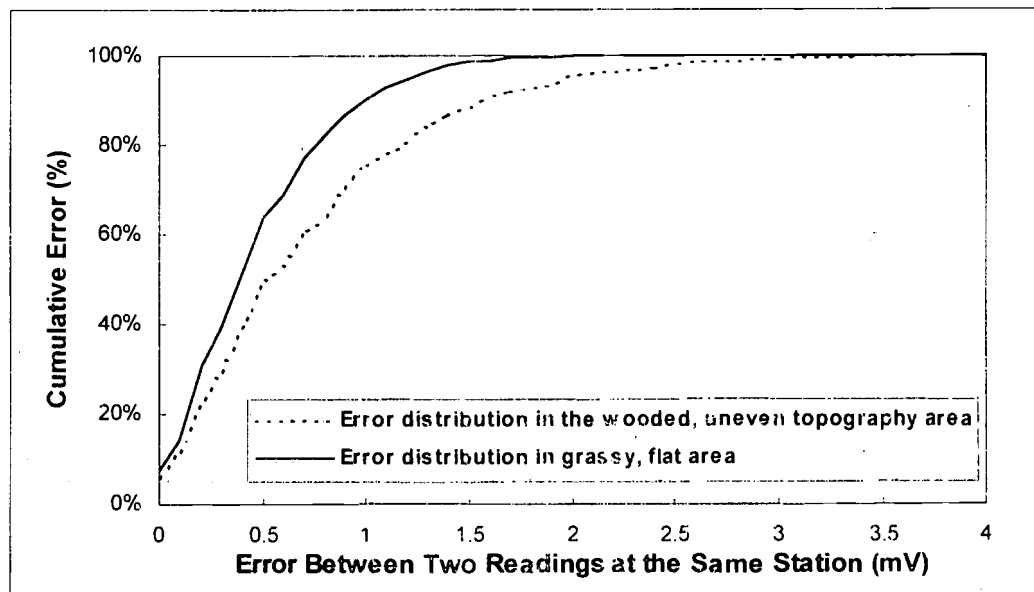
NP surveys may be impacted by various sources of interference. Telluric currents generated by temporary variations in Earth's magnetic field may sometimes affect NP measurements. Disregarding rare magnetic storms, the electric field may vary several mV per mile. During this investigation, closely spaced measurements and short profiles were used to minimize the influence of such currents (Ernstson and Scherer, 1986).

Electrical resistivity of the ground is another important factor affecting NP measurements. Field data has indicated that variation in topography and vegetation may distort the patterns of current flow. On the east side of the site where dense woods and uneven topography are present (Lines 1 through 21), the noise level is apparently higher than in the flat, grassy area (Lines 22 through 41), as shown in Figure V-9. The maximum error (difference between duplicate measurements at a station) in the uneven, wooded area is 3.4 mV with 90 percent of the errors less than 1.6 mV. The maximum error in the grassy area is only 2.2 mV, with 90 percent of the errors less than 1 mV. The greater apparent noise in the wooded area may contribute to the relatively low linear correlation between drift-corrected NP and elevation for the data collected on January 7, 1997.

Temporal drift in the NP response is caused by temperature changes in the electrodes, as well as temperature, moisture, and chemical fluctuations in the soil. Temporal drift was corrected by assuming that the temperature was constant at the buried reference electrode and that the temporal drift at the base station was representative of the whole

P.E. LaMoreaux & Associates

FIGURE V-9 Natural Potential Noise Levels at the Site



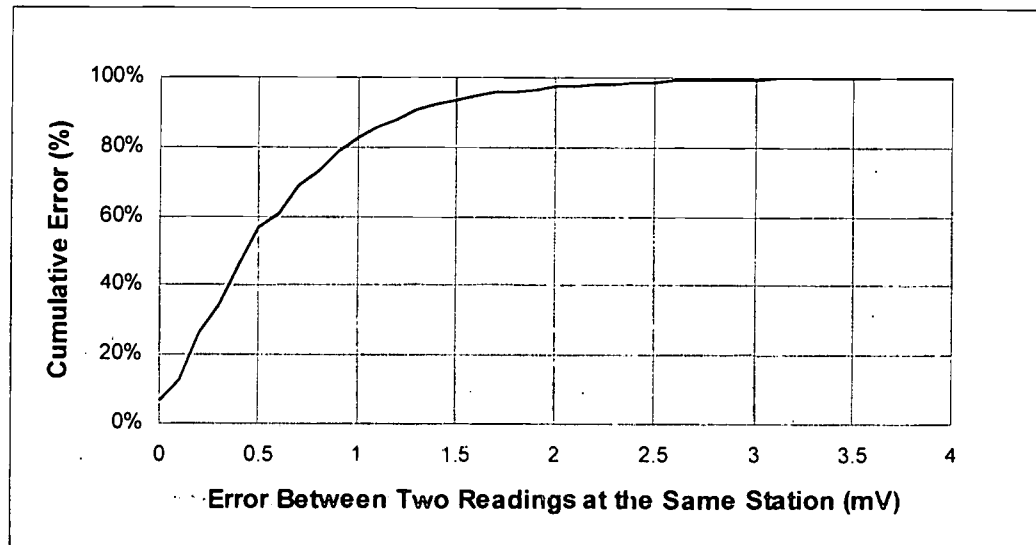
site. Careful field observations were made within the survey area to locate buried metallic debris which may cause interference and misinterpretation of NP signals.

As a result of precautionary efforts to minimize the noise level, the NP data collected during this investigation are considered reliable. Figure V-10 shows the cumulative error distribution for all of the NP measurements. The maximum error is only 3.4 mV, with 90 percent of the measurements having an error less than 1.3 mV.

b) Topographic Effect—Streaming Potential from Lateral Groundwater Flow

Many previous investigations have demonstrated the existence of the linear topographic effect (Corwin and Hoover, 1979), but the phenomenon has not been explained clearly. The role of thermoelectric effects and a hypothetical "vertical telluric current" have been much disputed. In recent years, however, it has become more widely accepted that the observed phenomenon results from streaming potentials induced by groundwater activity. Controlled field experiments have clearly demonstrated a correlation between precipitation and NP, although there was a one-month delay in the NP response (Ernstson and Scherer, 1986). This one-month time lag excludes surface runoff as a cause for the phenomenon.

A streaming potential mechanism also provides a reasonable explanation for the correlation of NP with elevation observed during this study. Rock Lick Branch has an elevation of about 605 feet adjacent to the site. The water level in four on-site

FIGURE V-10 Cumulative Error Distribution for Natural Potential

exploratory boreholes ranged from 617 to 622 feet. This suggests that groundwater beneath the site is discharged along Rock Lick Branch. Although the exact flow pathways cannot be determined, groundwater tracing has verified that site groundwater does indeed discharge to Rock Lick Branch. As groundwater flows from recharge areas to discharge areas along the stream, potential gradients develop along the flow paths. Therefore, the observed linear correlation between NP and elevation is to be expected. Because the lateral groundwater flow is regional in scale, the resulting streaming potentials are also regional in nature. The time-dependence of the topographic effect results from the dynamic characteristics of groundwater flow.

Based on the data collected during this investigation, the streaming potential explanation for the topographic effect is valid for this site. NP is generated by numerous mechanisms, and streaming potential is only one of them. In other areas, similar linear trends have been attributed to cathodic protection of pipelines (Lange and Kilty, 1991). However, no evidence was found for this form of interference at the Lehigh site. Streaming potential caused by flowing groundwater appears to be the primary component of the NP at this site.

c) Residual NP—Streaming Potential from Vertical Groundwater Recharge

After correcting for temporal drift and the effects of topography (lateral groundwater flow), the NP data represent the effects of localized streaming potentials. Negative anomalies exist on some individual transects (Appendix D) and on the NP map (Figure V-8). According to Ernstson and Scherer (1986), groundwater infiltration in carbonate rock can cause such anomalies, and their polarity is dependent on the pH of

the water. They suggest that infiltration of neutral water (pH of 7) causes a negative anomaly, although they did not actually confirm this. Negative anomalies have been observed in the field in areas of active infiltration (Lange and Kilty, 1991; Ishido and Mizutani, 1981). Because groundwater in uncontaminated limestone aquifers has a pH of about 7, it is possible that the negative anomalies at the site are caused by vertical groundwater infiltration.

Exploratory boreholes BH-1 and BH-2 (Figure II-6) have revealed the presence of groundwater in the limestone on the east side of the site, and groundwater tracing has demonstrated that Rock Lick Branch is the local discharge zone for this water (Chapter VI). The groundwater level at Sinkholes B and C is presumably between 605 feet (Rock Lick Branch) and 617 feet (BH-1 and BH-2), which is below the elevation of the bottom of the deeper sinkhole (Sinkhole C). Therefore, vertical infiltration from this sinkhole appears to take place in the epikarstic zone.

Because the magnitudes of the negative anomalies are directly proportional to the infiltration rate (Erchul and Slifer, 1987), the greatest infiltration appears to occur at Station 350 on Line 6; Station 375 on Line 7; Station 425 on Line 8; and Stations 400-425 on Line 9. The NP map in Figure V-8 indicates that the greatest groundwater recharge coincides with Sinkholes B and C. This is not surprising since sinkholes generally function as discrete groundwater recharge sites in karst areas. However, this association verifies the applicability of the NP technique for identifying vertical recharge zones at the site. It should be noted that the term "vertical flow" is an oversimplification of the actual flow patterns in the epikarstic zone. In this context, vertical flow refers to the infiltration and percolation of soil water into fractures in the underlying limestone—flow that is dominated by the vertical component.

There is only one negative anomaly within the footprint of the site. It is a low-magnitude anomaly, covering a broad area between Lines 29 and 37 and Stations 125 and 800. Because its magnitude is less than 5 mV, it may be caused by background noise (Corwin and Hoover, 1979), although it could be a response to vertical groundwater recharge in the epikarstic zone. Its magnitude is lower and it is much less concentrated than the anomalies associated with Sinkholes B and C, therefore any groundwater recharge associated with this anomaly must be smaller and much more diffuse.

It should be noted that the presence of concentrated groundwater recharge zones identified by an NP survey would not necessarily indicate a sinkhole collapse risk. Collapses are only likely to occur where groundwater recharge occurs through an open fracture or conduit in the limestone, wide enough to permit the downward transport of soil particles. Such features are usually associated with a depression in the limestone surface. An NP survey might also identify areas where water is moving vertically through narrow fractures. However, ground collapses are extremely rare in these cases because there is no mechanism for removal of the overburden material. Therefore, an independent geophysical survey was conducted, using electrical

P.E. LaMoreaux & Associates—

resistivity tomography to search for depressions in the limestone surface (see Section B).

The only negative NP anomaly detected within the site boundary is low in magnitude (less than 5 mV) and may be partially attributable to background noise and/or diffuse groundwater recharge. By itself, it is certainly not an indication of a sinkhole-collapse risk.

B. ELECTRICAL RESISTIVITY TOMOGRAPHY

Electrical resistivity tomography was used to identify depressions in the limestone surface, which can indicate the existence of enlarged channels in the bedrock. If the channels draining a depression in the limestone surface are capable of transmitting water and soil particles into the underlying karst aquifer, there is a potential for the development of a cover-collapse sinkhole.

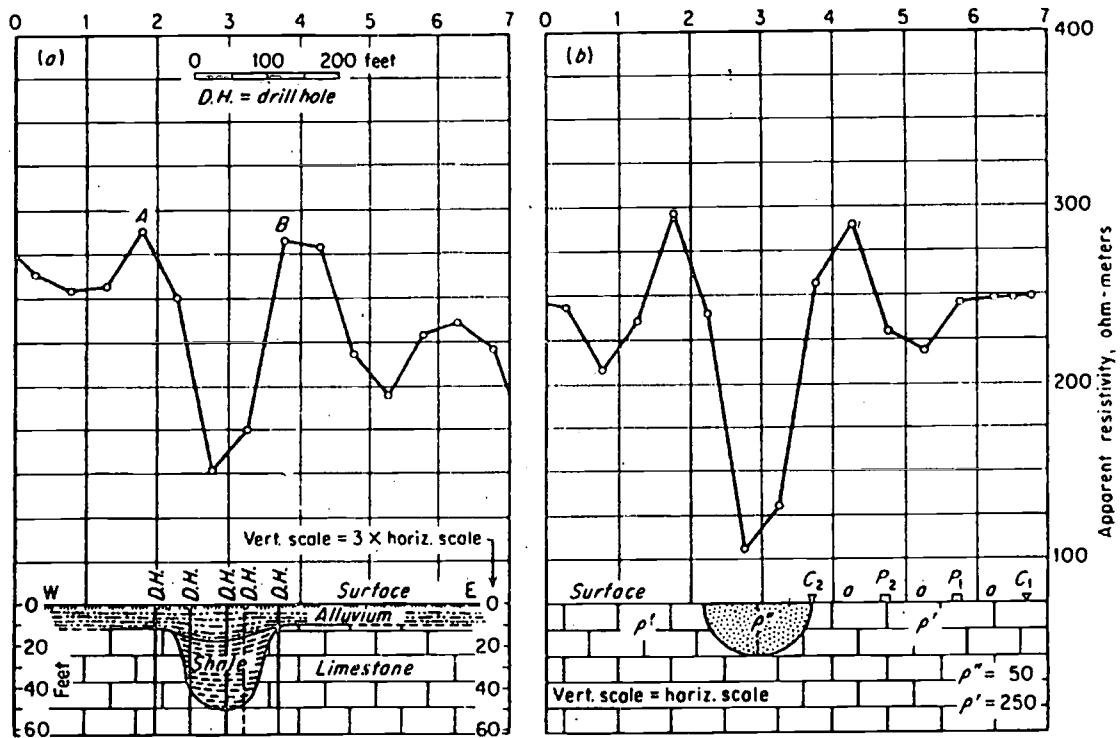
1. INTRODUCTION TO ELECTRICAL RESISTIVITY TOMOGRAPHY

Electrical resistivity methods involve the measurement of variations in the electrical resistivity of geologic materials and the interpretation of subsurface geologic conditions based on the measured electrical properties. Resistivity surveys are most applicable at sites with a large resistivity contrast among the various geologic materials. Because the resistivity values of clay and limestone are generally very different, resistivity methods may be the most frequently used (and most successful) geophysical techniques for site investigations in karst areas (Franklin and others, 1981).

Soil borings and exploratory boreholes have shown that the lithology at the site consists generally of brown/red clay and limestone bedrock (Kessler, 1994). The resistivity of this type of clay is normally less than 100 ohm-meters. The limestone is primarily calcisiltite and calcarenite, which generally has a resistivity over 1,000 ohm-meters. This high resistivity contrast is ideal for using electrical resistivity techniques to characterize the limestone/clay contact. Any depressions in the bedrock surface should produce negative anomalies similar to the one shown in Figure V-11, which results from the presence of a shale-filled sinkhole. In that case, a theoretical calculation indicated that the resistivity contrast between the shale and the limestone was only one to five (Cook and Van Nostrand, 1954). That survey was conducted by traditional horizontal profiling, which is labor intensive, time consuming, and generally cost prohibitive for covering large areas.

Electrical resistivity tomography is a relatively new version of traditional electrical methods. It was developed for the investigation of areas with complex geology where the use of traditional resistivity methods is difficult. In geological applications, tomographic surveys normally employ arrays of electrodes on the ground surface. Data is collected in a series of traverses in which the electrode separation is constant for each traverse and increases with each successive traverse. Modern computerized

FIGURE V-11 Resistivity Anomaly Caused by a Shale-Filled Sinkhole



Source: Adapted from Cook and Van Nostrand (1954).

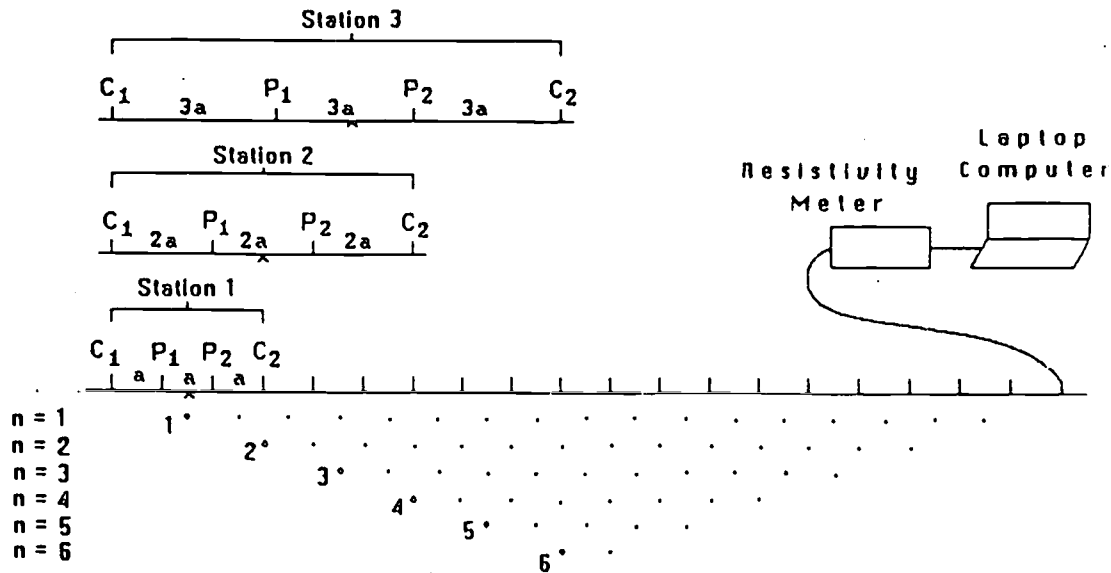
Commonly used resistivity configurations include the following arrays: Wenner, Schlumberger, pole-dipole, and dipole-dipole. Figure V-12 shows the typical measurement sequence for the Wenner array. The dipole-dipole array was used during the current investigation.

instrumentation permits automatic selection of three or four electrodes from the array to be used for each measurement. This facilitates the collection of multiple data points within a relatively short period of time.

Larger electrode spacing provides data from greater depths. The measured resistivities ("apparent resistivities") are commonly presented in a vertical cross section known as a pseudosection. The unit electrode spacing is determined by the length of the profile, the desired depth of penetration, and the required resolution.

The apparent resistivity is affected by all the geologic layers through which the induced electric current flows. An inversion program is utilized to convert the array of apparent resistivity data into a model of the geology that would yield the observed distribution of apparent resistivity values. The product of the data inversion process is a two-dimensional image (a tomograph) showing a distribution of true resistivity values that

FIGURE V-12 Generalized Layout of Multiple-Electrode Electrical Resistivity Tomography Surveys



a-Electrode spacing; n-Layer of data; C₁, C₂-current electrodes; P₁, P₂-potential electrodes

NOTE: Although the measurement sequence shown in this diagram is applicable to the Wenner array, the equipment and resulting data pattern are similar to that used with the dipole-dipole array during this investigation.

would produce the apparent resistivity values observed in the field data. An iterative process refines the model until the apparent resistivity distribution matches the raw data as closely as possible. No *a priori* information on the resistivity distribution is involved, so the resulting image is free of interpreter bias (Griffiths and Barker, 1993). However, proper interpretation of the images does require knowledge of local geological conditions. Dipole-dipole resistivity tomography has been used successfully to map the thickness of a clay layer over microdiorite bedrock (Loke and Barker, 1996). Application of this technique in karst areas has indicated that it is particularly well suited for determining depth to limestone bedrock (Lambert, 1997). Electrical resistivity was applied in this project to map the surface of the limestone bedrock beneath the clay overburden at the site and to identify any depressions in that surface. This information was used to evaluate potential sinkhole-collapse hazards at the site.

2. RESISTIVITY DATA ACQUISITION

Resistivity data collection occurred between June 3 and June 20, 1997 and between July 28 and August 29, 1997. Data were collected using the Sting R1 Memory Earth Resistivity Meter and the Swift Automatic Smart Electrode System.

The resistivity transects (Figure V-13) were designed to coincide with the lines used for collecting NP data (see Section A). The transects were spaced 50 feet apart in the north-south direction and 75 feet apart in the east-west direction. Forty-nine transects were established over an area of approximately 17.8 acres. Sinkhole C was crossed by Transects 5 through 11. In addition, two control transects (C1 and C2) were established to evaluate the method's response to known sinkholes near the site. Transect C1 crosses Sinkhole B, and Transect C2 lies between Sinkholes A and B.

The electrode spacing along each transect is 3 meters, or approximately 10 feet. The lengths of the transects vary from 81 meters (266 feet) to 249 meters (817 feet). In cases of electrode malfunction, the affected electrode was moved to the end of the transect, effectively shortening its length slightly. Each transect included the use of 28, 56, or 84 electrodes, producing data for 8, 11, and 13 layers (depths), respectively.

Table V-4 lists the parameters for each transect. Because the electrical cross section is trapezoidal, some transects consist of overlapping lines to achieve full coverage of the site. Resistivity data were collected along a total survey length of about 6 miles.

Throughout most of the site, the ground surface consisted of clay-rich soil, ensuring good electrical contact between the stainless steel electrodes and the ground. Where Transects 29A through 41A and Transects 1 through 19 crossed the CKD Haul Road, the electrodes were placed in 2-inch holes which were drilled through the road surface (1.5 feet deep). Electrical contact between the electrodes and the ground was facilitated by filling the holes with clay mud and salt water. Each transect measurement was preceded by a contact test of each electrode in the array per recommendation of the instrument manufacturer (Advanced Geosciences, Inc., 1996).

Highly conductive material (metallic debris) at the site affected the resistivity data. Considerable effort was made to remove wire fences, metal poles, and other material from the site with a backhoe. Transects measured before debris removal—e.g., Transects 31B through 45B—were measured again after the removal to ensure collection of the best quality data possible.

Rain also had a significant impact on data collection at the site. In addition to slowing the data-collection process, it also changed the near-surface soil conditions in a dramatic manner with respect to electrical resistivity. Very noisy data were produced along several transects where data collection occurred during or immediately after rainfall—e.g., Transects 150A, 225B, 300A and 450A. These transects were measured again at a later time.

—P.E. LaMoreaux & Associates—

FIGURE V-13
ELECTRICAL RESISTIVITY
TOMOGRAPHY TRANSECTS

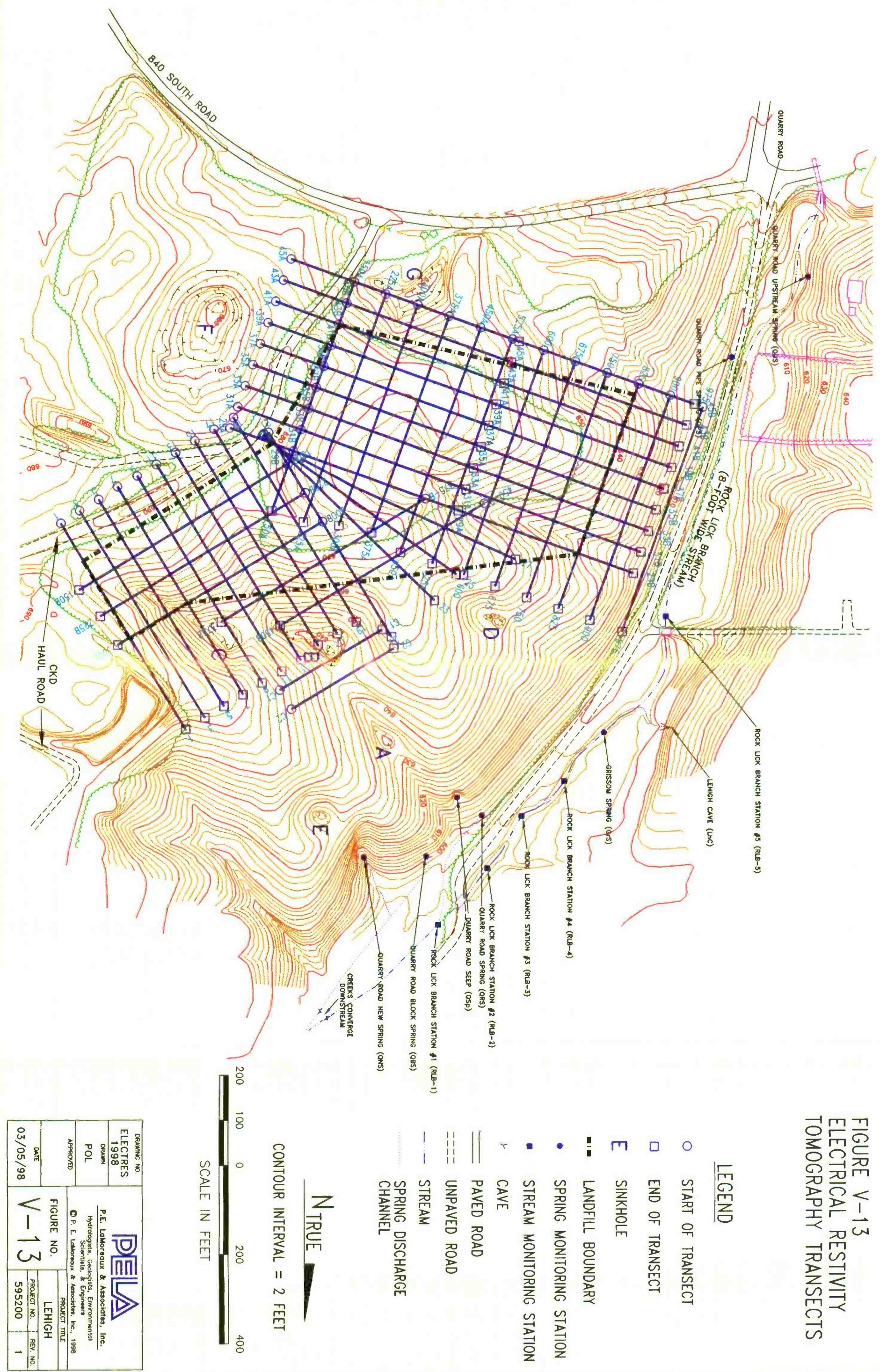


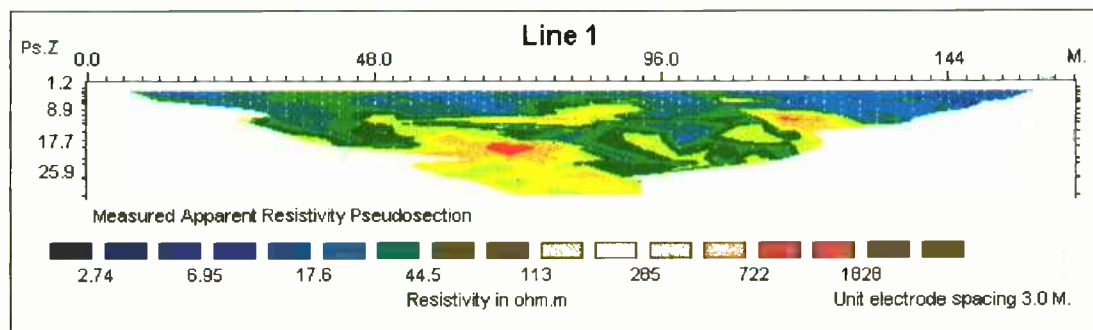
TABLE V-4 Electrical Resistivity Tomography Transects

LINE NO.	LENGTH (m)	SPACING (m)	ELECTRODES	STATIONS
Control Transects				
C1	81	3	28	Centered on Sinkhole B
C2	81	3	28	Centered between Sinkholes A & B
South-North Transects				
45A	165	3	56	Starting at Station 0
45B	246	3	83	Starting at Station 150
43A	165	3	56	Starting at Station 0
43B	246	3	83	Starting at Station 150
41A	162	3	55	Starting at Station 0
41B	246	3	83	Starting at Station 150
39A	162	3	55	Starting at Station 0
39B	246	3	83	Starting at Station 150
37A	162	3	55	Starting at Station 0
37B	246	3	83	Starting at Station 150
35A	162	3	55	Starting at Station 0
35B	246	3	83	Starting at Station 150
33A	162	3	55	Starting at Station 0
33B	246	3	83	Starting at Station 150
31A	162	3	55	Starting at Station 0
31B	246	3	83	Starting at Station 150
29A	162	3	55	Starting at Station 0
29B	246	3	83	Starting at Station 150
27	162	3	55	Ending at Station 600
25	162	3	55	Ending at Station 600
23	162	3	55	Ending at Station 600
21	162	3	55	Ending at Station 600
19	162	3	55	Starting at Station 0
17	162	3	55	Starting at Station 0
15	162	3	55	Starting at Station 0
13	165	3	56	Starting at Station 0
11	165	3	56	Starting at Station 0
9	165	3	56	Starting at Station 0
7	165	3	56	Starting at Station 0
5	165	3	56	Starting at Station 0
3	165	3	56	Starting at Station 0
1	165	3	56	Starting at Station 0
West-East Transects				
150A	165	3	56	Starting at Line 45
150B	165	3	56	Starting at Line 21
225A	165	3	56	Starting at Line 45
225B	162	3	55	Starting at Line 21
300A	159	3	54	Starting at Line 45
300B	162	3	55	Starting at Line 21
375A	156	3	53	Starting at Line 45
375B	162	3	55	Starting at Line 29
450A	162	3	55	Starting at Line 45
450B	162	3	55	Ending at Line 13
525	162	3	55	Starting at Line 45
600	162	3	55	Starting at Line 45
675	162	3	55	Starting at Line 45
750	162	3	55	Starting at Line 45
825	162	3	55	Starting at Line 45
900	162	3	55	Starting at Line 45
975	162	3	55	Starting at Line 45

P.E. LaMoreaux & Associates

On average, 300 data points were collected for each 28-electrode transect; 700 data points were collected for each 56-electrode transect; and 1,200 data points were collected for each 84-electrode transect. The time required for data collection along each transect ranged from 1.5 to 5 hours, excluding instrument setup. Approximately 40,000 data points were collected, each of which consists of the location, the average and standard deviation of three apparent resistivity measurements, and the time at which the measurement was made. The raw data are presented in the measured apparent resistivity pseudosections, which are the top graphs on each page in Appendix E. The measured apparent resistivity pseudosection for Transect 1 is shown in Figure V-14 to illustrate the general format. Each pseudosection is constructed by plotting each measured apparent resistivity value below the center point of the corresponding array at a depth that is a fraction of the corresponding electrode spacing. The apparent resistivity values are presented using a logarithmic color scale. The vertical axis is the pseudo-depth (in meters) below the ground surface, and the horizontal axis is the distance from the first electrode. Each tick mark along the horizontal axis represents one electrode.

FIGURE V-14 Measured Apparent Resistivity Pseudosection



3. DATA ANALYSIS AND RESULTS

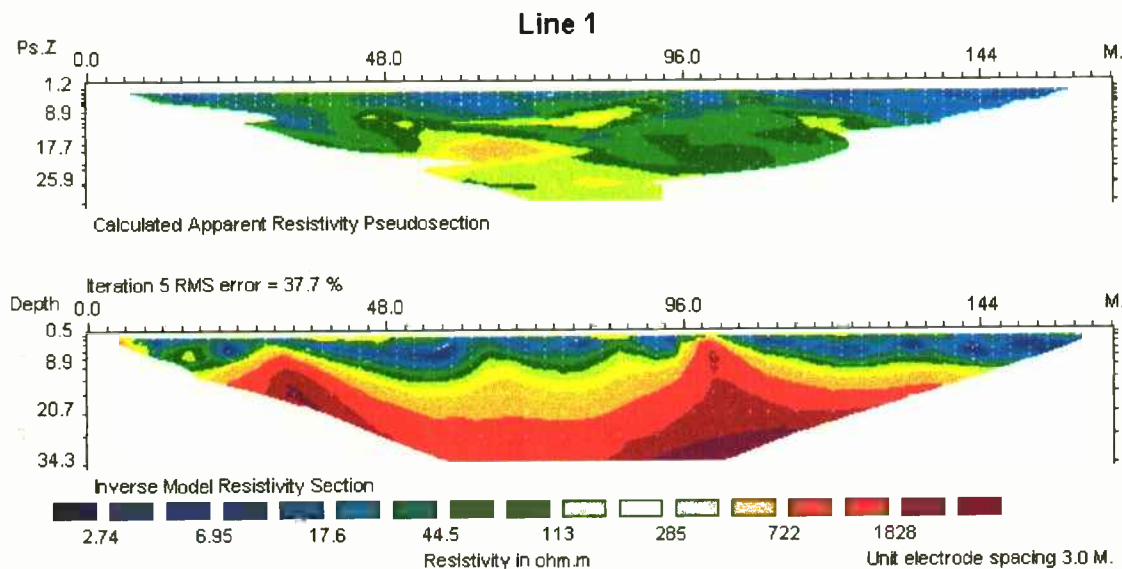
Data quality can be affected by various factors, such as wind, clouds, animals, and even solar flares. As recommended by the instrument manufacturer (Lagmanson, 1997), the raw data were edited by removing any apparent resistivity values that were less than zero, which is theoretically impossible, or had standard deviations greater than 20 percent. Abnormally low (less than 5 ohm-meters) and high (greater than 100,000 ohm-meters) apparent resistivity values were also removed from the data set.

Edited data were processed to generate two-dimensional resistivity models of the subsurface using RES2DINV, computer software developed by Loke (1996) and distributed by Advanced Geosciences, Inc. RES2DINV is an automatic iterative imaging program that estimates true resistivity values and approximates the positions of the corresponding geologic materials and structures. The process uses a finite difference algorithm during each iteration to produce a cross section of calculated

apparent resistivity. The program compares it with the measured apparent resistivity section and modifies the model until an acceptable match is achieved between the measured and calculated pseudosections. The difference between the two pseudosections is quantified as the Root-Mean-Square (RMS) error. Small RMS values indicate close matches between the measured data and the modeled geological profile. The acceptable match is defined by the convergence limit, the default value of which is 5 percent change in the RMS error between two iterations.

Of the 51 transects, 59 percent required five iterations; 37 percent required four iterations; 2 percent required three iterations; and 2 percent required six iterations to obtain an acceptable match. The iteration with the least error was selected to best represent the true resistivity distribution for each transect. The model tomographs are presented in the Inverse Model Resistivity Sections (lower graphs of each page) in Appendix E. The calculated apparent resistivity distributions are shown in the Calculated Apparent Resistivity Pseudosections (middle graphs of each page) in Appendix E. Figure V-15 shows the results and RMS error calculated by RES2DINV at Iteration 5 for Transect 1. The true resistivity image clearly shows a layered geologic structure. Visual comparison reveals a general match between the calculated apparent resistivity and the measured apparent resistivity in Figure V-14. In this case, the minor discrepancies account for an RMS error of 37.7 percent. In general, the calculated and measured apparent resistivity images appear similar when the RMS error is less than 50 percent.

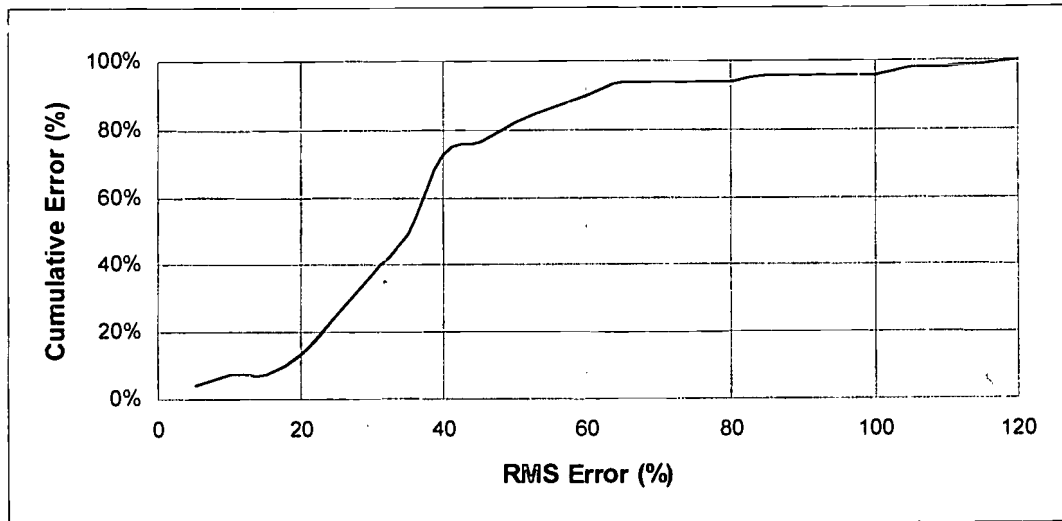
FIGURE V-15 Calculated Apparent Resistivity Pseudosection and Inverse Model Resistivity Section



RMS error results from the data collection and data inversion processes. Every effort was made to reduce noise in the data by repeating measurements on transects with

noisy data and editing the raw data as described above. Figure V-16 shows the RMS error distribution for all 51 transects. The average RMS error is 37.1 percent, with a minimum of 1.8 percent along control Transect C2 and a maximum of 118.2 percent along Transect 975. About 82 percent of the lines have RMS errors less than 50 percent.

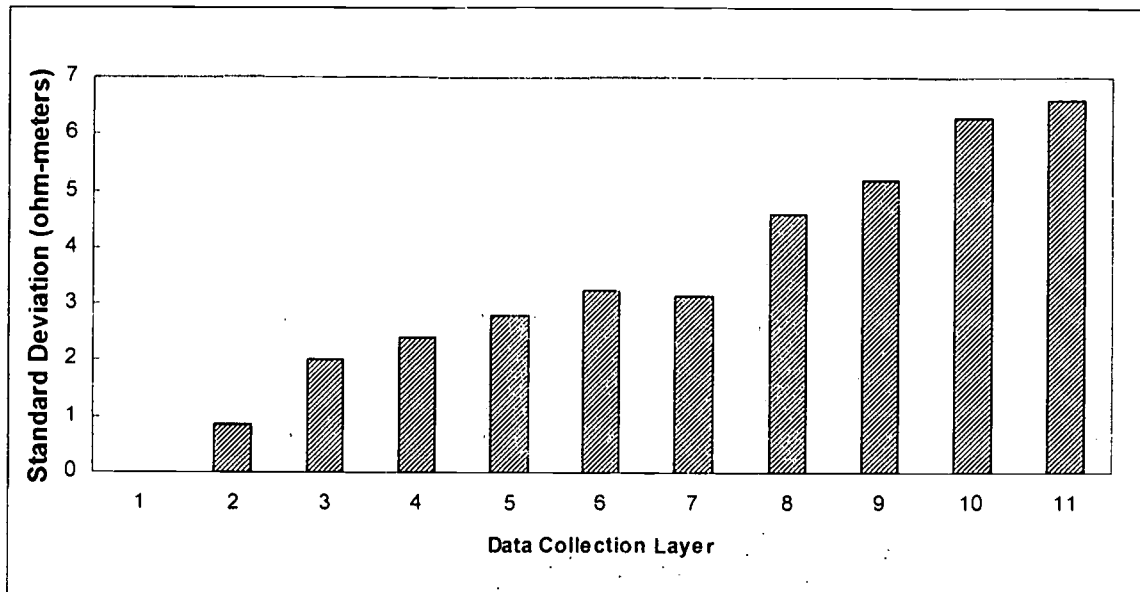
FIGURE V-16 RMS Error Distribution Obtained from RES2DINV



It should also be noted that data resolution decreases with depth. Data provide less detail at greater depth because larger volumes of materials are being measured. This effect is inherent to resistivity tomography techniques (Griffiths and Barker, 1993). The depth of data collected during this investigation varies from 15 meters (49 feet) to 40 meters (131 feet), depending on the number of electrodes employed. Each reported resistivity value is the average of three individual measurements. To evaluate the effect of depth on the resistivity investigation at the site, the data from all the 56-electrode profiles were assessed. Figure V-17 shows the average standard deviations of the measurements at various depths (data collection layers). The standard deviations observed during this investigation were quite small, probably because of the small electrode spacing maintained during measurement and careful data editing.

When applying a two-dimensional resistivity model in a karst area, variations in the lower (deeper) sections of the model may be caused by significant variations in the subsurface geology in a direction perpendicular to the survey transect. This effect is most pronounced when the survey line passes near a localized feature with different electrical properties than the surrounding material, such as a clay-filled sinkhole. To minimize such effects during this investigation, data collected along transects with different orientations were evaluated, interpreted, and combined, as discussed in Section 4.

FIGURE V-17 Variation of Standard Deviation of Measured Apparent Resistivity with Depth



4. INTERPRETATION AND DISCUSSION

The tomographs are interpreted by converting them to a geological cross-section. As shown in the lower portion of Figure V-15, most of the true resistivity sections reveal the presence of a thin, low-resistivity surface layer, below which the resistivity increases steadily with depth (see also Appendix E). Exploratory drilling has shown that there is generally a gradual transition from fully weathered, low-resistivity material to fractured or unfractured, high-resistivity limestone. However, even a sharply contrasting limestone/clay boundary appears transitional on the processed image. Therefore, data from the soil borings drilled in 1994 were used to determine the actual depth of the boundary at specific locations on the tomographs.

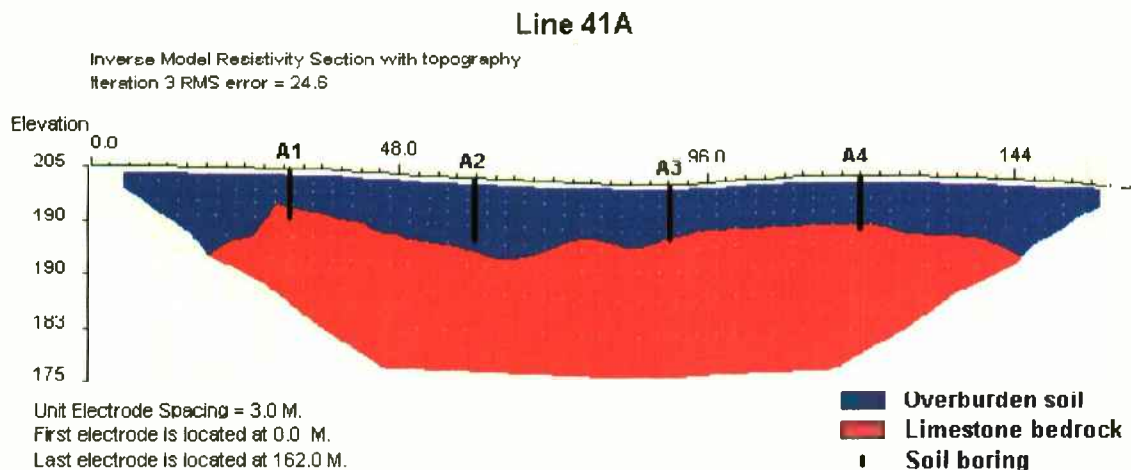
Topographic irregularities on the site introduce distortions in the tomographs that can affect interpretations regarding the target boundary (Spiegel and others, 1980). To properly compensate for this topographic effect, surface elevations obtained from the Site Map (Figure I-1) were incorporated in the program RES2DINV. The depth of the clay/limestone boundary was estimated by averaging the depth to bedrock determined in the closest borings drilled in 1994. Because the true resistivity sections are obtained from volume-averaged apparent resistivity, the boring data are only one of the criteria used to interpret the depth to the limestone/clay contact. Two assumptions must also be made.

- (1) The contact is assumed to be laterally continuous between two layers of uniform resistivity;
- (2) The contact is assumed to be sharp rather than gradational—i.e., it is located where the vertical resistivity gradient is greatest.

Because these assumptions are not appropriate in all cases, the interpreted boundary does not always match the data from all the borings. The absolute resistivity value for the boundary varies from transect to transect, ranging from 30 to 300 ohm-meters. The lower end of this range is lower than might be expected because the actual contact is not sharp, but rather is characterized by a weathered zone where clay and limestone fragments coexist.

The diagrams in Appendix F show the interpreted limestone/clay boundaries for all transects at the site. An example for Transect 41A is shown in Figure V-18. The limestone and clay are depicted in red and blue, respectively. The interpreted limestone surface illustrates various irregularities. Depressions are clearly shown in Transects 7, 13, 21, 23, 33A, 35B, 45A, and 825. However, the surface is basically flat in Transects 15, 31A, 35A, 37A, 39A, 41A, 41B, 43A, 45B, 150B, 225A, 300A, and 600. The remaining transects appear to have relatively small pinnacles and depressions. In Transects 29A, 825, 900, and 975, resistivity decreases with depth (instead of increasing) at some locations. This may be caused by localized ground conditions—i.e., the ground may be too resistive for electrical current to penetrate effectively, or it may be conductive enough to cause electrical “short circuits” near the surface.

FIGURE V-18 Interpreted Limestone/Clay Contact Along Line 41A



Comparison of the interpreted bedrock surface with additional boring data which was not used to establish the boundary provides information regarding the accuracy of the interpretation. Table V-5 lists the interpreted elevation of the bedrock surface for transects which directly cross soil borings. When borings were intercepted by more than one transect, the elevation from each transect is given, but only the average value is used for comparison. Boreholes DA3 and DA4 are not included because the tomograph from Transect 25 does not appear to be geologically meaningful and was disregarded. Borehole A7 is not included because it is not crossed by any of the transects. However, data from all the boreholes are used to evaluate the validity of the bedrock surface map derived from the resistivity data (see below).

The interpreted elevations of the limestone surface can be higher or lower than the elevations determined in the borings. The average elevation difference between the borings and the interpretation is 5.8 feet, and the maximum is 22 feet. More than 80 percent of the data points differ by less than 10 feet, as shown in Figure V-19.

Differences between the interpreted and observed bedrock-surface elevations arise from a variety of causes, as discussed previously. For all of these reasons, the interpreted limestone/clay boundary should only be considered a generalized trend. It may be used to characterize the bedrock surface and to locate areas of high and low resistivity. However, it should not be used to "pinpoint" the exact location of features in the field, especially in karst areas where the features of interest may be highly localized.

An effective way to reduce the discrepancies between the interpreted and observed bedrock elevations is to average the elevations interpreted from more than one transect with different orientations. If similar elevations are interpreted from more than one transect, their average value may be considered more reliable. A third-dimensional feature for one transect may be crossed by transects in other directions. The elevations of all transect junctions (Figure V-13) have been determined from the graphs in Appendix F and presented in the form of a contour map (Figure V-20)¹. A 10-foot contour interval is used for the bedrock surface because most (80 percent) of the interpreted elevations appear to be accurate within 10 feet, as explained above.

Soil borings from 1994 that were not used to define the limestone/clay boundary and exploratory boreholes drilled in 1997 were used to evaluate the accuracy of the map. Table V-6 compares the results derived by comparing the bedrock-surface elevations in Figure V-20 with the elevations determined by drilling. The average difference is only 3.5 feet. The error is less than 5 feet for six of the seven boreholes, and the maximum error is 12 feet at Boring DA3. In the 1997 exploratory boreholes for which detailed geologic logs are available, the average error is as small as 1.1 feet. Therefore, the

¹ Because the landfill boundary was modified to maintain the required waste-disposal volume while avoiding Sinkholes B, C, and D, the contour map presented in Figure V-20 does not completely cover the area within the landfill boundary. However, no NP anomalies were identified in this area (Figure V-8).

TABLE V-5 Comparison of Bedrock Elevations Interpreted from True Resistivity and Borings

(Part 1 of 2)

BORING		ELECTRICAL RESISTIVITY TOMOGRAPHY			DIFFERENCE (feet)
NUMBER	ELEVATION (feet)	TRANSECT	ELEVATION (feet)	AVERAGE ELEVATION (feet)	
A1	647	41A	650	650.0	-3.0
A2	641	41A 41B	636 641	638.5	2.5
A3	633	41A 41B 300A	634 635 622	630.3	3.3
A4	638	41A 41B	640 635	637.5	0.5
A5	638	41B	634	634.0	4.0
A6	638	41B 600	636 638	637.0	1.0
B1	647	37A	650	650.0	-3.0
B2	646	37A	640	640.0	6.0
B3	639	37A 37B 300A	635 638 637	636.7	2.3
B4	639	37A 37B	640 642	641.0	-1.0
B5	638	37B	642	642.0	-4.0
B6	636	37B 600	639 636	637.5	-1.5
C1	662	33A	662	662.0	0.0
C2	653	33A	634	634.0	19.0
C3	643	33A 33B 300A	641 635 642	639.3	3.7
C4	654	33A 33B	646 636	641.0	13.0

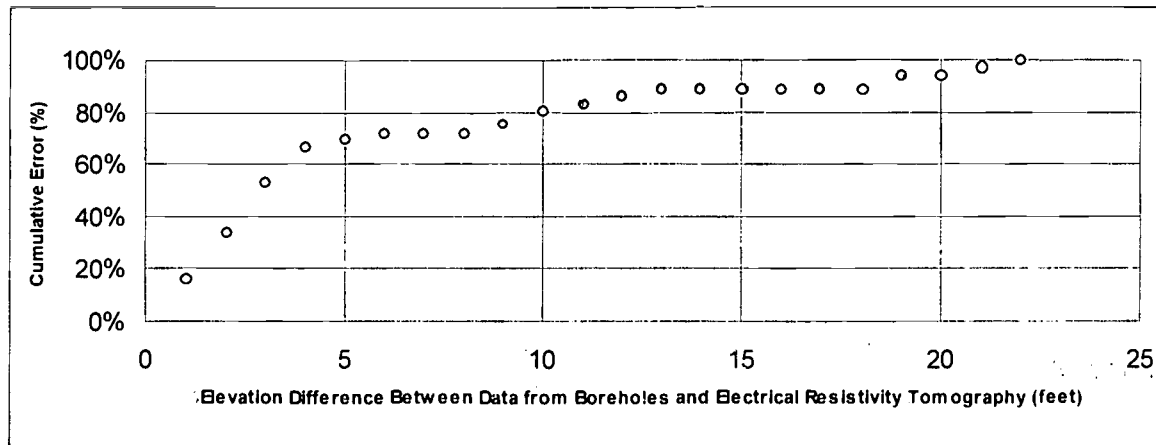
TABLE V-5 Comparison of Bedrock Elevations Interpreted from True Resistivity and Borings (Continued)

(Part 2 of 2)

BORING		ELECTRICAL RESISTIVITY TOMOGRAPHY			DIFFERENCE (feet)
NUMBER	ELEVATION (feet)	TRANSECT	ELEVATION (feet)	AVERAGE ELEVATION (feet)	
D1	641	29A 21	644 639	641.5	-0.5
D2	640	29A 29B	645 638	641.5	-1.5
D3	654	29A 29B 300A	625 628 652	635.0	19.0
D4	650	29A 29B	628 660	644.0	10.0
DB2	646	21	636	636.0	10.0
DB3	648	21	646	646.0	2.0
DB4	670	21	673	673.0	-3.0
E1	652	17	673	673.0	-21.0
E2	639	17	641	639.0	-2.0
E3	634	17 300B	628 634	631.0	3.0
E4	631	17	643	643.0	-12.0
F1	651	13	651	651.0	0.0
F2	639	13	617	617.0	22.0
F3	645	13 300B	648 662.5	655.3	-10.3
F4	639	13	642	642.0	-3.0
G1	656	9	665	665.0	-9.0
G2	645	9	650	650.0	-5.0
G3	640	9 300B	641 643	642.0	-2.0
H1	655	5	657	657.0	-2.0
H2	656	5	652	652.0	4.0

P.E. LaMoreaux & Associates

FIGURE V-19 Limestone Elevation Differences Between Data from Borings and Resistivity



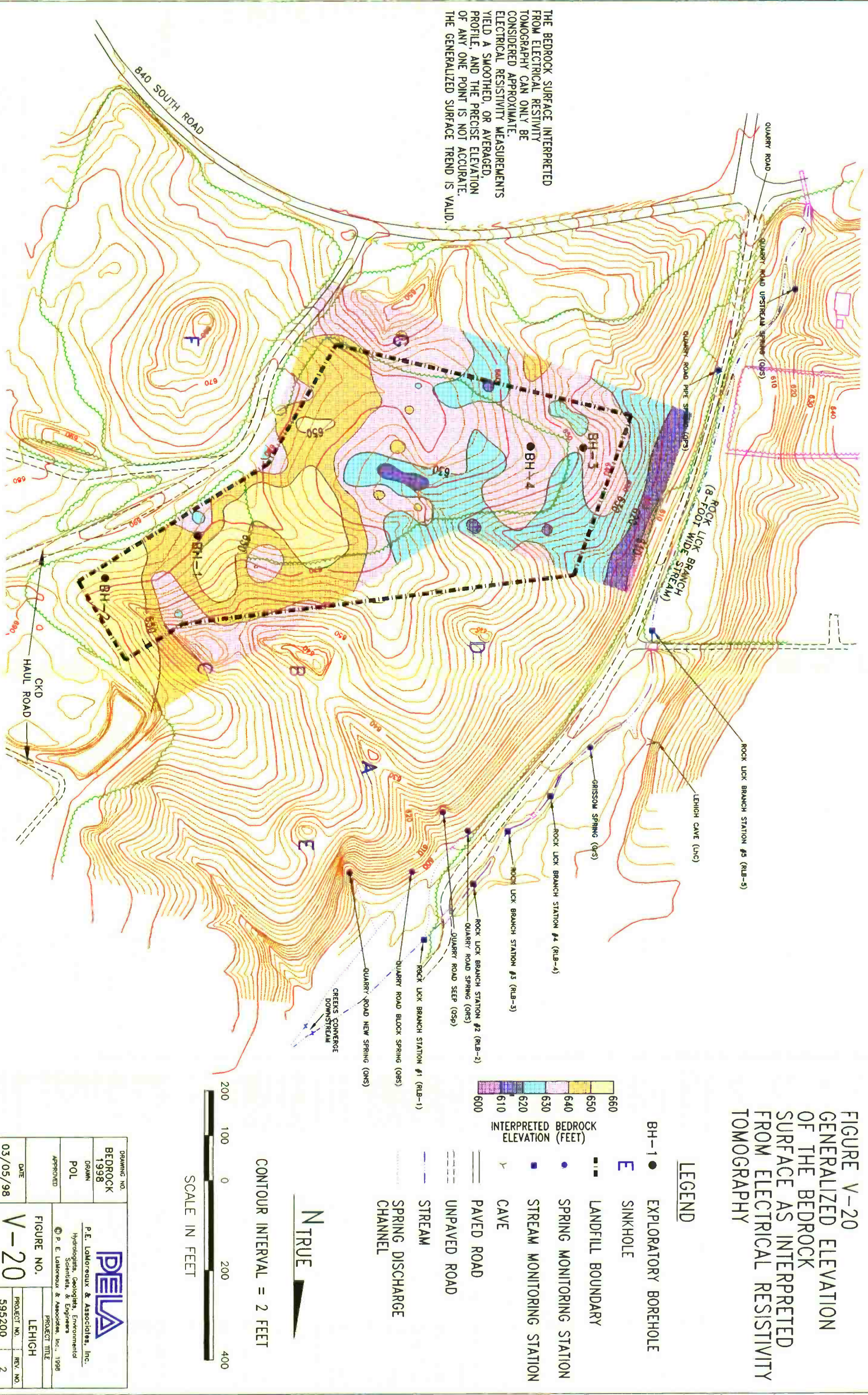
map presented in Figure V-20 appears to give a good approximation of the configuration of bedrock surface.

According to Figure V-20, the limestone dips generally westward toward Rock Lick Branch. It is exposed at the land surface immediately east of Quarry Road, which was confirmed by field observation. The coincidence of a trough with Sinkhole C demonstrates again that electrical resistivity tomography can provide information on the general configuration of the bedrock surface. The bedrock surface interpreted from this technique is undulating in nature, which is not uncommon in karst areas. The identified depressions may be isolated features in the limestone surface, or they may be locations where the groundwater collects and flows in a concentrated manner. Only the latter possibility is of concern because any location with a potential sinkhole-collapse hazard should be characterized by a depression in the limestone surface *and* an area of groundwater recharge. In other words, the areas of potential concern are those which appear as anomalies in *both* the resistivity *and* NP data—i.e., in Figure V-20 *and* in Figure V-8.

Comparison of Figures V-20 and V-8 reveals two anomaly areas that are common to the resistivity and NP surveys. One is located around Sinkhole C where a negative NP anomaly coincides with a trough in the limestone surface. This area is not within the site boundary.

Another area with anomalies common to both surveys lies between Lines 29 and 35 and between Stations 250 and 700. Like the area around Sinkhole C, a negative NP anomaly coincides with a trough in the limestone surface. The limestone surface lies generally between 620 and 630 feet in most of the trough, although three small areas within it appear to lie below that. The area of common anomalies is generally aligned

FIGURE V-20
GENERALIZED ELEVATION
OF THE BEDROCK
SURFACE AS INTERPRETED
FROM ELECTRICAL RESISTIVITY
TOMOGRAPHY



DRAWING NO.	BEDROCK		
1998	POL		
DRAWN	APPROVED		
DATE	03/05/98		
			
<u>P.E. LAMOREAUX & Associates, Inc.</u> Hydrologists, Geologists, Environmental Scientists, & Engineers			
P. E. Lamoreaux & Associates, Inc., 1998			
FIGURE NO.		PROJECT TITLE	
V-20		LEHIGH	
PROJECT NO.		REV. NO.	
595200		2	

TABLE V-6 Verification of the Bedrock Surface Elevation by Drilling

BOREHOLE	BEDROCK SURFACE ELEVATION (feet)		
	Borehole	Resistivity	Difference
A7	636	633	3.0
DA3	640	652	-12.0
DA4	630	635	-5.0
BH-1	643	641	2.0
BH-2	652	653	-1.0
BH-3	632	631	1.0
BH-4	634.5	634	0.5

with a small valley in the land surface. Based on the relative magnitudes of the anomalies in Figures V-8 and V-20, it appears that the area of greatest possible concern lies between Transects 29 and 31 and between Stations 575 and 625.

Another area with anomalies common to both surveys lies between Lines 29 and 35 and between Stations 250 and 700. Like the area around Sinkhole C, a negative NP anomaly coincides with a trough in the limestone surface. The limestone surface lies generally between 620 and 630 feet in most of the trough, although three small areas within it appear to lie below that. The area of common anomalies is generally aligned with a small valley in the land surface. Based on the relative magnitudes of the anomalies in Figures V-8 and V-20, it appears that the area of greatest possible concern lies between Transects 29 and 31 and between Stations 575 and 625.

Sinkhole collapses occur where groundwater recharge occurs through an open fracture or conduit in the limestone, allowing the downward transport of soil particles. Such features are usually associated with a depression in the limestone surface. Therefore, the geophysical techniques used in this project were selected to identify these subsurface characteristics. NP was used to detect areas of localized groundwater infiltration and percolation; electrical resistivity tomography was used to identify depressions in the limestone surface, which might be indicative of the presence of enlarged channels capable of transmitting infiltrating water and soil into the underlying karst aquifer. Every effort was made to ensure the reliability of the results, from data collection through data processing to interpretation.

The only obvious anomalies detected by both methods coincided with an off-site, mature, solution sinkhole and a small valley in the in the west-central portion of the site. Because of the small magnitude and dispersed nature of the on-site NP anomaly, it does not appear to result from a significant zone of concentrated groundwater recharge of the type necessary to produce a sinkhole collapse.

VI. GROUNDWATER TRACING

A groundwater tracing investigation was conducted to determine whether groundwater at the site can be monitored effectively and to provide data to design an effective monitoring strategy. Information from this investigation is also applicable to evaluating the sinkhole collapse potential at the site. Generalized flow routes of groundwater passing beneath the site in discrete fractures or conduits have been determined by introducing fluorescent dyes into sinkholes near the site and monitoring their discharge at nearby springs, seeps, and streams. The delineation of flow routes provides the information necessary to assist with the development of a groundwater monitoring strategy by identifying natural discharge features (such as springs) which are often more appropriate than monitoring wells for sampling groundwater downgradient from the site (McCann and Krothe, 1992; Quinlan, 1990). Groundwater-tracing data are also relevant to assessing the sinkhole collapse potential because the primary mechanism responsible for sinkhole collapse is subsurface erosion associated with the movement of groundwater into and through fractures and conduits.

A. DESIGN OF GROUNDWATER TRACING INVESTIGATION

During the planning stages of the groundwater tracing investigation, published maps and reports were reviewed to determine the extent of the area to be studied. Additionally, an inventory was conducted to identify karst groundwater features in the site area. Once the extent and characteristics of the study area were known, appropriate tracers were selected; and dye insertion, dye monitoring, and analytical methods were determined. These activities were conducted in conjunction with an assessment of background conditions in the field. Following the tracing experiments, generalized groundwater flow routes were determined, as explained in the following sections.

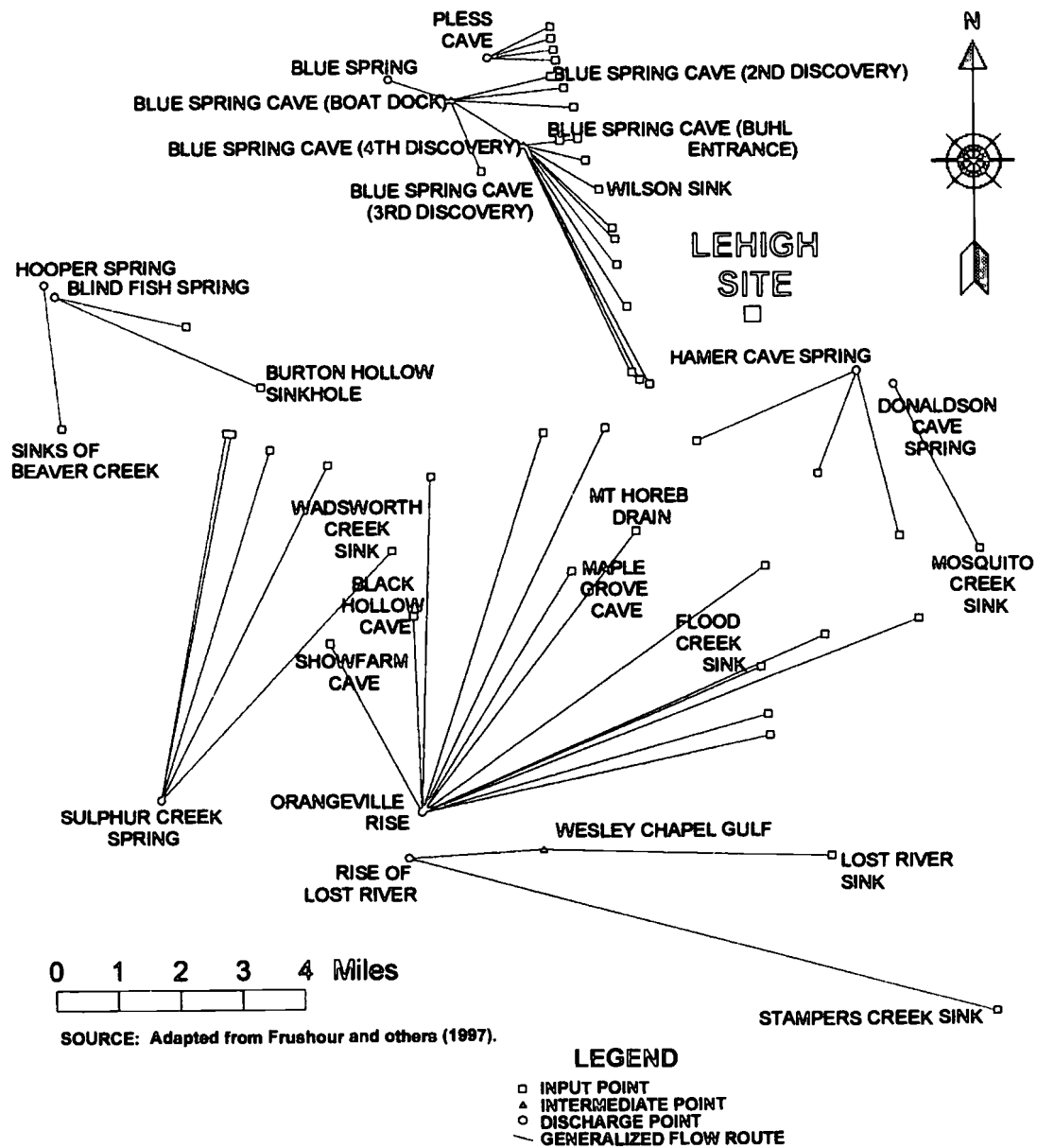
1. PREVIOUS GROUNDWATER TRACING

Prior to this investigation, a considerable amount of groundwater tracing had been conducted in the Mitchell area. Review of the published results of these studies provided valuable information for determining the extent of the area to be inventoried and monitored during this investigation. The availability of this information allowed coverage of approximately 150 square miles by monitoring numerous features relatively near the site and only three distant locations where previous work has shown that groundwater is discharged from large areas surrounding the site: Spring Mill State Park, Blue Spring Cave, and Orangeville Rise (Figure VI-1).

Frushour and others (1997) provide a generalized map summarizing previous groundwater traces conducted in the Mitchell area; and Powell and others (1997) show the general locations of sinkhole areas, sinking-stream basins, caves, and springs. Both maps are produced from a Geographic Information System (GIS) database. As

—P.E. LaMoreaux & Associates—

FIGURE VI-1 Results of Previous Groundwater Tracing near Mitchell



presented, the scale of these maps does not provide enough detail to be directly useful. However, the relevant karst features and groundwater tracing results are covered in more detail in other publications.

For example, Bassett and others (1996) and Duwelius and others (1994 and 1995) present maps at larger scales, depicting generalized flow routes for groundwater traces which emerged at Pless Cave, Blue Spring Cave, Sulphur Spring, Orangeville Rise, Hamer Cave, Blindfish Spring, and Hooper Spring. Duwelius and others (1994 and 1995) present descriptions of most of these features. Data presented in these papers show that the Blue Spring groundwater basin extends northwest from Mitchell toward East Fork White River. The discharge at Blue Spring has been observed to exceed 300,000 gallons per minute (Palmer, 1967). This basin is characterized by rapid groundwater flow through a well integrated underground drainage system. These data further indicate that groundwater west of State Route 37 in the Mitchell area flows either northwest to Blue Spring Cave or southwest to Orangeville Rise. No sinkholes along Highway 37 *north* of Mitchell were found to drain eastward (updip) toward Erwin Spring Cave, Rabbitville Quarry Rise, Lehigh Quarry Spring Cave, Rock Lick Spring (Lehigh Cave), Wind Cave, Whistling Cave, or CCC Spring¹. According to Duwelius and others (1995, p. 230), "The ground water basins for...these streams or springs appear to be small and located entirely east of State Route 37."

The upper Lost River drainage basin (south and southwest of the site) and groundwater tracing within it is discussed by Bassett and Ruhe (1974) and Bassett (1976). Hobbs and Wells (1972) also include a general description of the Lost River basin, and a guidebook produced by the National Speleological Society (1973, p. 69-77) presents a Lost River Field Trip, including a road log, a groundwater tracing map, and photographs of Orangeville Rise. The basin covers approximately 163 square miles and contains several significant sinking streams and two large springs. In the eastern portion of the basin, a network of surface streams provides recharge to the karst aquifer where it flows onto the sinkhole plain. Groundwater tracing has demonstrated that two large, independent karst groundwater drainage systems exist within the basin. One discharges at Orangeville Rise and has a drainage area of at least 46 square miles in the northwestern portion of the basin. The other discharges at the Rise of Lost River and has a drainage basin of at least 110 square miles, primarily in the eastern part of the basin. As described by Powell (1987, p. 375 & 379), "The Orangeville Rise is the spring head of Lost River in the town of Orangeville in northwestern Orange County. The site is about...9 miles (14.4 km) southwest of Mitchell.... [It is] not the actual resurgence of underground Lost River. The Rise of Lost River is located about a mile (1.6 km) to the south of and downstream from the Orangeville Rise." Quantitative tracing has shown that groundwater flow velocities within the aquifer can be as high as 5.5 miles per day. Under storm-flow conditions, the discharge at Orangeville Rise is estimated to be as high as 190 cubic feet per second (Bassett and Ruhe, 1973).

¹ One trace originating near the intersection of Highways 37 and 60 *south* of Mitchell was detected to the northeast at Hamer Cave (southeast of the site).

Bayless and others (1994) summarize the generalized groundwater flow routes demonstrated by water-level measurements and numerous traces originating south of Mitchell, including the area around Orleans. With two minor, localized exceptions, all the traces documented in their report flowed generally southwestward to Lost River Rise or Orangeville Rise or generally northward to Spring Mill State Park (Hamer Cave or the Twin Caves-Bronson Cave-Donaldson Cave system). Based on this information, Bayless and others (1994) determined the approximate location of the groundwater drainage divide between the Orangeville Rise/Lost River and Spring Mill State Park drainage basins. They note that portions of the divide have been shifted by subsurface stream piracy, causing groundwater to pass beneath topographic (surface-water) drainage divides. This observation is also reported by Bayless and Taylor (1994), Bayless and others (1995), and Powell (1987).

2. INVENTORY OF KARST FEATURES

At the outset of this tracing investigation, it was apparent from the published results of previous studies that several relatively large karst groundwater basins exist in the region surrounding the site. Groundwater is discharged from these basins at Blue Spring Cave, Orangeville Rise, and several locations within Spring Mill State Park (Figure VI-1). Among previous researchers, it was also widely accepted that most karst groundwater flow beneath the Mitchell Plain occurs in the downdip direction (Ash, 1984; Duwelius and others, 1995; Johnson, 1992; Johnson and Gomez, 1994; Palmer, 1967; Palmer and Palmer, 1975).

Field reconnaissance was conducted to locate karst features relevant to the flow of groundwater in the vicinity of the site. The search was carried out in all directions relatively near the site (generally within 3 miles), with emphasis in the direction of the regional dip (generally westward toward Rock Lick Branch). Seventy-one (71) features were identified, including sinkholes, sinking streams, caves, springs, seeps, and a quarry-water discharge pipe (NPDES Outfall Permit No. 004). In addition to locations that had been documented in previously published maps and literature, some were identified by the staff at Lehigh or Spring Mill State Park¹, while others were found by PELA during field reconnaissance. Many of the springs and seeps were considered to be of no value for the groundwater tracing study because they were located at elevations higher than the site or because their discharge rates were too small to indicate a significant flow route. Excluding these features, the locations shown in Figure VI-2 and Table VI-1 were selected for routine monitoring during the tracing investigation². The relative locations of Blue Spring Cave and Orangeville Rise are shown in Figure VI-1, and features in the immediate vicinity of the site are shown at a

¹ For example, locations of caves and "active" sinkholes within Spring Mill State Park are shown on a map by Huffman and Martin (1991).

² For simplicity, the group of adjacent springs identified in Figure IV-2 and Table IV-1 as QRS, QBS, and QNS are referred to in this document as the "Three Springs" area. It should also be noted that the name "Blue Spring Cave" has been used in the literature for at least three decades, although "Bluespring Caverns" is the commercial name used by the current owner.

FIGURE VI-2
TRACER MONITORING
LOCATIONS

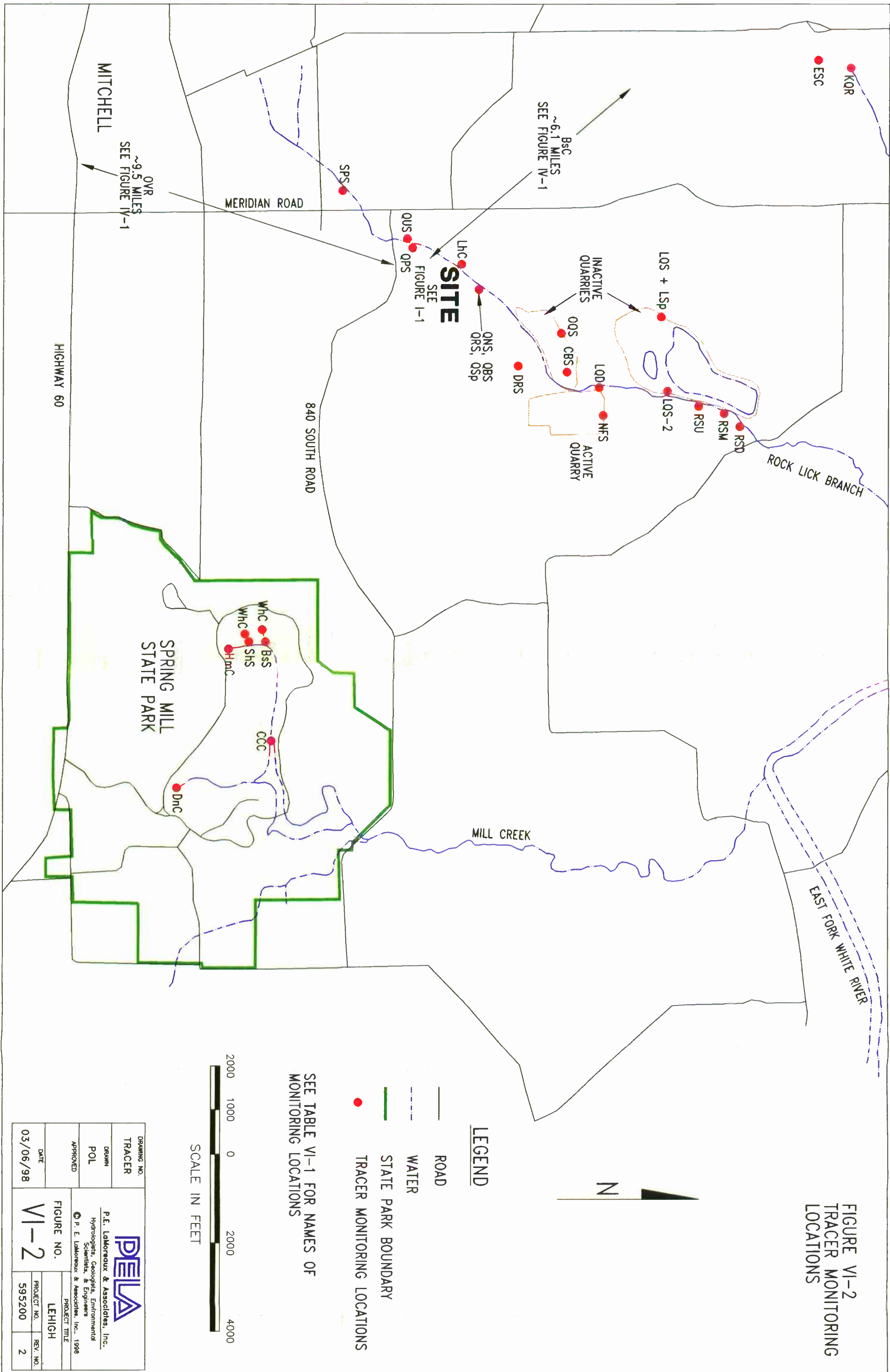


TABLE VI-1 Tracer Monitoring Locations (with Abbreviations)

LOCATION	CODE
Blue Spring Cave	BsC
Blacksmith Spring	BsS
Crusher Building Spring	CBS
CCC Spring	CCC
Donaldson Cave-main stream	DnC-1
Donaldson Cave-small stream	DnC-2
Donaldson Cave-PVC pipe	DnC-3
Downhill from Rockpile Seep	DRS
Erwin Spring (Rock Lick) Cave	ESC
Hamer Cave	HmC
Lehigh Cave	LhC
Lehigh Quarry Discharge	LQD
Lehigh Quarry Spring Cave	LQS
Lehigh Quarry Spring #2	LQS-2
Lehigh Quarry Seep	LSp
North Face Seepage	NFS
Old Quarry Seep	OQS
Orangeville Rise	OvR
Quarry Road Block Spring	QBS
Quarry Road New Spring	QNS
Quarry Road Pipe Spring	QPS
Quarry Road Spring	QRS
Quarry Road Seep	QSp
Quarry Road Upstream Spring	QUS
Rabbitville Quarry Rise	RQR
Rock Lick Br. Spr.-downstream	RSD
Rock Lick Br. Spr.-middle	RSM
Rock Lick Br. Spr.-upstream	RSU
Springhouse Seep	ShS
Sewage Plant Spring	SPS
Whistling Cave-main stream	WhC-1
Whistling Cave-downstream	WhC-B
Wind Cave	WnC

—P.E. LaMoreaux & Associates—

larger scale in Figure I-1. In addition to the features listed in Table VI-1, five locations monitored in Rock Lick Branch at various times during the traces are also shown in Figure I-1.

Springs were identified along both sides of Rock Lick Branch. Groundwater discharging along the east side of the stream appears to be flowing generally down the regional dip, whereas springs on the west side of the stream have presumably developed in response to localized reversal of the regional dip. According to Palmer and Palmer (1975, p. 28), "No cave was observed conclusively to have been formed by [groundwater] flow against the dip, since the caves containing flow toward the east, against the regional dip, were found to be situated in areas of local dip reversal."

During groundwater tracing activities, virtually the entire flow of Rock Lick Branch adjacent to the site was derived from Quarry Road Upstream Spring (QUS). Immediately upstream of that location, the streambed was dry. However, the stream channel contained flowing water further upstream at the sewage treatment plant operated by the City of Mitchell. Based on this and the observed variability of discharge and water quality at QUS, it is apparent that the flow of Rock Lick Branch sinks into the ground downstream of the sewage plant and resurges at QUS.

3. GROUNDWATER TRACING METHODOLOGY

Tracers used in hydrology include gases, particulate material, biological material, thermal energy, ionized substances, radioactive substances, and fluorescent dyes. Reviews of tracers are provided by Davis and others (1985) and Reid (1981). When selecting a tracer, consideration should be given to its potential physical and chemical interactions with the groundwater and the aquifer media (Davis and others, 1985). Atkinson and Smart (1981) describe the ideal tracer as "non-toxic and easily measured at great dilutions. It should be absent from the groundwater to be studied or present in only very low concentrations. It should not react chemically with the groundwater or be adsorbed on to the aquifer rock, and should move at the same rate as the water carrying it. Finally, it should be cheap and readily available." They add, "No tracer substance yet discovered meets all of these criteria."

However, fluorescent dyes have proven effective for most groundwater tracing applications in karst aquifers. Quinlan (1986) estimates that 90 percent of groundwater tracing experiments in the U.S. have been conducted with dyes in karst aquifers. Because of their flow characteristics, karst systems are ideally suited for groundwater tracing. Smart and Laidlaw (1977) assess eight fluorescent dyes for sensitivity and detectability, natural (background) fluorescence, effect of water chemistry, photochemical and biological decay rates, adsorption by organic matter and sediments, toxicity to humans and aquatic organisms, and cost. They conclude that rhodamine WT is the most favorable of the tested dyes. Smart (1984) reviews the potential toxicity of twelve fluorescent dyes and concludes that fluorescein, rhodamine WT, and an optical brightener (Tinopal CBS-X) are neither carcinogenic nor mutagenic.

P.E. LaMoreaux & Associates

Two commonly used dyes were selected for use during this investigation—a 50 percent solution of fluorescein (CI Acid Yellow 73) and a 20 percent solution of rhodamine WT (CI Acid Red 388). Both can be detected in water samples and quantified using a filter fluorometer or a spectrofluorophotometer. Alternatively, passive monitoring can be performed by deploying a dye receptor (“bug”) consisting of activated carbon in the water at each monitoring location. Dye adsorbed by the bug can be eluted from the carbon in the laboratory and analyzed fluorometrically. The analysis of a water sample is truly quantitative, allowing a precise determination of the dye concentration at a point in time. However, the analysis of a bug is only semi-quantitative—i.e., the dye concentration measured in the dye-eluant mixture cannot be related directly to its original concentration in the water. Because of the nature of the dye adsorption process, a low concentration of dye passing through a bug over an extended period of time can produce a higher-concentration analytical result than a high concentration of dye passing through a bug relatively quickly.

During this investigation, both dye monitoring methods were used. Bugs were deployed on September 3, 1997, prior to the initiation of groundwater tracing. They were retrieved for analysis and replaced with fresh ones at one- to two-week intervals until the final retrieval on December 8. On September 22, October 27-28, and November 10-11, water samples were collected at locations with sufficient flow. The bugs and water samples were analyzed for dye using a scanning spectrofluorophotometer. Water samples were also collected more intensively during the groundwater tracing events and analyzed with a filter fluorometer, as described in Section (b). The scanning spectrofluorophotometer was used for the routine analyses because of its ability to differentiate multiple dyes and to distinguish between the project dyes and other fluorescent compounds.

a) Background Monitoring

At the beginning of field work, it is essential to monitor background conditions at area springs and streams with respect to the presence of the tracers to be used during the study. This facilitates the selection of dyes for use during the project and reduces the risk of obtaining misleading results—i.e., false positives. At each feature to be monitored, dye receptors (bugs) were placed into the water on September 3, 1997. On September 22 (prior to the first dye insertion), they were replaced with fresh bugs, and water samples were collected at locations with sufficient flow. The bugs and water samples were analyzed for dye using a scanning spectrofluorophotometer.

According to data reported by Duwelius and others (1995, p. 229), background fluorescence within the spectral range of fluorescein was detected at low parts-per-billion concentrations at seven locations, and optical brightener—presumably from septic-tank effluent—was also detected in background samples. They detected no background fluorescence within the spectral ranges for rhodamine WT, eosine, or direct yellow. During this investigation, no monitoring sites were found to have

background levels of fluorescein or rhodamine WT that would preclude the use of these dyes during the study.

b) Groundwater Tracing Events

Five solution sinkholes adjacent to the site (Sinkholes B through F) were used to facilitate the introduction of dye into the karst aquifer (Figure I-1). At four of these locations, dye was inserted through natural openings (Figure VI-3). At Sinkhole D, dye was inserted into a small cavity exposed by excavating with a backhoe.

Prior to each dye insertion, a 2,000-gallon slug of potable water was introduced into the sinkhole. The water slugs were used to confirm that each sinkhole "drain" was permeable enough to allow the passage of dye into the subsurface. They also served to "pre-wet" the underground passages to increase the flow of dye. The dye was inserted with the beginning of a second 2,000-gallon slug of water, which was followed with one or two additional slugs. The use of pre- and post-dye water insertions has proven to be an effective means for introducing dye into karst aquifers via sinkholes (Mull and others, 1988).

Initially, it was hypothesized that dye from each sinkhole would be discharged from the karst groundwater system via the Three Springs area. Based on that hypothesis, a small quantity of dye was used for the initial traces so that it would be flushed from the groundwater system relatively quickly without perceptibly discoloring Rock Lick Branch. During a series of traces on September 23-25, 1997, Rhodamine WT (25 mL) was inserted into Sinkholes B and C, and fluorescein was inserted into Sinkholes E (25 mL) and F (100 mL). A larger amount of dye was used at Sinkhole F because of its greater distance from the hypothesized discharge area. The purpose of these initial traces was to evaluate the hypothesis that the four Sinkholes are hydrologically connected with the Three Springs area on Rock Lick Branch before using larger quantities with the potential to have a more significant visual impact on the stream.

During each of these initial traces, water samples were collected manually at QRS, QNS, and Quarry Road Block Spring (QBS). Samples were also collected just downstream of the location where discharge from QRS enters Rock Lick Branch (Rock Lick Branch Station #1, RLB-1). Immediately upon collection, water samples were analyzed in the field with a filter fluorometer (Figure VI-4). By determining dye concentrations at each feature immediately, it was possible to adjust the sampling frequency as necessary to provide higher data resolution during the rapidly increasing "rising limb" of the dye breakthrough curves. It also made it possible to determine when dye from one trace had been flushed from the groundwater system sufficiently to permit the next trace to be conducted. Following initial dye insertions at Sinkholes B, C, E, and F, dye bugs were replaced on October 6-7, 1997 and analyzed for dye using a scanning spectrofluorometer.

—P.E. LaMoreaux & Associates—

FIGURE VI-3 Dye Insertions at Sinkholes B and F



A. Rhodamine WT insertion at Sinkhole B on September 25, 1997 at 08:32.



B. Preparation for fluorescein insertion at Sinkhole F on October 15, 1997 at 13:05.

FIGURE VI-4 Dye Monitoring at QRS



- A. Fluorescein flowing through weir at Quarry Road Spring (QRS) on the morning of October 16, 1997 after being inserted into Sinkhole F on October 15, 1997 at 13:05. Large numbers on staff gage in background are 10 centimeters apart.



- B. Fluorometer used for on-site dye analyses; photograph made October 16, 1997.

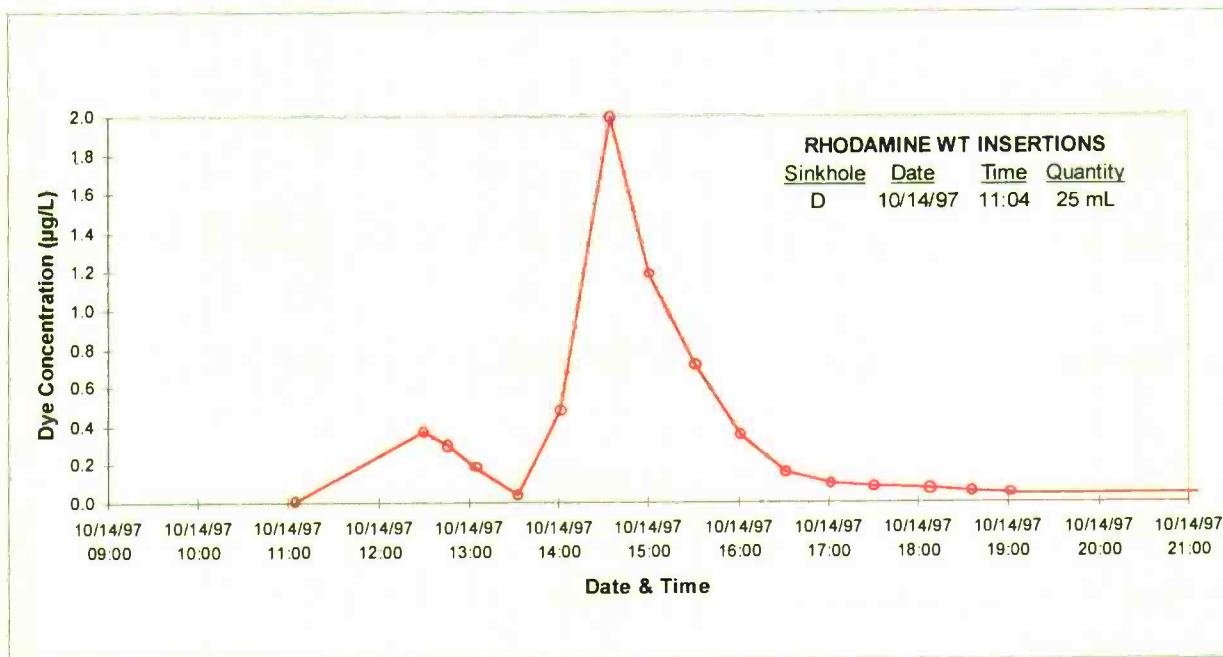
The initial trace from Sinkhole D was conducted on October 14 using 25 mL of rhodamine WT. In conjunction with that activity, a second trace was conducted from Sinkhole F on October 15 using 1 liter of fluorescein. The purpose of using a larger quantity of dye for this trace was to determine whether any of the monitoring locations more distant than the Three Springs area are also hydrologically connected with the most upgradient sinkhole at the site. Because the initial tracing indicated that at least some of the dye would be discharged into Rock Lick Branch, the Lawrence County Health Department and other local authorities were notified of the anticipated discoloration. During these traces, samples were collected from QRS, QBS, and QNS, as well as several features further upstream along Rock Lick Branch: QUS, Quarry Road Pipe Spring (QPS), Lehigh Cave, and Rock Lick Branch Station #2 (RLB-2). Dye bugs replaced before these traces on October 13-14 and one week later on October 20-21 were analyzed for dye using a scanning spectrofluorophotometer.

As discussed in Section B, the hypothesis was confirmed for initial traces from Sinkholes B, C, E, and F—i.e., the dye was discharged in the Three Springs area. However, based on analyses conducted in the field during the initial trace from Sinkhole D, it was not immediately evident that the dye had been detected at any of the monitoring locations. Moreover, rhodamine WT was not detected in any of the dye bugs retrieved from the field on October 27-28 or November 10-11, as discussed in Section B.

Upon replicate analysis of the samples in the laboratory (and a more thorough analysis of the data from the field-based analyses), it was apparent that a small concentration of rhodamine WT had been detected in Rock Lick Branch (at RLB-2) soon after its introduction at Sinkhole D (Figure VI-5 and pages B-18 and B-19 in Appendix B). The double peaks in Figure VI-5 indicate that the dye entered the stream in conjunction with two water insertions at Sinkhole D. Because the dye was not detected at any other monitoring location, it was hypothesized that it had been discharged through a previously unidentified feature in the stream channel. In order to locate the suspected discharge point, 1 gallon of rhodamine WT was introduced into Sinkhole D on November 18. A large amount of dye was used to ensure that its emergence into Rock Lick Branch would be visible. Following the final dye insertion, dye bugs were retrieved from the field on November 24-25 and December 8.

All water samples analyzed in the field were kept on ice in the dark and returned to the laboratory for reanalysis following each tracing event. Laboratory-based analysis permits instrument and sample temperatures to stabilize in a controlled environment and allows turbidity to settle in the samples. Both factors make measurements more precise and more accurate. All dye concentrations reported in this document were determined by analyses in the laboratory.

FIGURE VI-5 Dye Breakthrough Curve for RLB-2



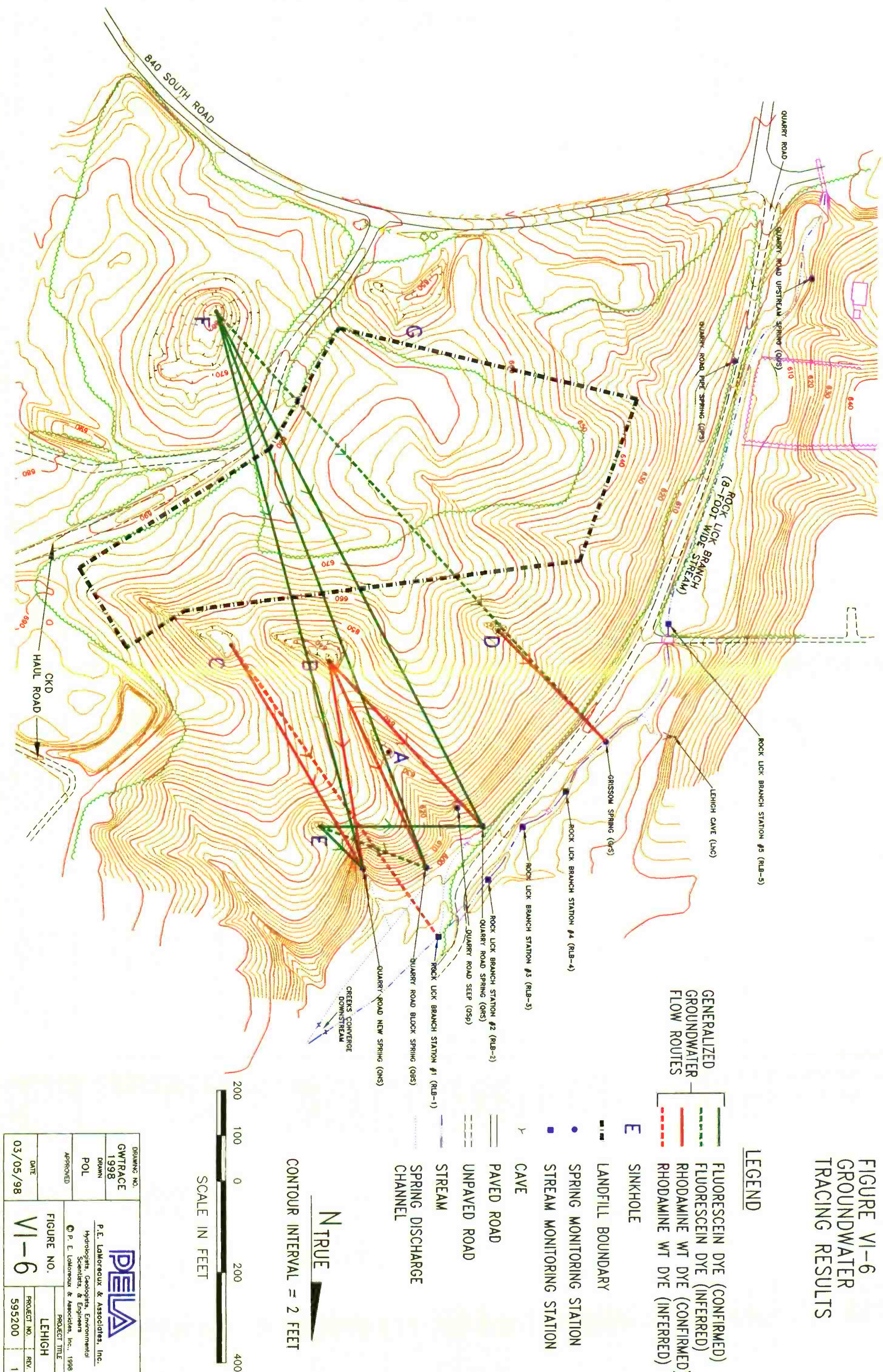
This pair of peaks at Rock Lick Branch Station #2 (RLB-2) results from the introduction of rhodamine WT into Sinkhole D. Presumably, the dye reached RLB-2 after being discharged from Grissom Spring (GrS), which had not been identified at the time of this trace. Each peak corresponds with the insertion of a slug of water at Sinkhole D.

B. RESULTS OF GROUNDWATER TRACING INVESTIGATION

The results of the groundwater tracing investigation are summarized in Figure VI-6 and Table VI-2. The generalized routes of subsurface flow depicted in Figure VI-6 were determined by interpretation of dye breakthrough curves developed from the fluorometric analyses of water samples (Appendix A) collected during tracing activities (see example curve in Figure VI-7).

Dye was inserted on seven occasions, and twelve locations were actively monitored at various times during those traces (Table VI-2). More than 650 water samples were collected and analyzed. Each sample was analyzed once in the field for fluorescein and/or rhodamine WT. In the laboratory, 666 samples were analyzed for fluorescein, and 609 samples were analyzed for rhodamine WT. The interpretations in Table VI-2 were made from the results of the 1,275 laboratory-based analyses. These fluorometric results and the associated dye breakthrough curves (at various scales) are presented in Appendices A and B, respectively.

FIGURE VI-6
GROUNDWATER
TRACING RESULTS



LEGEND

- FLUORESCEN DYE (CONFIRMED)
- FLUORESCEN DYE (INFERRED)
- RHODAMINE WT DYE (CONFIRMED)
- RHODAMINE WT DYE (INFERRED)

- E SINKHOLE
- LANDFILL BOUNDARY
- SPRING MONITORING STATION
- STREAM MONITORING STATION
- CAVE
- PAVED ROAD
- UNPAVED ROAD
- STREAM
- SPRING DISCHARGE CHANNEL

TRUE N
CONTOUR INTERVAL = 2 FEET

SCALE IN FEET
200 100 0 200 400

DRAWING NO. GWTRACE 1998	P. E. LaMoreaux & Associates, Inc. Hydrologists, Geologists, Environmental Scientists, & Engineers © P. E. LaMoreaux & Associates, Inc., 1998	FIGURE NO. VI-6	PROJECT TITLE LEHIGH	
DRAWN POL			PROJECT NO. 595200	REV. NO. 1
APPROVED				
DATE 03/05/98				

TABLE VI-2 Summary of Groundwater Tracing Results

(Part 1 of 2; see notes on next page)

TRACER INSERTION			DISCHARGE OR MONITORING LOCATION (See Table VI-1 and Figure VI-4)												
LOCATION	DATE	DYE	VOLUME	QUS	QPS	RLB-5	LhC	GrS	RLB-4	RLB-3	RLB-2	RLB-1	QRS	QBS	QNS
	TIME	TYPE		Hydrologic Connection Indicated? (YES or NO) Time from Dye Insertion to First Detection (hours:minutes) Page Numbers in Appendix B Containing the Dye Breakthrough Curves on which the Interpretation is Based											
Sinkhole B	09/25/97 08:32	Rhodamine WT	25 mL	*	*	*	*	*	*	*	*	YES (1) 1:56 27,30	YES 1:08 38,39	YES 3:08 51,52	YES 2:39 60,61, 62,65
Sinkhole C	09/24/97 10:02	Rhodamine WT	25 mL	*	*	*	*	*	*	*	*	YES (2) 1:59 27,28, 29	? (3) 38,39	NO 51,52	YES 1:29 60,61,62, 63,64
Sinkhole D	10/14/97 11:04	Rhodamine WT	25 mL	NO 3,4	NO 7	*	NO 11	YES (4) 1:26 8,12,13,16, 17,18,19, 20,21	*	*	YES 1:26 16,17, 18,19	NO? (5) 40,41, 42,44	NO? (6) 51,53,54	NO? (7) 60,66, 67,68	
Sinkhole D	11/18/97 12:23	Rhodamine WT	1 Gallon	*	*	NO 8	NO 11	YES 0:37 8,12,13,16, 17,18,19, 20,21	YES 0:37 12	YES 0:38 16,17, 20,21	*	NO 45	*	*	
Sinkhole E	09/25/97 11:04	Fluorescein	25 mL	*	*	*	*	*	*	*	*	NO (8) 22,23,24 25,26	YES 0:06 31,32, 33,34	YES? (9) N/A 31-34, 47-52, 55-58	YES 0:07 55,56, 57,58
Sinkhole F	09/23/97 10:34	Fluorescein	100 mL	*	*	*	*	YES? (4) ?? :?? 14,15	*	*	*	YES (1) 21:29 22,23,24, 25,26	YES 5:46 31,32,33	YES 10:00 46,47,48	YES 1:25 55,58
Sinkhole F	10/15/97 13:05	Fluorescein	1 Liter	NO 1,2	NO 5,6	*	NO 9,10	YES? (4) 7 days 14,15	*	YES 7 days 14,15	*	YES 3:55 31,36,37	YES 4:54 49,50	YES 4:57 55,59	

TABLE VI-2 Summary of Groundwater Tracing Results (Continued)

(Part 2 of 2)

NOTES

The interpretations in this table are based on the data presented in Appendix A and the associated dye breakthrough curves in Appendix B. Quarry Road Seep (QSp) was not actively monitored during groundwater tracing because there was no perceptible discharge to sample. However, passive monitoring was conducted with dye receptors.

* Not monitored.

YES? Hydrologic connection appears to be indicated by the data in Appendices B and C, but the data are not conclusive. (See appropriate footnote.)

NO? Hydrologic connection does not appear to be indicated by the data in Appendices B and C, but the data are not conclusive. (See appropriate footnote.)

? Determination regarding the existence of a hydrologic connection cannot be made based on the data in Appendices B and C. (See appropriate footnote.)

(1) Rock Lick Branch Station #1 (RLB-1) is downstream of the discharge from Quarry Road Spring (QRS). Fluorescein inserted into Sinkhole F was discharged from QRS prior to detection at RLB-1. Thus, it is assumed that dye detected at RLB-1 came from QRS.

(2) Rock Lick Branch Station #1 (RLB-1) is upstream of the discharge from Quarry Road New Spring (QNS). Rhodamine WT inserted into Sinkhole C was detected at both locations (QNS & RLB-1). Therefore, dye detected at RLB-1 must have emerged from an unidentified groundwater discharge feature, presumably a joint in the bedrock bottom of Rock Lick Branch (analogous to Grissom Spring, GrS).

(3) There is not enough data to determine conclusively whether the double rhodamine WT peaks at Quarry Road Spring (QRS) on 09/25/97 and 09/26/97 result from dye injections in Sinkholes B and C or from Sinkhole B only.

(4) Traces from Sinkhole D (10/14/97 @ 11:04) and Sinkhole F (10/15/97 @ 13:05) revealed connections with Rock Lick Branch Station #2 (RLB-2), strongly suggesting that dye from these sinkholes passed through Grissom Spring (GrS), which had not been identified until the trace from Sinkhole D on 11/18/97 @ 12:23.

(5) The peak concentration of apparent rhodamine WT on 10/15/97 @ 13:22 (0.28 µg/L) may be a product of turbidity induced by the injection of water and dye into Sinkhole F on 10/15/97 @ 13:05, as it was demonstrated that Sinkhole F is connected with Quarry Road Spring (QRS). The peak concentration of apparent rhodamine WT on 10/16/97 @ 07:35 (5.24 µg/L) is a product of a high concentration of fluorescein in the sample (~65,500 µg/L).

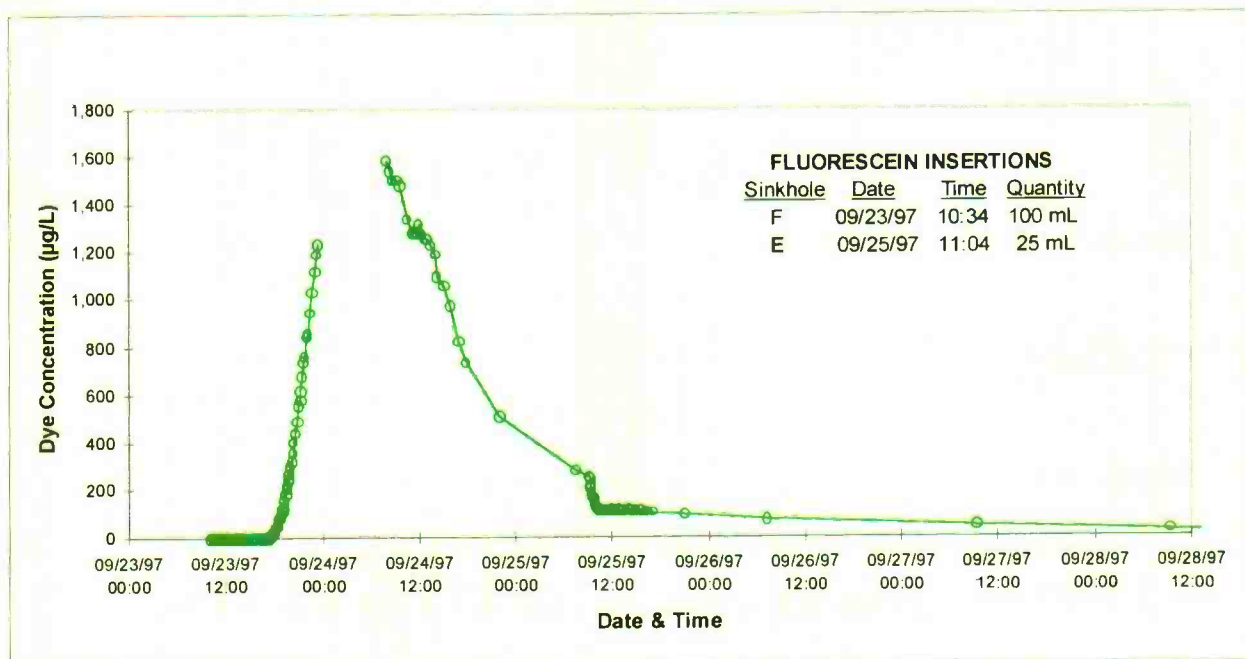
(6) The peak concentration of apparent rhodamine WT on 10/16/97 @ 07:31 (1.92 µg/L) is a product of a high concentration of fluorescein in the sample (~25,000 µg/L), which would also obscure any very low concentration of rhodamine WT that may actually be present.

(7) The peak concentration of apparent rhodamine WT on 11/01/97 @ 13:34 (0.02 µg/L) is only twice the background level (0.01 µg/L), which is approximately at the limit of detection.

(8) The fluorescein peak on 09/25/97 at 10:28 occurred before dye was inserted into Sinkhole E at 11:04. Therefore, this peak must result from dye inserted into Sinkhole F on 09/23/97 @ 10:34.

(9) Traces from Sinkholes B and F suggest that Quarry Road Block Spring (QBS) is in hydraulic communication with Quarry Road Spring (QRS) and Quarry Road New Spring (QNS). The trace from Sinkhole E indicates a hydraulic connection to QRS and QNS. Therefore, it is assumed that Sinkhole E is also hydraulically connected to QBS, although the data do not explicitly demonstrate this.

FIGURE VI-7 Typical Dye Breakthrough Curve



This peak represents a "classic" dye breakthrough curve for fluorescein inserted into Sinkhole F and detected at Quarry Road Spring (QRS). The data gap results from human samplers going to bed during the night.

As indicated in Section A3(b), the results of the initial trace from Sinkhole D suggested the existence of a previously unidentified spring located adjacent to the site along Rock Lick Branch. In order to make its location visible, a subsequent tracing experiment was conducted by introducing 1 gallon of rhodamine WT into Sinkhole D. Approximately one-half hour after the dye was inserted, it was observed flowing into the stream via two adjacent features (Figure VI-8). The discharge of dye is also documented by the dye breakthrough curves from three downstream monitoring locations (Figure VI-9 and pages B-12, B-13, and B-21 in Appendix B). The features are referred to collectively as Grissom Spring (GrS). They occur where a major joint intersects a bedding-plane parting, both of which have been enlarged by dissolution.

The presence of a similar feature further downstream is suggested by data collected during the trace from Sinkhole C (Figure VI-10 and page B-28 in Appendix B). Rhodamine WT inserted into Sinkhole C was detected at RLB-1, even though it was not detected at any spring upstream of that location. (It was also detected at QNS at approximately the same time, but the discharge from QNS enters Rock Lick Branch downstream of RLB-1.) Therefore, dye detected at RLB-1 must have emerged from an unidentified groundwater discharge feature, such as another set of joints and bedding-plane partings observed in the streambed of Rock Lick Branch (Figure VI-11).

FIGURE VI-8 Rhodamine WT Discharging from Grissom Spring

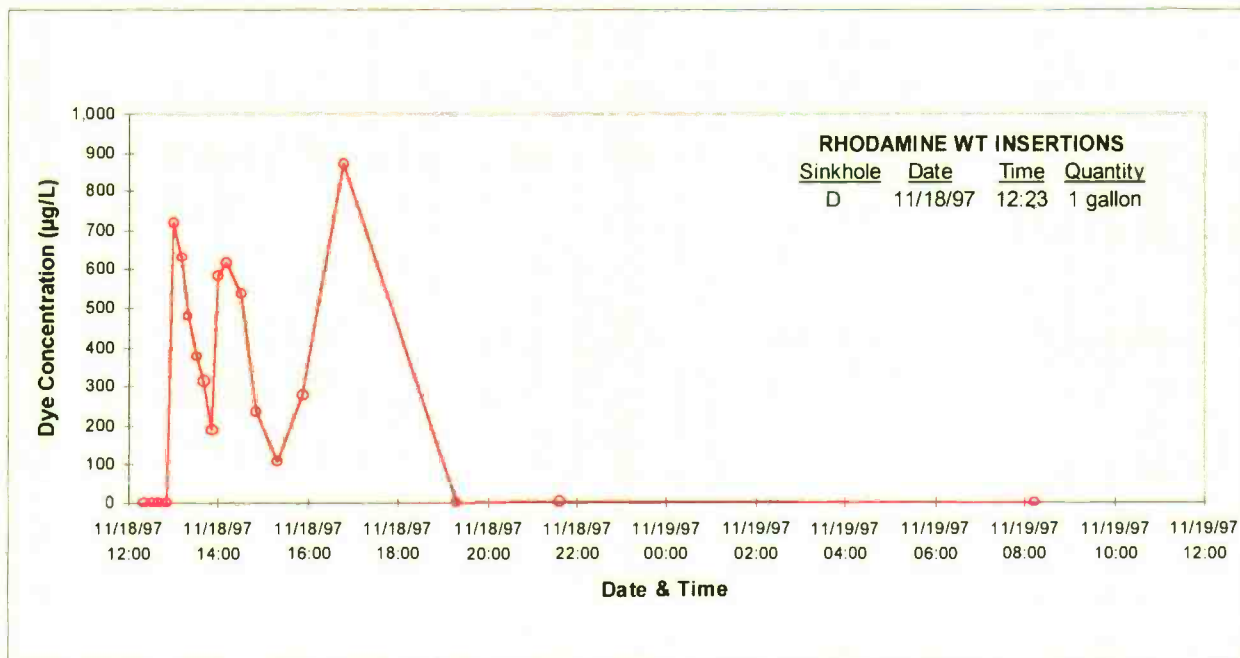


A. Rhodamine WT discharging into Rock Lick Branch from Grissom Spring (GrS) on November 18, 1997 at about 14:00 after being inserted into Sinkhole D at 12:23.



B. Rhodamine WT discharging into Rock Lick Branch from Grissom Spring (GrS) on November 18, 1997 at about 14:00 after being inserted into Sinkhole D at 12:23.

FIGURE VI-9 Dye Breakthrough Curve for RLB-4

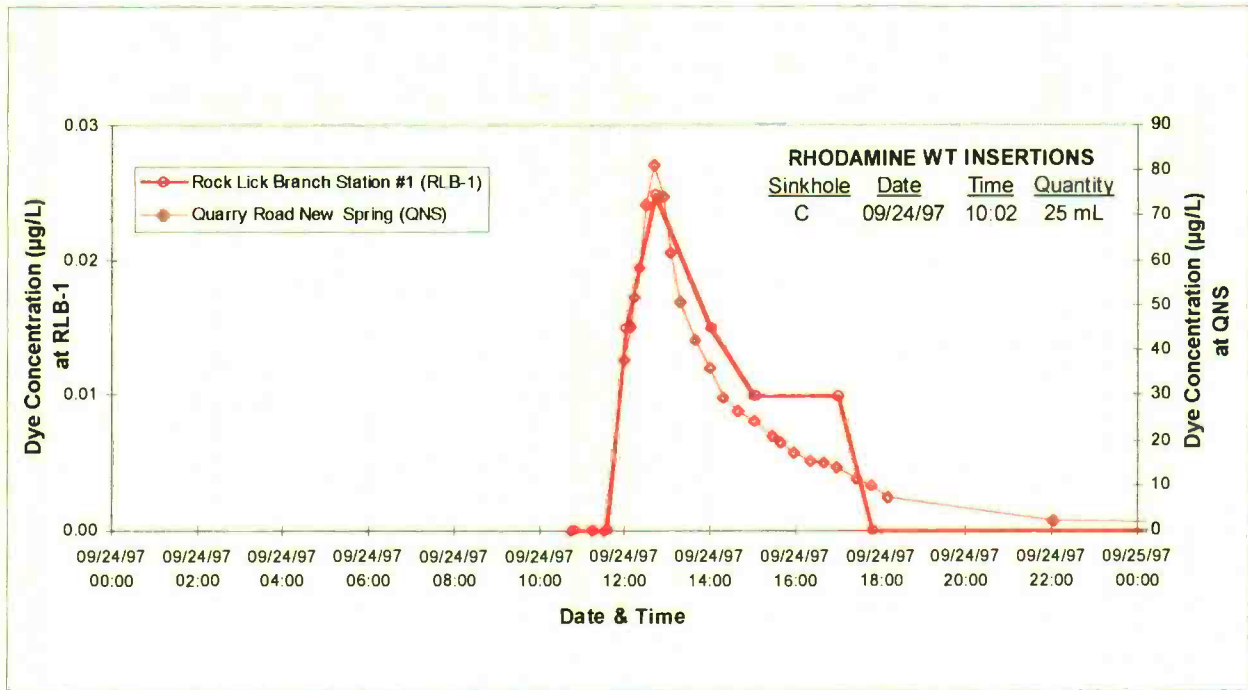


These Rhodamine WT concentrations were measured at Rock Lick Branch Station #4 while the dye was (visually) observed discharging from Grissom Spring (GrS). Individual peaks result primarily from water insertions at Sinkhole D.

Tables VI-3 through VI-6 show the results of the spectrofluorophotometric analyses of water samples and dye bugs. These results apply primarily to the monitoring locations which are not immediately adjacent to the site¹—i.e., those locations where intensive sampling and on-site fluorometric analysis did not occur. Analysis of these results confirms the detection of dye at QRS, QBS, and QNS. Moreover, **the data do not indicate the existence of any karst groundwater connections between sinkholes at the site and the monitoring locations at Spring Mill State Park, Blue Spring Cave, or Orangeville Rise.** Therefore, the results of this tracing investigation demonstrate that **site groundwater discharges from four (possibly five) springs located adjacent to the site along Rock Lick Branch: GrS, QRS, QBS, QNS, and possibly an unidentified feature between RLB-2 and RLB-1 (Figure VI-6).**

¹ Because dispersion of dye increases with the length of its flow route, bugs at relatively distant monitoring locations are exposed to a passing dye cloud for a longer period of time than bugs very near the dye insertion point. As noted above in Section A3, longer contact time between the dye and the bug makes relatively low concentrations more readily detectable.

FIGURE VI-10 Dye Breakthrough Curves for RLB-1 and QNS



Rhodamine WT inserted into Sinkhole C is detected at Rock Lick Branch Station #1 (RLB-1) and Quarry Road New Spring (QNS). The discharge from QNS enters Rock Lick Branch downstream of RLB-1, and the dye is not detected at Quarry Road Spring (QRS; see Page B-29 in Appendix B). Therefore, dye detected at RLB-1 must have emerged from an unidentified groundwater discharge feature, presumably a joint in the bedrock bottom of Rock Lick Branch (analogous to Grissom Spring, GrS).

FIGURE VI-11 Joints in Bedrock Streambed of Rock Lick Branch



View downstream along Rock Lick Branch from bridge on Quarry Road. Note the prominent jointing in the bedrock streambed. A bedding-plane parting is present beneath the small cascade downstream of the joints. Photograph made June 5, 1997.

TABLE VI-3 Results of Analyses for Fluorescein in Dye Bugs

LOCATION	CODE	FLUORESCENCE CONCENTRATION IN DYE BUGS (µg/L)							
		Date of Bug Retrieval from the Field in 1997							
		09/22	10/06	10/13	13/20	10/27	11/10	11/24	12/08
			10/07	10/14	10/21	10/28	11/11	11/25	
Blue Spring Cave	BsC	2.8	10.1	0.3	1.1	1.7	3.2		6.7
Blacksmith Spring	BsS		2.2	BDL	1.6	2.8	BDL	3.4	2.8
Crusher Building Spring	CBS	1.4		0.2	0.6				
CCC Spring	CCC	1.6	1.3	BDL	0.4	BDL	1.6		0.7
Donaldson Cave-main stream	DnC-1		1.6	BDL	1.7	0.8	2.5 ^(?)	2	3.6 ⁽¹⁾
Donaldson Cave-small stream	DnC-2		2.5	1.2	2 ^(?)	1.8	0.6	4.5	2.4 ^(?)
Donaldson Cave-PVC pipe	DnC-3	1.6	2	BDL	1.1	BDL	5.6	2.8	2.8
Downhill from Rockpile Seep	DRS	1	1.7	0.2	0.8				
Erwin Spring (Rock Lick) Cave	ESC	3.9	2.5	3.6	1.8	1.8	2.1	2.1	3.6
Hamer Cave	HmC	4.7	2.9	4.2	2.1	3.4	5.1	3.2	3.8
Lehigh Cave	LhC	4.8	5.8	20	5.9	7	10.1	4.6	4.6
Lehigh Quarry Discharge	LQD	3.8	5.4	BDL	2.4	3.9	5.6	2.8	4.4
Lehigh Quarry Spring Cave	LQS	1.1	0.8	0.2	0.3	0.5	0.8	0.7	0.6 ^(?)
Lehigh Quarry Spring #2	LQS-2	1.4	0.6	0.2	0.6	0.7	0.5		1.7
Lehigh Quarry Seep	LSp	3.6	2	1.6	1.6 ^(?)	5.4	4		3.3
North Face Seepage	NFS	3.6	0.4	0.3	0.7	BDL	4.4	2.2	2.8
Old Quarry Seep	OQS	1.9	1.5	BDL	BDL	0.7	2.6	0.4	3
Orangeville Rise	OvR		2.5	9	2.8	1.6	6.3	10.2 ⁽²⁾	4.8
Quarry Road Block Spring	QBS	3.6	2600	950	500	700	2200	3300⁽³⁾	4400
Quarry Road New Spring	QNS		650	23	17	24	19	27	10.3
Quarry Road Pipe Spring	QPS		4.3	4.6	3.6	6.5	7.7	4.9	10.2
Quarry Road Spring	QRS	2.8	7500	520	800	900	1800	7100⁽⁴⁾	3700
Quarry Road Seep	QSp	0.9	0.9	0.4	0.4				
Quarry Road Upstream Spring	QUS		2.4	3.6	5.0	5.8	19	7.7	6.5
Rabbitville Quarry Rise	RQR	1.8	0.8	0.4	0.6	BDL	1.1	0.6	1.9
Rock Lick Br. Spr.-downstream	RSD	1.2	1.1	3 ^(?)	2.4 ^(?)	3.6	3.8		
Rock Lick Br. Spr.-middle	RSM	3.6	0.2	0.4	1.2	0.7	2.7		1.7
Rock Lick Br. Spr.-upstream	RSU	3.4	90	2.3	110	16	9.3		
Springhouse Seep	ShS	1.8	0.7	BDL	0.3	BDL ^(?)	BDL ^(?)		0.5 ^(?)
Sewage Plant Spring	SPS	4.4	3.7	5.6	4.6	4.6	9.5	4.2	10.4
Whistling Cave-main stream	WhC-1	0.9	0.6	0.4	0.5	0.9	1	1.9	0.8
Whistling Cave-downstream	WhC-B	3.3	4.6	4.7	3.2	BDL	6	5	3 ⁽⁵⁾
Wind Cave	WnC	3.4	3.5	BDL	1.4	BDL	3.8	3.2	2.7

NOTES:

Analyses were performed on a Shimadzu RF 5000 U spectrofluorophotometer.

Values in **boldface** type are interpreted to represent concentrations of project dye.

BDL Below Detection Limit

^(?) Peak is not distinct or well matched to the typical dye emission spectrum.

⁽¹⁾ The result of an analysis of an additional dye bug was 1.5 µg/L.

⁽²⁾ The result of an analysis of an additional dye bug was 1.2 µg/L.

⁽³⁾ The result of an analysis of an additional dye bug was 3200 µg/L.

⁽⁴⁾ The result of an analysis of an additional dye bug was 5500 µg/L.

⁽⁵⁾ The result of an analysis of an additional dye bug was 1.9 µg/L.

P.E. LaMoreaux & Associates

TABLE VI-4 Results of Analyses for Rhodamine WT in Dye Bugs

LOCATION	CODE	RHODAMINE WT CONCENTRATION IN DYE BUGS (µg/L)							
		Date of Bug Retrieval from the Field in 1997							
		09/22	10/06 10/07	10/13 10/14	13/20 10/21	10/27 10/28	11/10 11/11	11/24 11/25	12/08
Blue Spring Cave	BsC	BDL	BDL	BDL	BDL	BDL	BDL		BDL
Blacksmith Spring	BsS		BDL	BDL	BDL	BDL	BDL	BDL	BDL
Crusher Building Spring	CBS	BDL		BDL	BDL				
CCC Spring	CCC	BDL	BDL	BDL	BDL	BDL	BDL		BDL
Donaldson Cave-main stream	DnC-1		BDL	BDL	BDL	BDL	BDL	BDL	BDL
Donaldson Cave-small stream	DnC-2		BDL	BDL	BDL	BDL	BDL	BDL	BDL
Donaldson Cave-PVC pipe	DnC-3	BDL	BDL	BDL	BDL	BDL	BDL	BDL	BDL
Downhill from Rockpile Seep	DRS	BDL	BDL	BDL	BDL				
Erwin Spring (Rock Lick) Cave	ESC	BDL	BDL	BDL	BDL	BDL	BDL	BDL	BDL
Hamer Cave	HmC	BDL	BDL	BDL	BDL	BDL	BDL	BDL	BDL
Lehigh Cave	LhC	BDL	BDL	BDL	BDL	BDL	BDL	BDL	BDL
Lehigh Quarry Discharge	LQD	BDL	BDL	BDL	BDL	BDL	BDL	BDL	BDL
Lehigh Quarry Spring Cave	LQS	BDL	BDL	BDL	BDL	BDL	BDL	BDL	BDL
Lehigh Quarry Spring #2	LQS-2	BDL	BDL	BDL	BDL	BDL	BDL		BDL
Lehigh Quarry Seep	LSp	BDL	BDL	BDL	BDL	BDL	BDL		BDL
North Face Seepage	NFS	BDL	BDL	BDL	BDL	BDL	BDL	BDL	BDL
Old Quarry Seep	OQS	BDL	BDL	BDL	BDL	BDL	BDL	BDL	BDL
Orangeville Rise	OvR		BDL	BDL	BDL	BDL	BDL	BDL	BDL
Quarry Road Block Spring	QBS	BDL	22⁽¹⁾	BDL	BDL	BDL	BDL	BDL	BDL
Quarry Road New Spring	QNS		0.8⁽¹⁾	BDL	BDL	BDL	BDL	BDL	BDL
Quarry Road Pipe Spring	QPS		BDL	BDL	BDL	BDL	BDL	BDL	BDL
Quarry Road Spring	QRS	BDL	1.5⁽¹⁾	10^(?)	BDL	BDL	BDL	BDL	BDL
Quarry Road Seep	QSp	BDL	BDL	BDL	BDL				
Quarry Road Upstream Spring	QUS		BDL	BDL	BDL	BDL	BDL	BDL	BDL
Rabbitville Quarry Rise	RQR	BDL	BDL	BDL	BDL	BDL	BDL	BDL	BDL
Rock Lick Br. Spr.-downstream	RSD	BDL	BDL	BDL	BDL	BDL	BDL		
Rock Lick Br. Spr.-middle	RSM	BDL	BDL	BDL	BDL	BDL	BDL		BDL
Rock Lick Br. Spr.-upstream	RSU	BDL	BDL	BDL	BDL	BDL	BDL		
Springhouse Seep	ShS	BDL	BDL	BDL	BDL	BDL	BDL		BDL
Sewage Plant Spring	SPS	BDL	BDL	BDL	BDL	BDL	BDL	BDL	BDL
Whistling Cave-main stream	WhC-1	BDL	BDL	BDL	BDL	BDL	BDL	BDL	BDL
Whistling Cave-downstream	WhC-B	BDL	BDL	BDL	BDL	BDL	BDL	BDL	BDL
Wind Cave	WnC	BDL	BDL	BDL	BDL	BDL	BDL	BDL	BDL

NOTES:

Analyses were performed on a Shimadzu RF 5000 U spectrofluorophotometer.

Values in **boldface type** are interpreted to represent concentrations of project dye.

BDL Below Detection Limit

^(?) Peak is not distinct or well matched to the typical dye emission spectrum.

⁽¹⁾ This result is "depressed" because acidification was used to reduce interference from fluorescein.

TABLE VI-5 Results of Analyses for Fluorescein in Water Samples

LOCATION	CODE	FLUORESCCEIN CONCENTRATION IN WATER (µg/L)		
		Date of Sample Collection in 1997		
		09/22	10/27 10/28	11/10 11/11
Blue Spring Cave	BsC	BDL	BDL	BDL
Blacksmith Spring	BsS	BDL	BDL	
Crusher Building Spring	CBS			
CCC Spring	CCC		BDL	
Donaldson Cave-main stream	DnC-1	BDL	BDL	BDL
Donaldson Cave-small stream	DnC-2	0.03	0.1	0.1 ^(?)
Donaldson Cave-PVC pipe	DnC-3			
Downhill from Rockpile Seep	DRS			
Erwin Spring (Rock Lick) Cave	ESC	BDL	BDL	BDL
Hamer Cave	HmC	BDL	BDL	
Lehigh Cave	LhC	BDL	BDL	BDL
Lehigh Quarry Discharge	LQD	BDL	BDL	0.2
Lehigh Quarry Spring Cave	LQS			
Lehigh Quarry Spring #2	LQS-2			
Lehigh Quarry Seep	LSp	<0.01	BDL	0.08 ^(?)
North Face Seepage	NFS		BDL	BDL
Old Quarry Seep	OQS		BDL	BDL
Orangeville Rise	OvR	<0.01	<0.01	
Quarry Road Block Spring	QBS	<0.01	340	63
Quarry Road New Spring	QNS		BDL	BDL
Quarry Road Pipe Spring	QPS		BDL	BDL
Quarry Road Spring	QRS	BDL	250	34
Quarry Road Seep	QSp			
Quarry Road Upstream Spring	QUS		<0.01	0.03 ^(?)
Rabbitville Quarry Rise	RQR	BDL	BDL	BDL
Rock Lick Br. Spr.-downstream	RSD		<0.01 ^(?)	0.03 ^(?)
Rock Lick Br. Spr.-middle	RSM			
Rock Lick Br. Spr.-upstream	RSU	BDL	1.2	0.1
Springhouse Seep	ShS	BDL	BDL	
Sewage Plant Spring	SPS	BDL	BDL	BDL
Whistling Cave-main stream	WhC-1			
Whistling Cave-downstream	WhC-B	BDL	BDL	
Wind Cave	WnC	BDL	BDL	

NOTES:

Values in **boldface** type are interpreted to represent concentrations of project dye.

BDL Below Detection Limit

^(?) Peak is not distinct or well matched to the typical dye emission spectrum.

TABLE VI-6 Results of Analyses for Rhodamine WT in Water Samples

LOCATION	CODE	FLUORESCCEIN CONCENTRATION IN WATER (µg/L)		
		Date of Sample Collection in 1997		
		09/22	10/27 10/28	11/10 11/11
Blue Spring Cave	BsC	BDL	BDL	BDL
Blacksmith Spring	BsS	BDL	BDL	
Crusher Building Spring	CBS			
CCC Spring	CCC		BDL	
Donaldson Cave-main stream	DnC-1	BDL	BDL	BDL
Donaldson Cave-small stream	DnC-2	BDL	BDL	0.2 ^(?)
Donaldson Cave-PVC pipe	DnC-3			
Downhill from Rockpile Seep	DRS			
Erwin Spring (Rock Lick) Cave	ESC	BDL	BDL	BDL
Harner Cave	HmC	BDL	BDL	
Lehigh Cave	LhC	BDL	BDL	BDL
Lehigh Quarry Discharge	LQD	BDL	BDL	BDL
Lehigh Quarry Spring Cave	LQS			
Lehigh Quarry Spring #2	LQS-2			
Lehigh Quarry Seep	LSp	BDL	BDL	BDL
North Face Seepage	NFS		BDL	BDL
Old Quarry Seep	OQS		BDL	BDL
Orangeville Rise	OvR	BDL	BDL	
Quarry Road Block Spring	QBS	BDL	BDL	BDL
Quarry Road New Spring	QNS		BDL	BDL
Quarry Road Pipe Spring	QPS		BDL	BDL
Quarry Road Spring	QRS	BDL	<1 ^(?)	BDL
Quarry Road Seep	QSp			
Quarry Road Upstream Spring	QUS		BDL	BDL
Rabbitville Quarry Rise	RQR	BDL	BDL	BDL
Rock Lick Br. Spr.-downstream	RSD		BDL	BDL
Rock Lick Br. Spr.-middle	RSM			
Rock Lick Br. Spr.-upstream	RSU	BDL	BDL	BDL
Springhouse Seep	ShS	BDL	BDL	
Sewage Plant Spring	SPS	BDL	BDL	BDL
Whistling Cave-main stream	WhC-1			
Whistling Cave-downstream	WhC-B	BDL	BDL	
Wind Cave	WnC	BDL	BDL	

NOTES:

Analyses were performed on a Shimadzu RF 5000 U spectrofluorophotometer.

Values in **boldface** type are interpreted to represent concentrations of project dye.

BDL Below Detection Limit

^(?) Peak is not distinct or well matched to the typical dye emission spectrum.

VII. DISCUSSION

This multiphase investigation was undertaken to answer three questions.

- 1) Is there a significant risk of sinkhole collapse or subsidence at the site?
- 2) If so, what can be done to minimize the potential hazards?
- 3) Can groundwater at the site be monitored effectively?

The origin of sinkholes and the risk of sinkhole collapse at the site are discussed in Chapter III. The largest and deepest sinkholes on the Mitchell Plain have formed by cave-roof collapse. However, authorities on sinkholes agree that this is an extremely rare event within the human time frame (as compared with the geologic time frame). Moreover, on the Mitchell Plain such collapses have only occurred over large cave passages with major underground streams running through them.

A thorough inventory of karst features was conducted in the vicinity of the site. Open drainage holes were found in Sinkholes A, B, C, E, and F, which lie around the immediate site area. However, none is large enough to be entered, much less to be considered a large cave. Although only 400 feet from the site boundary, Lehigh Cave is located on the other side of Rock Lick Branch and is not hydrologically connected to the site. A stream flows from the small cave entrance, but the cave can only be entered for a short distance before the stream level completely fills the small passage. Dye tracing has shown that groundwater beneath the site is discharged through the series of small springs along Rock Lick Branch downslope from the site. They are far too small to be entered, and their drainage channels show no indication of high discharge events. Although an exploratory boring on the site (BH-1) did intercept a cavity 4 feet high, all hydrologic indications are that the continuous, interconnected channels beneath the site are no larger than this void and are generally considerably smaller. There is certainly no evidence which indicates the presence of large active cave passages beneath the site. In light of this evidence it can be concluded that the risk of a sinkhole developing on the site by cave-roof collapse is negligible.

Although the largest and deepest sinkholes have formed by cave-roof collapse, most sinkholes on the Mitchell Plain have formed by a combination of long-term limestone dissolution and erosion of the unconsolidated cover material. Almost all sinkhole collapses which occur within the human time frame are cover-collapse sinkholes which form as a part of this process. However, as discussed in Chapter III, cover-collapse sinkholes on the Mitchell Plain generally form in the bottom of pre-existing sinkhole basins which are plugged or partially filled with unconsolidated material. There are no sinkhole depressions within the landfill boundary. Furthermore, examination of the site by a geologist prior to excavation and grading activities *circa* 1995 confirmed that there were no topographic depressions in the modified area at that time either. Therefore, it is highly improbable that a sinkhole will develop at the site by cover collapse.

P.E. LaMoreaux & Associates

NP and electrical resistivity tomography surveys were undertaken to investigate the possible existence of significant vertical drainage conduits in the limestone beneath the site. The results of the NP survey were corroborated by observations of visible recharge areas in the sinkholes adjacent to the site, and they may indicate the existence of one other area of concentrated groundwater recharge. If this area of potential groundwater recharge is associated with a significant vertical channel through the limestone, it should also be associated with a depression in the limestone surface. Results of the resistivity survey identified only one possible depression which is coincident with the potential recharge area. However, both the resistivity and NP anomalies associated with this area were of very low magnitude and probably do not indicate a substantial risk of sinkhole collapse.

The results of the groundwater tracing study show that the introduced tracer dyes emerged via springs along Rock Lick Branch immediately adjacent to the site. The data do not indicate the existence of karst groundwater connections between sinkholes at the site and regional discharge areas: Spring Mill State Park, Blue Spring Cave, or Orangeville Rise. Therefore, the groundwater associated with any facility at the site can be monitored by analyzing samples collected at these nearby springs.

VIII. CONCLUSIONS

1. The karstic nature of the site does not preclude its acceptability for use as a Type III waste disposal facility.
2. The risk of a cave-collapse sinkhole developing in the 10.3-acre area selected for CKD disposal is infinitesimally small, because there is no evidence of any large caverns beneath the site.
3. Based on knowledge of the cover-collapse processes in the Mitchell area and data from exploratory drilling, geophysical, and groundwater-tracing investigations, the risk of a cover-collapse sinkhole developing beneath the 10.3-acre area selected for CKD disposal is negligible. The only possible exception is an area between Transects 29 and 31 and between Stations 575 and 625, which is characterized by minor geophysical anomalies. In general, the occurrence of a cover-collapse sinkhole is a very rare event, even in a mature karst area. Moreover, most cover-collapse sinkholes on the Mitchell Plain occur within existing sinkhole basins, and the site does not contain any sinkhole basins.
4. Groundwater tracing has demonstrated that groundwater beneath the site discharges through several small springs immediately adjacent to the site. Groundwater associated with any facility at the site can be monitored effectively by analyzing samples collected at these nearby springs.
5. There is no indication of the existence of any karst groundwater connections between sinkholes at the site and regional discharge areas, including Spring Mill State Park, Blue Spring Cave, and Orangeville Rise.

P.E. LaMoreaux & Associates

REFERENCES CITED

Advanced Geosciences, Inc., 1996, Sting R1 Instruction Manual, Release 2.0.2.

Ahmad, M., 1964, Laboratory study of streaming potential: Geophysical Prospecting, v. 12, p. 49-64.

Ash, D.W., 1980, Karst development in the Mitchell Plain and adjacent Crawford Upland in response to lithologic, structural, and hydrologic constraints: The Geological Society of America, North-Central Section, 14th Annual Meeting, Bloomington, Indiana, April 10-11, Abstracts with Programs, v. 12, no. 5, p. 218.

Ash, D.W., 1984, Evidence for deep-seated groundwater movement in Middle Mississippian carbonate lithologies of south-central Indiana: National Speleological Society, The NSS Bulletin, v. 46, p. 14-15.

Ash, D.W., and Ehrenzeller, J., 1983, Geochemical and hydrological analysis of Harrison Springs, Harrison County, Indiana: in Dougherty, P.H., ed., Environmental Karst, Proceedings of Karst Symposium, Louisville, Kentucky, April, 1980, p. 137-64.

Atkinson, T.C., and Smart, P.L., 1981, Artificial tracers in hydrogeology: A Survey of British Hydrogeology 1980, The Royal Society, London, p. 173-190.

Aubert, M., and Atangana, Q.Y., 1996, Self-potential method in hydrogeological exploration of volcanic areas: Ground Water, v. 34, no. 6, p. 1010-16.

Ault, C.H., 1989, Map of Indiana showing directions of bedrock jointing: Indiana Geological Survey, Miscellaneous Map 52, 1:380,160 scale.

Ault, C.H., 1993, Map of Indiana showing elevations or thickness of overburden on selected rock units containing thick deposits of limestone and dolomite: Indiana Geological Survey, Miscellaneous Map 56, 1:500,000 scale.

Barrows, L.J., 1995, Applications of geophysical surveying to solid waste landfills: The Professional Geologists, November, p. 9-18.

Bassett, J., 1976, Hydrology and geochemistry of the upper Lost River drainage basin, Indiana: National Speleological Society, The NSS Bulletin, v. 38, p. 79-87.

Bassett, J.L., and Ruhe, R.V., eds., 1973, Fluvial geomorphology in karst terrain: in Morisawa, M., ed., Fluvial geomorphology, Proceedings, Binghamton, New York, 4th Annual Geomorphology Symposia Series, p. 74-89.

Bassett, J.L., and Ruhe, R.V., 1974, Geomorphology, hydrology, and soils in karst, southern Indiana: Field Conference, April 24-25, Water Resources Research Center, Indiana University, Bloomington, Indiana, p. 54 p.

P.E. LaMoreaux & Associates

Bassett, J.L., Keith, J.H., and Duwelius, A., 1996, Karst features of the Sulphur Spring drainage basin, the Beaver Creek Karst Valley, and Indiana State Highway 37: Indiana Geologists Field Trip, November 9, 16 p.

Bates, R.L. and Jackson, J.A., 1987, Glossary of Geology: Alexandria, Virginia, American Geological Institute, 788 p.

Bayless, E.R., and Taylor, C.J., 1994, Determination of ground-water flow directions and subsurface basin boundaries in the Lost River watershed near Orleans, Indiana: in Turco, R.F., ed., Proceedings of the Fifteenth Annual Water Resources Symposium—Understanding, Managing, and Protecting Indiana's Watersheds, Indiana Water Resources Association, June 1-3, Spring Mill State Park, p. 13-14.

Bayless, E.R., Taylor, C.J., and Hopkins, M.S., 1994, Directions of ground-water flow and locations of ground-water divides in the Lost River watershed near Orleans, Indiana: U.S. Geological Survey, Report of Water-Resources Investigations 94-4195, 25 p. + 2 sheets.

Bayless, E.R., Taylor, C.J., Hopkins, M.S., and Arvin, D.V., 1995, Directions of ground-water flow in the Lost River watershed near Orleans, Indiana: U. S. Geological Survey, Fact Sheet 0211-95, 2 p.

Beck, B.F., 1984, Sinkhole terminology: in Beck, B.F., ed., Sinkholes: Their Geology, Engineering and Environmental Impact, Proceedings, Orlando, Florida, A.A. Balkema, Rotterdam, p. ix-x.

Beck, B. F., 1988a, Environmental and engineering effects of sinkholes—the processes behind the problems: in Daoxian, Y., ed., Proceedings of Karst Hydrogeology and Karst Environment Protection, 21st Congress of the International Association of Hydrogeologists, Guilin, China, October 10-15, v. 176, p. 17-29.

Beck, B.F., 1988b, Environmental and engineering effects of sinkholes—the processes behind the problems: Environmental Geology and Water Science, v. 12, p. 71-78.

Beck, B.F., 1991, On calculating the risk of sinkhole collapse: in Kastning, E.H. and Kastning, K.M., eds., Appalachian Karst, Proceedings, Radford, Virginia, National Speleological Society, Huntsville, Alabama, p. 231-36.

Birch, F.S., 1993, Testing Fournier's method for finding water table from self-potential: Ground Water, v. 31, no. 1, p. 50-56.

Bleuer, N.K., 1970, Geologic considerations in planning solid-waste disposal sites in Indiana: Indiana Department of Natural Resources, Geological Survey, Special Report 5, 7 p.

Bogoslovsky, V.A., and Ogilvy, A.A., 1972, The study of streaming potentials on fissured media models: Geophysical Prospecting, v. 51, no. 1, p. 109-17.

—P.E. LaMoreaux & Associates—

Bogoslovsky, V.A., and Ogilvy, A.A., 1973, Deformation of natural electric fields near drainage structures: *Geophysical Prospecting*, v. 21, no. 4, p. 716-23.

Cook, K.L., and Van Nostrand, R.G., 1954, Interpretation of resistivity data over filled sinks: *Geophysics*, v. 19, p. 761-90.

Cooper, S.S., Koester, J.P., and Franklin, A.G., 1982, Geophysical Investigation at Gathright Dam: U.S. Army Corps of Engineers, WES Report GL-82-2.

Corwin, R.F., and Hoover, D.B., 1979, The self-potential method in geothermal exploration: *Geophysics*, v. 44, no. 2., p. 226-45.

Davies, W.E., 1951, Mechanics of cavern breakdown: *National Speleological Society Bulletin*, no. 13, p. 36-43.

Davis, S.N., Campbell, D.J., Bentley, H.W., and Flynn, T.J., 1985, Ground water tracers: U.S. Environmental Protection Agency and National Water Well Association, 200 p.

Droste, J.B., and Carpenter, G.L., 1990, Subsurface stratigraphy of the Blue River Group (Mississippian) in Indiana: Indiana Department of Natural Resources, Geological Survey, Bulletin 62, 45 p.

Duwelius, J.A., Bassett, J.L., and Keith, J.H., 1994, Delineation of sinkhole drainage routes utilizing fluorescent dye tracing procedures, Highway 37 improvement project, Lawrence [County], Indiana: in Turco, R.F., ed., *Proceedings of the Fifteenth Annual Water Resources Symposium—Understanding, Managing, and Protecting Indiana's Watersheds*, Indiana Water Resources Association, June 1-3, Spring Mill State Park, p. 33-37.

Duwelius, J.A., Bassett, J.L., and Keith, J.H., 1995, Application of fluorescent dye tracing techniques for delineating sinkhole drainage routes, Highway 37 improvement project, Lawrence County, Indiana: in Beck, B.F., ed., *Karst GeoHazards—Engineering and Environmental Problems in Karst Terrane*, *Proceedings of the Fifth Multidisciplinary Conference on Sinkholes and the Engineering and Environmental Aspects of Karst*, Gatlinburg, Tennessee, p. 227-33.

Erchul, R.A., and Slifer, D.W., 1987, The use of spontaneous potential in the detection of groundwater flow patterns and flow rate in karst areas: Beck, B.F. (ed.): *Second Multidisciplinary Conference on Sinkholes and the Environmental Impacts of Karst*, Orlando, Florida, p. 217-26.

Ernstson, K., and Scherer, H.U., 1986, Self-potential variations with time and their relation to hydrogeologic and meteorological parameters: *Geophysics*, v. 51, no. 10, p. 1967-77.

Fenneman, N.M., 1938, Physiography of the Eastern United States: McGraw-Hill, New York, 714 p.

Ford, T.D., and Cullingford, C.H.D., 1976, The science of speleology: London, Academic Press, 593 p.

Ford, D.C., and Williams, P.W., 1989, Karst geomorphology and hydrology: London, Unwin Hyman, 601 p.

Franklin, A.G., Patrick, D.M., Butler, D.K., Strohm, W.E., Hynes-Griffin, M.E., Jr., 1981, Foundation Considerations in Siting of Nuclear Facilities in Karst Terrain and Other Areas Susceptible to Ground Collapse: U.S. Army Engineer Waterways Experiment Station, NUREG/CR-2062, 229 p.

Frushour, S.S., 1997, Personal communication: geologist, Indiana Geological Survey.

Frushour, S.S., Harper, D., and Dintaman, C., 1997, Dye-trace experiments in the karst region of Indiana (DRAFT): series of seven maps at various scales.

Gilmore, T.J., and Clayton, E.A., 1997, Mapping the top of the permafrost using surface direct current resistivity survey, Environmental Geology, v. 30, nos. 1/2, p. 29-33.

Gray, H.H., 1983, Map of Indiana showing thickness of unconsolidated deposits: Indiana Geological Survey, Miscellaneous Maps 37 and 38, 1:500,000 scale.

Gray, H.H., and Powell, R.L., 1965, Geomorphology and groundwater hydrology of the Mitchell Plain and Crawford Upland in southern Indiana: Indiana Geological Survey Field Conference, Guidebook 11, 26 p.

Gray, H.H., Wayne, W.J., and Wier, C.E., 1970, Geologic map of the 1° x 2° Vincennes quadrangle and parts of adjoining quadrangles, Indiana and Illinois, showing bedrock and unconsolidated deposits: Indiana Geological Survey, Regional Geologic Map No. 3, Parts A & B, 1:250,000 scale.

Gray, H.H., Droste, J.B., Patton, J.B., Rexroad, C.B., and Shaver, R.H., 1985, Correlation chart showing paleozoic stratigraphic units of Indiana: Indiana Department of Natural Resources, Geological Survey, Supplement to Miscellaneous Map 48, 1 sheet.

Gray, H.H., Ault, C.H., and Keller, S.J., 1987, Bedrock geologic map of Indiana: Indiana Department of Natural Resources, Geological Survey, Miscellaneous Map 48, 1:500,000 scale.

Griffiths, D.H., and Barker, R.D., 1993, Two-dimensional resistivity imaging and modeling in areas of complex geology: Journal of Applied Geophysics, v. 29, p. 211-26.

Gruver, B.L., and Krothe, N.C., 1991, Evidence for epikarstic storage in a classic sinkhole plain, Mitchell Plain, Indiana: Proceedings of the American Geophysical Union 1991 Fall Meeting, Programs and Abstracts, December 9-13, San Francisco, California, p. 206.

Hall, R.D., 1973, Stratigraphy and sedimentation of a sinkhole in south central Indiana: Geological Society of America, North-Central Section, 7th Annual Meeting, Abstracts with Programs, v. 5, no. 4, p. 319.

Hall, R.D., 1976a, Investigations of sinkhole stratigraphy and hydrogeology, south-central Indiana: National Speleological Society, The NSS Bulletin v. 38, p. 88-92.

Hall, R.D., 1976b, Stratigraphy and origin of surficial deposits in sinkholes in south-central Indiana: Geology, v. 4, no. 8, p. 507-09.

Hansel, A., 1983, Form as an indicator of origin of karst landscapes in Indiana: in Dougherty, P.H., ed., Environmental Karst, Proceedings of Karst Symposium, Louisville, Kentucky, April, 1980, p. 109-18.

Hasenmueller, N.R., and Tankersley, J.R., 1987, Annotated bibliography of Indiana geology 1956 through 1975: Indiana Department of Natural Resources, Geological Survey, Bulletin 60, 425 p.

Hobbs, H.H., and Wells, S.G., 1972, The Lost River karst—Problems in conservation and land management: NSS News, v. 30, no. 8, August, p. 123-28.

Huffman, H., and Martin, M., 1991, Ecological evaluation of Spring Mill State Park: Indiana Department of Natural Resources, Division of Nature Preserves, 24 p.

Ishido, T., and Mizutani, H., 1981, Experimental and theoretical basis of electrokinetic phenomena in rock-water systems and its applications to geophysics: Journal of Geophysical Research, v. 86 (B3), p. 1763-75.

Jancin, M., and Clark, D.D., 1993, Subsidence-sinkhole development in light of mud infiltrate structures within interstratal karst of the Coastal Plain, Southeast United States: in Beck, B.F., ed., Applied Karst Geology, Proceedings, Panama City, Florida, A.A. Balkema, Rotterdam, p. 29-36.

Johnson, P.A., 1992, Cavern development along the East Fork of the White River, Lawrence County, Indiana: unpublished M.A. thesis, Indiana State University, Terre Haute, Indiana, 110 p.

Johnson, P.A., and Gomez, B., 1994, Cave levels and cave development in the Mitchell Plain following base-level lowering: Earth Surface Processes and Landforms, v. 19, no. 6, p. 517-24.

Jorgensen, D.B., and Carr, D.D., 1973, Influence of cyclic deposition, structural features, and hydrologic controls on evaporite deposits in the St. Louis Limestone in southwestern Indiana: Proceedings of the Eight Forum on the Geology of Industrial Minerals, Iowa Geological Survey Public Information Circular 5, p. 43-65.

Kessler, T.E., 1994, Mitchell, Indiana Plant Auger Drilling Program: Intracompany and Office Correspondence, August 26.

Kessler, T.E., 1997, Personal communication and file notes: geologist, Lehigh Portland Cement Company.

Kilty, K.T., and Lange, A.L., 1991, Electrochemistry of natural potential processes in karst: Proceedings of the Third Conference on Hydrogeology, Ecology, Monitoring, and Management of Ground Water in Karst Terrains, U.S. EPA and National Ground Water Association, December 4-6, Nashville, Tennessee, p. 163-77.

Lagmanson, M., 1997, Personal communication: Advanced Geosciences, Inc., Austin Texas.

Lambert, D.W., 1997, Dipole-dipole D.C. resistivity surveying for exploration of karst features: Beck, B.F., and Stephenson, J.B., eds., Proceedings of the Sixth Multidisciplinary Conference on Sinkholes and the Engineering and Environmental Impacts of Karst, April 6-9, Springfield, Missouri, p. 413-18.

Lange, A.L., and Barner, W.L., 1995, Application of the natural electric field for detecting karst conduits on Guam: in Beck, B.F., ed., Karst GeoHazards—Engineering and Environmental Problems in Karst Terrane, Proceedings of the Fifth Multidisciplinary Conference on Sinkholes and the Environmental Impacts of Karst, April 2-5, Gatlinburg, Tennessee, p. 425-41.

Lange, A.L., and Kilty, K.T., 1991, Natural-potential responses of karst systems at the ground surface: Proceedings of the Third Conference on Hydrogeology, Ecology, Monitoring, and Management of Ground Water in Karst Terrains, U.S. EPA and National Ground Water Association, December 4-6, Nashville, Tennessee, p. 179-96.

Lange, A.L., and Quinlan, J.F., 1988, Mapping caves from the surface of karst terranes by the natural potential method: Proceedings of the Second Conference on Environmental Problems in karst Terranes and Their Solutions Conference, National Water Well Association, November 16-18, Nashville, Tennessee, p. 369-90.

Lange, A.L., and Wiles, M., 1991, Mapping Jewel Cave—from the surface: Park Science, v. 11, No. 2, p. 6-7.

Lange, A.L., Walen, P.A., and Buecher, R.H., 1990, Cave mapping from the surface at Kartchner Caverns State Park, Arizona: American Society of Photogrammetry and Remote Sensing, Proceedings of the Third Forest Service Remote Sensing Applications Conference, Tucson, Arizona, p. 163-74.

P.E. LaMoreaux & Associates

Lehmann, H., 1975, On the morphology of the Mitchell Plain and the Pennyroyal Plain of Indiana and Kentucky (translated from the German by Eberhard Werner): Cave Geology (State College, Pennsylvania), v. 1, no. 2, p. 29-39.

Lineback, J.A., 1972, Lateral gradation of the Salem and St. Louis Limestones (Middle Mississippian) in Illinois: Illinois Geological Survey Circular 474, 21 p.

Loke, M.H., 1996, Manual for the RES2DINV. Distributed by Advanced Geosciences, Inc., Austin, Texas.

Loke, M.H., and Barker, R.D., 1996, Practical techniques for 3D resistivity surveys and data inversion: Geophysical Prospecting, v. 44, p. 499-23.

Loke, M.H., and Barker, R.D., 1996, Rapid least-square inversion of apparent resistivity pseudosections by a quasi-Newton method: Geophysical Prospecting, v. 44, p. 131-52.

Malott, C.A., 1919, The American Bottoms region of eastern Greene County, Indiana: Indiana University Studies No. 40, 61 p.

Malott, C.A., 1922, The physiography of Indiana: Handbook of Indiana Geology, Indiana Department of Conservation Publication 21, p. 59-256.

Malott, C.A., 1945, Significant features of the Indiana karst: Proceedings of the Indiana Academy of Science, v. 54 (1944), p. 8-24.

McCann, M.R., and Krothe, N.C., 1992, Development of a monitoring program at a Superfund site in a karst terrane near Bloomington, Indiana: National Ground Water Association, Proceedings of the Third Conference on Hydrogeology, Ecology, Monitoring, and Management of Ground Water in Karst Terranes, Nashville, Tennessee, December 4-6, p. 349-71.

McConnell, H., and Horn, J.M., 1972, Probabilities of Surface Karst—Applications in Mitchell Plain, Indiana: in Spatial Analysis in Geomorphology, Methuen & Co., Ltd., London, p. 111-33.

McGregor, D.J., 1954, Gypsum and anhydrite deposits in south-western Indiana: Indiana Geological Survey Report Prog. 8, 24 p.

Miller, T.E., and Waldron, T.B., 1988, Bibliography of Indiana karst and karst-related literature: National Speleological Society, The NSS Bulletin, v. 50, no. 2, p. 72-76.

Moore, H.L., 1980, Karst problems along Tennessee highways, an overview: 31st Annual Highway Geology Symposium (reprint), Austin, Texas, 68 p.

Moore, M.C., 1973, Karst areas of Indiana—The south-central karst area (stratigraphy and lithology of the karst-bearing units): in Guidebook for the 1973 Convention of the National Speleological Society, p. 6-10.

P.E. LaMoreaux & Associates

Mull, D.S., Liebermann, T.D., Smoot, J.L., and Woosley, L.H., 1988, Application of dye-tracing techniques for determining solute-transport characteristics of ground water in karst terranes: U.S. Environmental Protection Agency, EPA 904/6-88-001, 103 p.

National Speleological Society, 1973, NSS 73 Convention Guidebook: Guidebook for the 1973 Convention of the National Speleological Society, Bloomington, Indiana, June 16-24, 81 p.

Newton, J.G., 1976, Induced sinkholes—a continuing problem along Alabama highways: International Association of Hydrological Science, Anaheim [California] Symposium, Proceedings, no. 21, p. 453-63.

Newton, J.G., and Hyde, L.W., 1971, Sinkhole problem in and near Roberts Industrial Subdivision, Birmingham, Alabama—a reconnaissance: Alabama Geological Survey Circular 68, 42 p.

Ogilvy, A.A., 1967, Studies of underground water movement: Geological Survey of Canada Report #26, p. 540-43.

Ogilvy, A.A., Ayed, M.A., and Bogoslovsky, V.A., 1969, Geophysical studies of water leakage from reservoirs: Geophysical Prospecting, v. 22, no. 1, p. 36-62.

Olson, C.G., Ruhe, R.V., and Mausbach, J.J., 1980, The terra rossa limestone contact phenomenon in karst, southern Indiana: Soil Science Society of America Journal, v. 44, p. 1075-79.

Palmer, A.N., 1967, The survey and geologic investigation of Blue Spring Cave, Indiana (abstract): National Speleological Society Bulletin, v. 29, p. 103.

Palmer, A.N., 1968, The survey of Blue Spring Cave, Lawrence County, Indiana: Proceedings of the Indiana Academy of Science, v. 77 (1967), p. 245-49.

Palmer, A.N., 1969, A hydrologic study of the Indiana karst: unpublished Ph.D. dissertation, Indiana University, Bloomington, Indiana, 181 p.

Palmer, A.N., 1970, Hydrology of the limestone aquifers of southern Indiana (abstract): National Speleological Society Bulletin, v. 32, no. 2, p. 49.

Palmer, A.N., 1973, Karst areas of Indiana—The south-central karst area (introduction): in Guidebook for the 1973 Convention of the National Speleological Society, p. 3.

Palmer, M.V., 1976, The Mitchell Plain of southern Indiana: National Speleological Society, The NSS Bulletin, v. 38, p. 74-79.

Palmer, A.N., and Moore, M.C., 1976, Geomorphology and hydrology of the Indiana and Kentucky karst—A symposium: National Speleological Society, The NSS Bulletin, v. 38, p. 73-74.

P.E. LaMoreaux & Associates

Palmer, M.V., and Palmer, A.N., 1975, Landform development in the Mitchell Plain of southern Indiana—origin of a partially karsted plain: *Zeitschrift fur Geomorphologie*, v. 19, no. 1, p. 1-39.

Pinsak, A.P., 1957, Subsurface stratigraphy of the Salem Limestone and associated formations in Indiana: *Indiana Geological Survey Bulletin* 11, 62 p.

Powell, R.L., 1961, Caves of Indiana: *Indiana Geological Survey, Circular No. 8*, 127 p.

Powell, R.L., 1964, Origin of the Mitchell Plain in south-central Indiana: *Proceedings of the Indiana Academy of Science*, v. 73 (1963), p. 177-82.

Powell, R.L., 1966, Caves—Speleology and karst hydrology: in *The Indiana Sesquicentennial Volume, Natural Features of Indiana*, *Indiana Academy of Science*, p. 116-30.

Powell, R.L., 1970, Base level, lithologic, and climate controls of karst groundwater zones in south-central Indiana: *Proceedings of the Indiana Academy of Science*, v. 79 (1969), p. 281-91.

Powell, R.L., 1973, Karst areas of Indiana—The south-central karst area (physiography and development): in *Guidebook for the 1973 Convention of the National Speleological Society*, p. 3-6.

Powell, R.L., 1976, Some geomorphic and hydrologic implications of jointing in carbonate strata of Mississippian age in south-central Indiana: unpublished Ph.D. dissertation, Purdue University, West Lafayette, Indiana, 169 p.

Powell, R.L., 1977, Joint patterns and solution channel evolution in Indiana: in Tolson, J.S., and Doyle, F.L., eds., *Karst Hydrogeology, Proceedings of the 12th Congress of the International Association of Hydrogeologists*, v. XII, p. 255-69.

Powell, R.L., 1987, The Orangeville Rise and Lost River, Indiana: *Geological Society of America Centennial Field Guide, North-Central Section*, p. 375-80.

Powell, R.L., 1997, Personal communication: consulting geologist, Bloomington, Indiana.

Powell, R.L., Frushour, S.S., and Harper, D., 1997, Areas of sinkholes and sinking-stream basins with locations of cave openings and springs in central southern Indiana: *Indiana Geological Survey, Miscellaneous Map 65*, scale 1:250,000.

Quinlan, J.F., ed., 1986, Water-tracing techniques in karst terranes: *Practical Karst Hydrogeology with Emphasis on Groundwater Monitoring, a Short Course*, National Water Well Association, Dublin, Ohio, 25 p.

Quinlan, J.F., 1990, Special problems of ground-water monitoring in karst terranes: in Nielsen, D.M., and Johnson, A.I., eds., *Groundwater and Vadose Zone Monitoring*, American Society for Testing and Materials, Philadelphia, STP 1053, p. 275-304.

Reid, G.C., 1981, Literature evaluation of induced groundwater tracers, field tracer techniques, and hydrodynamic dispersion values in porous media: unpublished Master's Thesis, Texas Tech University, 92 p.

Rexroad, C.B., and Gray, L.M., 1979, Geologic story of Spring Mill State Park: State Park Guide no. 7, Indiana Geological Survey, Bloomington, Indiana, 4 p.

Ruhe, R.V., 1977, Summary of geohydrologic relationships in the Lost River watershed, Indiana, applied to water use and environment: in Dilamarter, R.R., and Csallany, S.C., eds., *Hydrologic Problems in Karst Regions*, Proceedings of the International Symposium on Hydrologic Problems in Karst Regions, Bowling Green, Kentucky, April 26-29, 1976, p. 64-78.

Shaver, R.H., Burger, A.M., Gates, G.R., Gray, H.H., Hutchison, H.C., Keller, S.J., Patton, J.B., Rexroad, C.B., Smith, N.M., Wayne, W.J., and Wier, C.E., 1970, *Compendium of rock-unit stratigraphy in Indiana*: Indiana Department of Natural Resources, Geological Survey, Bulletin 43, 229 p.

Shaver, R.H., Ault, C.H., Burger, A.M., Carr, D.D., Droste, J.B., Eggert, D.L., Gray, H.H., Harper, D., Hasenmueller, N.R., Hasenmueller, W.A., Horowitz, A.S., Hutchison, H.C., Keith, B.D., Keller, S.J., Patton, J.B., Rexroad, C.B., and Wier, C.E., 1986, *Compendium of Paleozoic rock-unit stratigraphy in Indiana—A revision*: Indiana Department of Natural Resources Geological Survey, Bulletin 59, 203 p.

Smart, P.L., 1984, A review of the toxicity of twelve fluorescent dyes used for water tracing: *National Speleological Society Bulletin*, v. 46, p. 21-33.

Smart, P.L., and Laidlaw, I.M.S., 1977, An evaluation of some fluorescent dyes for water tracing: *Water Resources Research*, v. 13, no. 1, p. 15-32.

Spiegel, R.J., Sturdivant, V.R., and Owen, T.E., 1980, Modeling resistivity anomalies from localized voids under irregular terrain: *Geophysics*, v. 45, no. 7, p. 1164-83.

Tharp, T.M., Holdrege, T.J., Coffin, D.T., Eberly, D., Ohlmacher, G.C., Schultz, R.A., Sittler, S.P., and Tomlinson, R.G., 1985, Behavior of roof-beams in limestone caves—Implications for cave morphology and character of karst landforms: *Geological Society of America*, 1985 Annual Meeting, Orlando, Florida, October 28-31, Abstracts with Programs, v. 17, no. 7, p. 734.

Thomas, J.A., 1985, *Soil Survey of Lawrence County, Indiana*: U.S. Department of Agriculture, Soil Conservation Service, 173 p. + 67 sheets.

U.S. Geological Survey, 1960, Mitchell quadrangle, Indiana: 7.5-minute topographic map, 1:24,000 scale.

U.S. Geological Survey, 1965, Georgia quadrangle, Indiana: 7.5-minute topographic map, 1:24,000 scale.

U.S. Geological Survey, 1978, Bedford East quadrangle, Indiana: 7.5-minute topographic map, 1:24,000 scale.

U.S. Geological Survey, 1979, Bedford West quadrangle, Indiana: 7.5-minute topographic map, 1:24,000 scale.

Waltham, A.C., 1989, Ground subsidence: New York, Chapman & Hall, 202 p.

White, W.B., 1988, Geomorphology and hydrology of karst terrains: New York, Oxford University Press, 464 p.

Williams, J.H., and Vineyard, J.D., 1976, Geological indicators of catastrophic collapse in karst terrane in Missouri: National Academy of Science, Transportation Research Record 612, p. 31-37.

EXTENDED BIBLIOGRAPHY

Adams, J., 1994, The Indiana Karst Conservancy: National Speleological Society News, February, v. 52, no. 2, p. 56-57.

Amadi, U.M.P., 1981, Ground-water chemistry and hydrochemical facies distribution as related to flow in the Mississippian carbonates, Harrison County, Indiana: unpublished A.M. thesis, Indiana University, Bloomington, Indiana.

Amadi, U.M.P., 1986, Flow pattern and changes in the chemistry of the ground water from the karst plains of southern Indiana, U.S.A.: in Gunay, G., and Johnson, A.I., eds., Karst Water Resources, International Symposium on Karst Water Resources, Ankara, Turkey, July 8-12, 1985, International Association of Hydrological Sciences Publication, v. 161, p. 433-48.

Amadi, U.M.P., and Krothe, N.C., 1981, Hydrodynamic influences on the ground-water chemistry of the Mississippian carbonates, Harrison County, southern Indiana: in Biggs, D.L., The Geological Society of America, North-Central Section, 15th Annual Meeting, Ames, Iowa, April 30-May 1, Abstracts with Programs, v. 13, no. 6, p. 269.

Amadi, U.M.P., and Krothe, N.C., 1988, Fluorite saturation and equilibrium trends in the groundwater system from the karst plains of southern Indiana, USA: in Daoxian, Y., ed., Proceedings of Karst Hydrogeology and Karst Environment Protection, 21st Congress of the International Association of Hydrogeologists, Guilin, China, October 10-15, v. 176, no. 2, p. 847-55.

Amadi, U.M.P., and Shaffer, N.R., 1986, Low sulfate ground water and its relationship to the gypsum-fluorite replacement in the karst terrains of southern Indiana, U.S.A.: in Gunay, G., and Johnson, A.I., eds., Karst Water Resources, International Symposium on Karst Water Resources, Ankara, Turkey, July 8-12, 1985, International Association of Hydrological Sciences Publication, v. 161, p. 449-66.

Ash, D.W., 1984, Aspects of recharge and ground-water flow in lower St. Louis carbonates in south-central Indiana: 29th Annual Midwest Groundwater Conference, Lawrence, Kansas, October 1-3, v. 29, p. 8.

Ash, D.W., and Ehrenzeller, J., 1979, Hydrological analysis of Harrison Spring, Harrison County, Indiana: Selected Abstracts of Papers, 1979 National Speleological Society Convention, Pittsfield, Massachusetts, The NSS Bulletin, v. 42 (1980), no. 2, p. 33.

Ash, D.W., and Powell, R.L., 1979, Geomorphology and karst development in the Mitchell Plain and adjacent Crawford Upland in south-central Indiana: Louisville Cave and Karst Symposium Field Trip Guidebook, p. 39-52.

Baedke, S.J., 1990, A model for the chemical evolution of spring waters in south-central Indiana: unpublished M.S. thesis, Indiana University, Bloomington, Indiana, 70 p.

P.E. LaMoreaux & Associates

Bassett, J.L., 1974, Hydrology and geochemistry of karst terrain, upper Lost River drainage basin, Indiana: unpublished A.M. thesis, Indiana University, Bloomington, Indiana, 102 p.

Bloomington Indiana Grotto (BIG), 1961, Guide to caves of the Mitchell area: National Speleological Society, Bloomington Indiana Grotto Newsletter, v. 4, p. 1-24.

Bolton, D.W., 1980, Water chemistry of springs and streams in the St. Louis Limestone, Lawrence County, Indiana: unpublished A.M. thesis, Indiana University, Bloomington, Indiana.

Brown, I.O., 1920, Limestone sinks in the Bloomington Indiana, Quadrangle: unpublished M.S. thesis, University of Chicago, Chicago, Illinois, 64 p.

Brune, G.M., 1949, Reservoir sedimentation in limestone sinkhole terrain: Agricultural Engineering, v. 30, no. 2, p. 73-77.

Bultman, B.E., and Hall, R.D., 1987, The effects of the formation of the Wadsworth Sinkhole on the drainage of Wadsworth and Landreth Hollows, south central Indiana: Proceedings of the Indiana Academy of Science, v. 97, p. 353-59.

Bushnell, T.M., 1929, Geological information from the Monroe and Lawrence County soil maps: Proceedings of the Indiana Academy of Science, Indianapolis, Indiana, v. 38, p. 245.

Campbell, C.E., 1967, A seismic refraction and electrical resistivity investigation of a karst environment in Lawrence County, Indiana: unpublished A.M. thesis, Indiana University, Bloomington, Indiana, 44 p.

Carter, D.S., Lydy, M.J., Crawford, C.G., 1995, Water-quality assessment of the White River basin, Indiana—Analysis of available information on pesticides, 1972-92: U.S. Geological Survey, Water-Resources Investigations Report WRI 94-4024, 60 p.

Childs, L., 1940, A study of a karst area in Orange and Lawrence Counties, Indiana: unpublished A.M. thesis, Indiana University, Bloomington, Indiana, 111 p.

Cohn, M.E., and Rudman, A.J., 1995, Orientation of near-surface fractures from azimuthal measurements of apparent resistivity: Society of Exploration Geophysicists, 65th Annual International Meeting, Houston, Texas, October 8-13, SEG Annual Meeting Expanded Technical Program Abstracts with Biographies, v. 65, p. 372-74.

Cumings, E.R., 1912, Geological conditions of municipal water supply in the driftless area of southern Indiana: Proceedings of the Indiana Academy of Science, p. 111-46.

Cutler, J.L., Krothe, N.C., and Shafer, N.R., 1988, Hydrogeochemical ground-water reconnaissance in Monroe County, Indiana: Geological Society of America, 22nd Annual Meeting, April 21-22, v. 20, no. 5, p. 341.

Des Marais, D.J., 1981, Subterranean stream piracy in the Garrison Chapel karst valley, Indiana, U.S.A.: in Beck, B.F., ed., Proceedings of the 8th International Congress of Speleology, v. 1, no. 8, p. 196-99.

Ehrenzeller, J.L., 1978, Geological and hydrological analysis of Harrison Spring, Harrison County, Indiana: unpublished A.M. thesis, Indiana State University, Terre Haute, 94 p.

Ehrenzeller, J., and Ash, D.W., 1979, Geochemical analysis of Harrison Spring, Harrison County, Indiana: Selected Abstracts of Papers, 1979 National Speleological Society Convention, Pittsfield, Massachusetts, The NSS Bulletin, v. 42 (1980), no. 2, p. 33.

Elrod, M.N., 1899, The geologic relations of some Saint Louis group caves and sinkholes: Proceedings of the Indiana Academy of Science, p. 258-67.

Fitch, J.R., 1994, A karst groundwater study to delineate the Quarry Spring basin groundwaters near the Lemon Lane Landfill, west-central Bloomington, Indiana: unpublished M.S. thesis, Indiana University, Bloomington, Indiana, 154 p.

Greene, F.C., 1909, Caves and cave formations of the Mitchell limestone: Proceedings of the Indiana Academy of Science, p. 175-84.

Gruver, B.L., and Krothe, N.C., 1990, Temporal variability of groundwater quality in karst-carbonate aquifers of the upper Lost River basin, south-central Indiana: Geological Society of America, 1990 Annual Meeting, Dallas, Texas, October 29-November 1, Abstracts with Programs, v. 22, no. 7, p. 66.

Gruver, B.L., and Krothe, N.C., 1992, Stable isotope separation of spring discharge in a major karst spring, Mitchell Plain, Indiana, U.S.A.: National Ground Water Association, Proceedings of the Third Conference on Hydrogeology, Ecology, Monitoring, and Management of Ground Water in Karst Terranes, Nashville, Tennessee, December 4-6, 1991, p. 265-85.

Hansel, A.K., 1980, Sinkhole form as an indicator of process in karst landscape evolution: unpublished Ph.D. dissertation, University of Illinois, Urbana, Illinois, 175 p.

Howe, M.R., 1981, The relationship of a potentiometric surface to conduit development in the carbonate lithologies of the Mitchell Plain, Harrison County, Indiana: unpublished M.S. thesis, Indiana State University, Terre Haute, Indiana, 154 p.

Iqbal, M.Z., 1994, A study of the infiltration processes responsible for contamination of groundwater by fertilizer-derived nitrate and other chemical compounds in the karst aquifers of Orange and Washington counties, Indiana: unpublished Ph.D. dissertation, Indiana University, Bloomington, Indiana, 192 p.

Iqbal, M.Z., and Krothe, N.C., 1995, Infiltration mechanisms related to agricultural waste transport through the soil mantle to karst aquifers of southern Indiana, USA: *Journal of Hydrology*, v. 164, no. 1-4, p. 171-92.

Iqbal, M.Z., Krothe, N.C., and Spalding, R.F., 1994, A nitrogen isotope study to determine sources of nitrate in karst aquifers of southern Indiana: Geological Society of America, 1994 Annual Meeting, Seattle, Washington, October 24-27, Abstracts with Programs, v. 26, no. 7, p. 321-22.

Keith, J.H., Bassett, J.L., and Duwelius, J.A., 1995, Modification of highway runoff quality by sinkhole drainage structures, Highway 37 improvement project, Lawrence County, Indiana: in Beck, B.F., ed., *Karst GeoHazards—Engineering and Environmental Problems in Karst Terrane*, Proceedings of the Fifth Multidisciplinary Conference on Sinkholes and the Engineering and Environmental Aspects of Karst, Gatlinburg, Tennessee, p. 273-84.

Krothe, N.C., 1987, Sulfur isotope studies in ground water of the karst Mitchell Plain, southern Indiana: in Dickinson, W.R., ed., *Geological Society of America, 1987 Annual Meeting and Exposition*, Phoenix, Arizona, October 26-29, Abstracts with Programs, v. 19, no. 7, p. 734.

Krothe, N.C., 1988, Hydrologic connection between spring water and the evaporite of the lower St. Louis Limestone, karst Mitchell Plain of southern Indiana: in Daoxian, Y., ed., *Proceedings of Karst Hydrogeology and Karst Environment Protection*, 21st Congress of the International Association of Hydrogeologists, Guilin, China, October 10-15, v. 176, no. 1, p. 406-16.

Krothe, N.C., 1989, Development of flow in Mississippian carbonate aquifer on Mitchell karst plain, Indiana: Abstracts of the 28th International Geological Congress, Washington, DC, July 9-19, v. 28, no. 2, p. 231-32.

Krothe, N.C., 1992, Hydrochemistry and sulfur isotope studies of carbonate springs on the karst Mitchell Plain and mineral springs in the Crawford Upland of southern Indiana: American Geophysical Union, 1992 Fall Meeting, San Francisco, California, December 7-11, EOS, Transactions, v. 73, no. 43, p. 173.

Krothe, N.C., 1995, Groundwater chemical transport in a karst terrain, Lost River basin, southern Indiana—An isotopic study: Geological Society of America, 29th Annual Meeting, North-Central Section, South-Central Section, Lincoln, Nebraska, April 27-28, Abstracts with Programs, v. 27, no. 3, p. 66.

Krothe, N.C., and Libra, R., 1979, The determination of flow systems in the karst terrain of southern Indiana using sulfur isotopes: Geological Society of America, Abstracts with Programs, v. 11, no. 7, p. 420-21.

Krothe, N.C., and Libra, R., 1980, Sulfur isotopes and hydrogeochemical variations as an indicator of flow systems in karst terranes: The Geological Society of America, 93rd Annual Meeting, Atlanta, Georgia, November 17-20, Abstracts with Programs, v. 12, no. 7, p. 466-67.

Krothe, N.C., and Libra, R., 1983, Hydrogeology and sulfur isotope variations of spring waters of southern Indiana, U.S.A.: in V.T. Stringfield Symposium, Processes in Karst Hydrology, Journal of Hydrology, v. 61, no. 1-3, p. 267-83.

Krothe, N.C., and Wells, E.R., 1989, Seasonal fluctuations in $\delta^{15}\text{N}$ of groundwater in mantled karst aquifer: Abstracts of the 28th International Geological Congress, Washington, DC, July 9-19, v. 28, no. 2, p. 232.

Krothe, N.C., Ash, D.W., and Smith, C.R., 1983, Hydrologic connection between spring water and evaporite units of the Lower St. Louis Limestone, southern Indiana: Geological Society of America, Abstracts with Programs, v. 15, no. 6, p. 619.

Krothe, N.C., Yu, H.G., and Baedke, S.J., 1993, Stable carbon isotope application to storm hydrograph separation of karst springs in south-central Indiana: Geological Society of America, 1993 Annual Meeting, Boston, Massachusetts, October 25-28, Abstracts with Programs, v. 25, no. 6, p. 91.

Lakey, B.L., and Krothe, N.C., 1996, Stable isotopic variation of storm discharge from a perennial karst spring, Indiana: Water Resources Research, v. 32, no. 3, p. 721-31.

Lewis, J.J., 1983, The obligatory subterranean invertebrates of glaciated southwestern Indiana: National Speleological Society, The NSS Bulletin, v. 45, no. 2, p. 34-40.

Libra, R.D., 1981, Hydrology and sulfur isotope variations of spring systems, south-central Indiana: unpublished A.M. thesis, Indiana University, Bloomington, Indiana, 116 p.

Malott, C.A., 1932, Lost River at Wesley Chapel Gulf, Orange County, Indiana: Proceedings of the Indiana Academy of Science, v. 41, p. 285-316.

Malott, C.A., 1939, Karst valleys: Geological Society of America Bulletin, v. 50, no. 12, part 2, p. 1984.

Malott, C.A., 1949, A stormwater cavern in the Lost River region of Orange County, Indiana: National Speleological Society, The NSS Bulletin, v. 11, p. 64-68.

Malott, C.A., 1952, The swallow-holes of Lost River, Orange County, Indiana: Proceedings of the Indiana Academy of Science, v. 61 (1951), p. 187-231.

McCann, M.R., and Krothe, N.C., 1989, Using tracers to delineate hydrologic zones of influence at a Superfund site: Proceedings of Tracers in Hydrogeology—Principles, Problems, and Practical Applications, Houston, Texas, October 30-November 1, National Water Well Association, Ground-Water Technology Division, Urbana, Illinois, Ground Water, v. 27, no. 5, p. 726.

McGregor, D.J., and Rarick, R.D., 1962, Some features of karst topography in Indiana: Guidebook for a Geologic Field Trip, Indiana Academy of Science, 20 p.

Miller, J.R., 1990, Influence of bedrock geology and karst processes on the morphology and dynamics of fluvial systems in the Crawford Upland, south-central Indiana: unpublished Ph.D. dissertation, Southern Illinois University, Carbondale, Carbondale, Illinois, 431 p.

Miller, J.R., Ritter, D.F., and Kochel, R.C., 1989, Lithologic controls on drainage basin morphology in the Crawford Upland, south-central Indiana: Geological Society of America, North-Central Section, 23rd Annual Meeting, Notre Dame, Indiana, April 20-21, Abstracts with Programs, v. 21, no. 4, p. 42.

Miller, J.R., Ritter, D.F., and Kochel, R.C., 1990, Morphometric assessment of lithologic controls on drainage basin evolution in the Crawford Upland, south-central Indiana: American Journal of Science, v. 290, no. 5, p. 569-99.

Miller, T., 1990, Regional correlation of cave levels in Indiana: Abstracts of the 11th Friends of Karst, Decorah 1990: Geo², v. 17, nos. 2-3, p. 71.

Murdock, S.H., and Powell, R.L., 1968, Subterranean drainage routes of Lost River, Orange County, Indiana: Proceedings of the Indiana Academy of Science, v. 77 (1967), p. 250-55.

Olson, C.G., 1979, A mechanism for origin of terra rossa in southern Indiana: unpublished Ph.D. dissertation, Indiana University, Bloomington, Indiana, 198 p.

Olson, C.G., and Ruhe, R.V., 1978, A mechanism for the origin of Terra rossa in humid karst, southern Indiana, U.S.A.: The Geological Society of America, North-Central Section, 12th Annual Meeting, Ann Arbor, Michigan, May 1-2, Abstracts with Programs, v. 10, no. 6, p. 280.

Palmer, A.N., 1965, The hydrogeology of Indiana: A Survey of Indiana Geology, Sigma Gamma Epsilon, Rho Chapter, Department of Geology, Indiana University, Bloomington, p. 22-28 (p. 75-81 in 1966 revised edition).

Palmer, A.N., 1965, The occurrence of ground water in limestone: Compass, v. 42, p. 246-55.

Palmer, A.N., 1965, The physiography of south-central Indiana: National Speleological Society Convention Guidebook, p. 1-3.

Palmer, A.N., 1984, Geomorphic interpretation of karst features: LaFleur, R.G., ed., Groundwater as a Geomorphic Agent, 13th Annual Geomorphology Symposium—Groundwater as a Geomorphic Agent, Troy, New York, September 1982, v. 13, p. 173-209.

Palmer, A.N., 1990, Groundwater processes in karst terranes: in Higgins, C.G., and Coates, D.R., eds., Groundwater Geomorphology—The Role of Subsurface Water in Earth-Surface Processes and Landforms, Geological Society of America, Special Paper, v. 252, p. 177-209.

Palmer, A.N., 1995, Geochemical models for the origin of macroscopic solution porosity in carbonate rocks: in Budd, D.A., Saller, A.H., and Harris, P.M., eds., Unconformities and Porosity in Carbonate Strata, American Association of Petroleum Geologists, Tulsa, Oklahoma, AAPG Memoir, v. 63, p. 77-101.

Palmer, M.V., Palmer, A.N., and Powell, R.L., 1981, Guidebook to the Indiana excursion: 1981 International Congress of Speleology, 37 p.

Pease, P.P., and Johnson, P.A., 1992, Limitations on regional correlation of cave levels, Indiana and Kentucky: in Peacock, N.D., ed., Proceedings of the National Speleological Society Annual Meeting, Salem, Indiana, August 3-7,

abstract in National Speleological Society, The NSS Bulletin, v. 54, no. 2, p. 89-90.

Pease, P.P., Gomez, B., and Schmidt, V.A., 1992, Magnetostratigraphy of cave sediments, Wyandotte Ridge, Crawford County, southern Indiana: Geological Society of America, 1992 Annual Meeting, Cincinnati, Ohio, October 26-29, Abstracts with Programs, v. 24, no. 7, p. 48-49.

Pease, P.P., Gomez, B., and Schmidt, V.A., 1994, Magnetostratigraphy of cave sediments, Wyandotte Ridge, Crawford County, Indiana—Towards a Regional Correlation: Geomorphology, v. 11, no. 1, p. 75-81.

Powell, R.L., 1961, A geography of the springs of Indiana: unpublished A.M. thesis, Indiana University, Bloomington, Indiana, 74 p.

Powell, R.L., 1963, Alluviated cave springs in south-central Indiana: Proceedings of the Indiana Academy of Science, v. 72 (1962), p. 182.

Powell, R.L., 1968, Geomorphic interpretations of unconsolidated deposits on the Mitchell Plain of Indiana: Geological Society of America, Special Paper, p. 396.

Powell, R.L., 1969, Unconsolidated deposits on the Mitchell Plain of Indiana: Proceedings of the Indiana Academy of Science, v. 78 (1968), 316 p.

Powell, R.L., and Forbes, J.R., 1982, Karst drainage basins in central southern Indiana: 16th Annual Meeting, North-Central Section of the Geological Society of America, West Lafayette, Indiana, April 29-30, Abstracts with Programs, v. 14, no. 5, p. 268.

P.E. LaMoreaux & Associates

Powell, R.L., and Krothe, N.C., 1983, Mitchell Plain, Indiana: in Shaver, R.H., and Sunderman, J.A., eds., Field Trips in Midwestern Geology, Geological Society of America, v. 2, p. 1-85.

Powell, R.L., and Maegerlein, S.D., 1977, Classification of springs in south-central Indiana: Proceedings of the Indiana Academy of Science, v. 86 (1976), p. 261-62.

Powell, R.L., and Thornbury, 1967, Karst geomorphology of south-central Indiana: Guidebook for North-Central Section, Geological Society of America, and Indiana Department of Geology and Geological Survey, p. 11-38.

Quinlan, J.F., Ewers, R.O., Ray, J.A., Powell, R.L., and Krothe, N.C., 1983, Ground-water hydrology and geomorphology of the Mammoth Cave region, Kentucky, and of the Mitchell Plain, Indiana (Field trip 7): in Shaver, R.H., and Sunderman, J.A., eds., Field Trips in Midwestern Geology, Geological Society of America, v. 2, p. 1-85.

Reams, M.W., 1992, Fractal dimensions of sinkholes: Geomorphology, v. 5, no. 1-2, p. 159-65.

Rexroad, C.B., 1976, Underground Indiana—Five famous caves: Outdoor Indiana, v. 41, no. 6, p. 23-35.

Ritter, C.D., 1975, Selected analyses of water quality at two sites in the Blue Spring Cave System, Lawrence County, Indiana: Department of Chemistry (C509), Indiana University, Bloomington, Indiana, 45 p.

Ruhe, R.V., 1975, Geohydrology of karst terrain, Lost River watershed, southern Indiana: Water Resources Research Center, Report of Investigations No. 7, Indiana University, Bloomington, Indiana, 91 p.

Ruhe, R.V., and Olson, C.G., 1980, The origin of terra rossa in the karst of southern Indiana: in Shaver, R.J., ed., Field Trips 1980 from the Indiana University Campus, Geological Society of America, North-Central Section, p. 84-122.

Saines, S.J., 1983, Hydrogeochemical well water reconnaissance in Orange County, Indiana: unpublished M.S. thesis, Indiana University, Bloomington, Indiana, 293 p.

Sunderman, J.A., 1968, Geology and mineral resources of Washington County, Indiana: Bulletin of the Indiana Geological Survey, Bloomington, Indiana, 90 p.

Tweddle, J.B., 1987, The relationship of discharge to hydrochemical and sulfur isotope variations in spring waters of south-central Indiana: unpublished M.S. thesis, Indiana University, Bloomington, Indiana, 165 p.

Waldron, T.B., and Miller, T.E., 1987, Bibliography of Indiana karst and karst-related literature: Indiana State University, Department of Geography and Geology, Terre Haute, Indiana, Professional Paper, v. 18, p. 41-52. (See Miller and Waldron, 1988.)

Wayne, W.J., 1950, Description of the Indiana karst: Compass of Sigma Gamma Epsilon, 1915-84, v. 27, no. 4, p. 215-23.

Wells, E.R., and Krothe, N.C., 1989, Seasonal fluctuation in delta ¹⁵N of groundwater nitrate in a mantled karst aquifer due to macropore transport of fertilizer-derived nitrate: Journal of Hydrology, v. 112, no. 1-2, p. 191-201.

West, T.R., Kallio, T., and Warder, D., 1981, Construction of an apartment/social center complex in karst terrain, Bloomington, Indiana: in Winslow, D.R., ed., Proceedings of the 1981 Fall Meeting of the Indiana Academy of Science, Crawfordsville, Indiana, November 5-7, v. 91, p. 348.

Wier, C.E., Wobber, F.J., Russeli, O.R., Amato, R.V., and Leshendok, T.V., 1974, Geological lineament map of the 1° X 2° Vincennes quadrangle, Indiana and Illinois: Indiana Geological Survey, Miscellaneous Map 25, 1:250,000 scale.

Woodson, F.J., 1981, Lithologic and structural controls on karst landforms of the Mitchell Plain, Indiana, and Pennyroyal Plateau, Kentucky: unpublished M.S. thesis, Indiana State University, Terre Haute, Indiana, 132 p.

Yu, G.H., and Krothe, N.C., 1994, Annual variation of stable carbon isotopes through the soil mantle to karst aquifers of southern Indiana: Geological Society of America 1994 Annual Meeting, Seattle, Washington, October 24-27, Abstracts with Programs, v. 26, no. 7, p. 322.

Yu, G.H., and Krothe, N.C., 1995, C¹³/C¹² signatures and their implication in hydrochemical studies of karst aquifers, southern Indiana: Geological Society of America, 1995 Annual Meeting, New Orleans, Louisiana, November 6-9, Abstracts with Programs, v. 27, no. 6, p. 180.